ASSESSING THE TREATABILITY OF

TEXTILE EFFLUENTS

IN AN ACTIVATED SLUDGE SYSTEM

Arnold Mashava

Dissertation submitted
in fulfilment of the academic requirements for the
Master of Science Degree in Chemical Engineering (MScEng Chemical Engineering)
in the School of Chemical Engineering, University of KwaZulu-Natal, Durban

December 2014

Research Supervisors: Professor Chris A. Buckley and Chris J. Brouckaert

The Pollution Research Group
School of Chemical Engineering
Howard College
University of KwaZulu-Natal
Durban 4041
South Africa

DECLARATION

I, Arnold Mashava, declare that:

1. the research reported in this dissertation/thesis, except where otherwise indicated, is my original work.

2. this dissertation/thesis has not been submitted for any degree or examination at any other university.

3. this dissertation/thesis does not contain other persons' data, pictures, graphs or other information, unless specifically acknowledged as being sourced from other persons.

4. this dissertation/thesis does not contain other persons' writing, unless specifically acknowledged as being sourced from other researchers. Where other written sources have been quoted, then:

5. their words have been re-written but the general information attributed to them has been referenced;

    a) where their exact words have been used, their writing has been placed inside quotation marks, and referenced.

    b) where I have reproduced a publication of which I am an author, co-author or editor, I have indicated in detail which part of the publication was actually written by myself alone and have fully referenced such publications.

6. this dissertation/thesis does not contain text, graphics or tables copied and pasted from the Internet, unless specifically acknowledged, and the source being detailed in the dissertation/thesis and in the References sections.

Arnold Mashava, December 2014

As the candidate's supervisor, I have approved this dissertation for submission.

1)	Name	Signature	Date
2)	Name	Signature	Date

ACKNOWLEDGEMENTS

I am forever indebted to Chris Brouckaert and Chris Buckley for their seemingly infinite patience with bad scientists, and their immensely astute academic supervision which was monumental in realising the completion of this project.

I also wish to acknowledge the invaluable input of Farai Mhlanga, Kavisha Nandhlal, Kitty Foxon, Merlin Reddy and all the past and present members of the Pollution Research Group.

I wish to thank the Water Research Commission, Chris Fennemore of eThekwini Municipality, Gunter Rencken, Arnaud Gisclon and Lorraine Hartwig, all from Veolia Water Solutions and Technologies for funding the research.

I salute my father, Clifford, for his initial and sustained hatred for Chemical Engineering as a dead-end career characterised by infinite nonsense, and I also wish to pay homage to him for providing food, beer and life to the family.

Thanks to my mates, who have been relentless with their onslaught on my shortcomings; by daring me to complete this project with their deafening reminders of the inherent genetic pre-dispositions that characterise the different genera of the human species, and all the perceived imperfections that have resulted in other genera of the same species being disesteemed with lesser decorum and correctitude.

Special acknowledgements to Beck's Brewery (Brauerei Beck & Co), Brandhouse and SABMiller plc. for providing draught, bottled and canned beer to Africa and to lands beyond.

ABSTRACT

Assessing the treatability of a textile effluent through the activated sludge process required the development of analytical protocols and evaluating their suitability in providing receiving municipal wastewater treatment plants with systematic methodologies for predicting: (i) soluble dye effluent decolourisation through the activated sludge process (ii) impact of surfactants on oxygen transfer in the activated sludge system (iii) subsequent biodegradability of these surfactant effluents.

Decolourisation was assessed through spectrophotometric computations of the mass of dye remaining in the activated sludge supernatant.

Oxygen transfer was quantified from estimates of volumetric oxygen transfer coefficients which were computed from the modified form of the Lewis-Whitman interfacial mass transfer model which took into account the oxygen uptake rate from the respiring microbial species

Biodegradability of the surfactant effluent was computed from the mass of soluble biodegradable substrates assimilated by the active sludge system during exogenous respiration

The mass of the dye particles removed from solution attained an asymptotic value after 1 h and this implied adsorption equilibrium. A comparison between the adsorption equilibrium attained after 1 h and the municipal activated sludge system hydraulic residence time of 6 h led to the conclusion that soluble colour removal in receiving municipal activated sludge systems is not rate limited and it was therefore not necessary to accurately predict the adsorption kinetics. Instead, the adsorptive capacity of the activated sludge and extent of dye effluent decolourisation is of greater significance.

Instantaneously after dosing the activated sludge system with the surfactant effluent, computed estimates of the volumetric oxygen transfer coefficient exhibited sudden and pronounced increments which simultaneously coincided with pronounced increments in the non-linear regression confidence level error bounds associated with each mass transfer coefficient computation. It was theorised that the surfactant effluent imparted some form of interference to the Clark dissolved oxygen sensor's dissolved oxygen measurement mechanism and this resulted in erratic data points that did not fit onto the model.

Comparative computations of volumetric oxygen transfer coefficients in the presence of a non-surfactant substrate such as CH_3COOH should be conducted for purposes of elucidating increments in the mass transfer coefficients as a result of reaction-enhanced mass transfer from increments resulting from the impact of the surfactant effluent on either the liquid film mass transfer coefficient or the interfacial area or both. Further refinements are required in automating the methodology for computing volumetric oxygen transfer coefficients and generating scatter plots of the mass transfer coefficients as a function of time from automated real-time feeds of dissolved oxygen time series data logged by dissolved oxygen online instrumentation.

Biodegradability numerical estimates were all far less than the estimates reported in literature by surfactant manufacturers and it was postulated that the erratic dissolved oxygen time series data points resulting from the dosing of the surfactant effluent were also extended to the biodegradability computations. It is also highly probable that the pronounced dissimilarities in biodegradability estimates were a result of either the presence of toxic components in the surfactant effluent which resulted in the gradual inhibition of microbial activity or a significant presence of slowly biodegradable and inert soluble substrates in the surfactant effluent which were not depleted through aerobic utilisation by heterotrophic microbial populations.

CONTENTS

LIST OF TABLES

LIST OF FIGURES

GLOSSARY

activated sludge	the term given to the active biological material (biomass) which results from the continuous flow of thick, viscous material from the secondary clarifiers to the aeration basin and during the circulation process, takes in some active aerobic bacteria which forms a brown floc
activated sludge process	a continuous aerobic biological wastewater treatment process which makes use of active biological material suspended in the wastewater so that it decreases the amount of pollutants in the wastewater
aerobic bacteria	micro-organisms which require free or dissolved oxygen to survive and grow
anoxic bacteria	micro-organisms which survive and grow in conditions without free or dissolved oxygen and yet biological oxidation still takes place as a result of oxygen being made available by dissolved inorganic components such as NO_3^- ions
autotrophic bacteria	micro-organisms which do not use organic carbon but rather use CO_2 as a source of the carbon needed for growth and survival
azo dye	a compound whose molecular structure contains the azo functional group $(R-N=N-R')$ and is very brightly coloured as a result of the interactions between the delocalized π electrons and the aryl functional groups
bacteria	unicellular micro-organisms which multiply through binary fission using carbon either obtained from CO_2 if they are autotrophic or from organic material if they are heterotrophic
biodegradable	capable of being decomposed biochemically into simpler products through the action of micro-organisms such as bacteria
biosorption	physiochemical attachment of wastewater components (adsorbates) onto activated sludge (adsorbent) through a process which allows biomass to agglomerate adsorbates onto its cellular structure and the amount of adsorbate the biomass can adsorb is dependent on kinetic equilibrium and the composition of the adsorbent cellular surface

BOD_5	$5-$ day biochemical oxygen demand and this is a measure of wastewater organic strength which quantifies the amount of oxygen consumed in 5 days and at 20 ℃ by biological processes breaking down biologically degradable material present in organic wastes
COD	chemical oxygen demand and it indirectly provides the means of quantifying the organic strength of both domestic and industrial wastewater
endogenous respiration	microbial oxygen uptake rate in the absence of substrates from external sources through a process in which active microbial populations oxidise some of their own cellular mass
exogenous respiration	microbial oxygen uptake rate in the absence of substrates from external sources
heterotrophic bacteria	micro-organisms which use organic carbon for survival and growth
oxygen uptake rate (OUR)	the rate of absorption of oxygen by aerobic bacteria during respiration and is expressed in terms of mass of dissolved oxygen per unit volume consumed per unit time
supernatant	the layer of liquid above the settled sludge layer in a settling tank
time constant	the numerical value of t required for a response variable (y) to rise from 0 to $1-(1/exp(1)) = 63.2\%$ of its final steady (asymptotic) value as it varies with t
Volatile Suspended Solids (VSS)	volatile suspended solids and these form the organic content of suspended or dissolved solids in wastewater which are oxidized to carbon dioxide at a temperature of 550 ℃

NOMENCLATURE

1. Greek symbols

ϵ	measurement error on the response which is equivalent to a statistical error with a normal distribution
λ	ultraviolet/visible light wavelength, (L)
τ	time constant, (T)

2. Latin symbols

a	interfacial area, $(1/L)$
A	visible light absorbance, $(dimensionless)$
C	concentration, (M/L^3)
d	day(s), (T)
h	hour(s), (T)
J	Jacobian matrix
k	iteration number, $(dimensionless)$
K_F	Freundlich adsorption constant, (L^3/M)
k_L	liquid film mass transfer coefficient, (L/T)
K_L	Langmuir adsorption model constant, (L^3/M)
$k_\mathrm{L}a$	volumetric mass transfer coefficient, $(1/T)$
m	mass, (M)
M_r	molar mass, (M/MOL)
n_F	Freundlich adsorption parameter, $(dimensionless)$
q	mass of adsorbate adsorbed per unit mass of adsorbent, (M/M)

Q	volumetric flow rate, (L^3/T)
S	activated sludge soluble component mass concentration, (M/L^3)
t	time, (T)
V	volume, (L^3)
x	predictor variable
X	activated sludge particulate component mass concentration, (M/L^3)
y	response variable
Y	aerobic yield of heterotrophic biomass

3. Abbreviations

ADMI colour	colour scale developed by the American Dye Manufacturers Institute which uses a spectral or a tristimulus method to determine a colour value that is independent of hue, $(ADMI\ units)$
ASM3	IAWQ Activated Sludge Model No.3
BOD_5	5-day Biochemical Oxygen Demand, (M/L^3)
COD	Chemical Oxygen Demand, (M/L^3)
DO	dissolved oxygen
F/M	food-to-microorganism ratio, (M/M)
OUR	oxygen uptake rate $(M/L^3/T)$,
OUR_{end}	endogenous oxygen uptake rate, $(M/L^3/T)$
OUR_{exo}	exogenous oxygen uptake rate, $(M/L^3/T)$
TDS	Total Dissolved Solids, (M/L^3)
TSS	Total Suspended Solids, (M/L^3)

UV	ultra-violet light
Vis	visible light
VSS	Volatile Suspended Solids, (M/L^3)

4. Subscripts

0	initial condition at $t = 0\ s\ or\ t = 0\ h$
1	initial state
2	final state
min	minimum
max	maximum
∞	equilibrium condition

1. INTRODUCTION

The five-year permitting system for industrial effluent discharges introduced in December 2004 by the Pollution and Environmental Department of the eThekwini Municipality required the development and setting up of permitting protocol. The protocol, which would enable the eThekwini Municipality to evaluate the ability of a receiving wastewater treatment plant to sufficiently treat the industrial effluents before releasing them to the environment, identified effluents generated by textile factories as high risk effluents.

With the establishment of permitting system, eThekwini Municipality would be in apposition to regulate the quality of discharged industrial effluents and the volumetric loading of such effluents on receiving municipal wastewater treatment plants. This is a critical input in the establishment of a performance monitoring system for municipal wastewater treatment plants, where there is need for sustaining minimum efficiencies required in treating industrial effluents to environmentally acceptable standards prior to releasing them into the environment.

This ultimately puts in place some significant means of pollution control and provides continuous improvement in the water quality in South African water bodies.

The critical resources that eThekwini Municipality has for managing the discharge treatment of industrial effluents are:

1. the receiving wastewater treatment plants

2. discharge permits which enforce limits on the quality parameters of the discharged effluent

3. discharge tariffs for bearing the cost of treating the received effluents and providing incentives and penalties to the users of the permitting system

This means that the effluent discharge permitting system also ensures the sustainability of municipal wastewater treatment plants by regulating the cost incurred in receiving and treating discharged industrial effluents, where non-conformances in the stipulated volumetric loading and effluent quality discharged by an industry result in monetary penalties or revision of the industry's effluent discharge permit.

Therefore the effluent discharge permitting system will provide an interface between eThekwini Municipality and industries discharging their effluents to municipal wastewater treatment plants whilst striking a balance between protection of the general public and sustaining the longevity of the ecosystems into which the treated effluents are released.

The Umbilo and Mariannridge wastewater treatments plants were selected as cases for the study and it has been widely speculated that the performance of both wastewater treatment plants is impeded by the presence of textile effluents.

Effluents from textile factories were selected as a case for the study because in comparison to other industries, textile factories consume significantly vast quantities of municipal water for their dyeing, scouring and washing processes and consequently discharge proportionally vast quantities of effluents to receiving municipal wastewater treatment plants.

The adverse effects of textile effluents on the performance of activated sludge systems that have been noted in receiving municipal wastewater treatment plants include:

1. high counts of soluble COD and BOD_5 and the presence of slowly biodegradable and inert soluble substrates in the received textile effluents. This then results in rapid depletion of dissolved oxygen which is often difficult to regulate and consequently inhibits the activity and performance of heterotrophic microbial populations. Inevitably the overall efficiency of the wastewater treatment plant in removing soluble biodegradable substrates is attenuated

2. dyestuffs, surfactants and other organic compounds, as well as acidic and alkaline contaminants exhibit inhibitory and toxicity effects to active microbial species and this often results in the following:

   (a) complete death of protozoa and other higher forms of activated sludge microbial species

   (b) loss of biomass flocs in the activated sludge mixed liquor and this is often accompanied by foaming

   (c) loss of COD and BOD_5 removal

(d) filamentous sludge bulking when the process recovers

Notable occurrences in the wastewater treatment plants attributed to textile effluents that were considered in this study are as follows:

1. heavy and dark colouration imparted onto the activated sludge in aeration tanks as illustrated in Fig.1, where a visible dark colouration is observed in the sludge in the aeration tank at the Umbilo wastewater treatment plant

Fig.1: Dark coloured sludge in the aeration tank at the Umbilo wastewater treatment plant

2. thick and stable layers of foam which blanket the activated sludge surface in aeration tanks as illustrated in Fig.2, where a visible layer of foam covers the surface of the activated sludge at the Umbilo wastewater treatment plant

Fig.2: Layers of foam in an industrial effluent being treated at the Umbilo wastewater treatment plant

Pictorial comparisons illustrating the differences between the states of activated sludge in a wastewater treatment plant which does not receive and treat textile effluents and the occurrences shown in Fig.1 and Fig.2 are respectively provided by Fig.3 and Fig.4 where both foaming and dark colourations imparted onto the sludge are absent.

Fig.3: Normal brown colour of activated sludge in the aeration tank at the Durban Water Recycling plant

Fig.4: The absence of foam in the aeration tank at the Durban Water Recycling plant

For this study, the observed adverse effects of textile effluents on the activated sludge system have been attributed to specific components in the effluent, namely soluble dyes which impart dark colourations to activated sludge and surfactants which are largely responsible for the layers of foam shown and as respectively shown in Fig.1 and Fig.2.

This resulted in the study being segmented into three separate investigations and treatability of the textile effluent being evaluated in terms of the following:

1. assessing the capabilities of a laboratory-scale activated sludge system in decolourising a Procion Red H-E7B dyestuff solution discharged to the Umbilo wastewater treatment plant by Dyefin textile factory in Durban

2. evaluating the Effect of Surfactant Effluents on Oxygen Transfer from air to the liquid phase of an activated sludge system. Surfactants in textile effluents have been suspected to be the source of foaming in municipal activated sludge systems. For this investigation, the textile effluent was synthesised from the combination of fresh H_2O and a pure surfactant reagent from JMV textile factory in Verulam

3. estimating the extent to which the activated sludge system was capable of biodegrading a quantified load of surfactant effluent from the JMV textile factory.

1.1 Soluble dye effluents decolourisation

The basis for the development of an analytical protocol employed in this segment of the study was derived from the hypothesised mechanism through which the activated sludge system would decolourise the Procion Red H-E7B soluble dye effluent. Since adsorption was the hypothesised mechanism, the development of the analytical protocol involved spectrophotometric estimates of the mass of dye effluent adsorbed from solution and representing the decolourisation process with adsorption equilibria models.

As fully described in the Methodology section, the analysis involved spectrophotometric estimates which required the establishment of a calibration curve correlating the concentration of the dye effluent to light absorbance of the dye effluent measured by a UV-Vis spectrophotometer at the dominant wavelength ($\lambda_{\max}$).

1.2 Effect of surfactant effluents on oxygen transfer

Oxygen transfer on the air-H_2O interface in activated sludge was quantified through $k_L a$ estimates. This was the basis for the formulation of a method which combined C_{DO} vs. t measurements in activated sludge with an empirical gas-liquid interfacial mass transfer model which was modified so that microbial oxygen uptake in the activated sludge system was taken into account.

Prior to and after dosing a load of the surfactant effluent in the activated sludge system, $k_L a$ estimates were then computed as best fit parameters of C_{DO} vs. t measurements onto the modified gas-liquid interfacial mass transfer model through the non-linear least squares estimation method.

The effect of the textile effluent on oxygen transfer would then be inferred of from scatter plots of estimates of $k_{\mathrm{L}}a$ vs. t where an increase in the estimated value of $k_{\mathrm{L}}a$ after dosing the activated sludge system with the surfactant effluent would indicate an increase in oxygen transfer and a decrease would imply the opposite.

1.3 Biodegradability of surfactant effluents

Estimates on the biodegradability of the same load of textile effluent referred to in Section 1.2 were computed from the mass ratio of soluble biodegradable substrate $m_{S_{\mathrm{S}}}$ consumed by the activated sludge to the mass of total soluble Chemical Oxygen Demand $m_{COD_{\mathrm{total\ soluble}}}$ in a load of the textile effluent contacted with activated sludge for a residence time equivalent to the operating hydraulic retention time at the receiving municipal wastewater treatment plant.

This necessitated the formulation of a methodology which involved the use of a standard titrimetric procedure for estimating $COD_{\mathrm{total\ soluble}}$ of the textile effluent in combination with respirometry experiments for measurements of microbial oxygen uptake rates (OUR vs. t) for computing estimates of $m_{S_{\mathrm{S}}}$ from the area under the curve of OUR vs. t measurements corresponding to the endogenous respiration phase for each experiment.

As a subset of a larger project for the establishment of a permitting system for the discharge of industrial effluents to municipal wastewater treatment plants, the primary emphasis of this study was on the development and testing of analytical methods through which treatability of industrial effluents can predicted.

2. LITERATURE REVIEW

Textile effluents are generally grouped into the following categories which require different pollution prevention methods and effluent treatment technologies (Subrata, 2006):

1. Hard to treat effluents – this is a category of effluents which are resist treatment and impede the efficient operation of wastewater treatment plants. Non-biodegradable organic or inorganic materials are the main sources of such effluents which contain dyes, phenolic compounds, non-ionic and anionic surfactants, toxic organic compounds etc.

2. Toxic effluents – these are effluents with adverse impacts on the environment an toxic wastes include textile bleaches, non-biodegradable organic materials and other compounds often are used for non-process applications such as cleaning of factory machinery

Studies on the treatability of wastewater from a textile mill have been reported in previous investigations by Abo-Elela et al. (1998) who evaluated the biological treatment of a textile effluent contacted with equal volumes of domestic effluent in a completely mixed activated sludge system and their study concluded that the process produced a very fairly clean effluent after treatment.

Other assessments by Kumar and Saravanan (2009) evaluated the treatability of a textile wastewater using a Pilot plant which combined an aerobic fluidized bed biofilm process and chemical coagulation. Enhancement of the biological treatment process efficacy was achieved through the incorporation of polyurethane cubes as supporting media for attached growth and Fenton's reagent was used as a coagulant in the study.

The fluidised bed biofilm process was then operated at four different residence times: 3 h, 4.5 h, 6h and 8 h and this resulted in $COD_{\text{soluble, total}}$ removal efficiencies increasing from 69% to 94% when the residence time increased from 3 h to 4.5 h and thereafter, the $COD_{\text{soluble, total}}$ removal efficiency became asymptotic at approximately 94%. After the treatment process significant reductions in the colour of the textile effluent were also observed.

Basibuyuk and Forster (1997) examined the treatability of a synthetic textile effluent containing a Maxilon Red BL-N dye using a cascade sequence of four biological aerated filters. In the study, 99% colour removal was reported and the decolourisation mechanism was an adsorption process in which the textile effluent-activated sludge system exhibited conformance to the Langmuir adsorption isotherm.

In another study by Ciner et al. (2003), dyestuffs and polyvinyl alcohols were identified as the major textile wastewater components which posed a higher risk to the environment and required rigorous treatment methods to meet municipal discharge effluent standards for the discharge of industrial effluents in terms of $COD_{\text{soluble, total}}$ and colour.

In the investigation, effluents from textile dyeing factories underwent both physico-chemical treatment and biological treatment in the form of the activated sludge process. In the physico-chemical treatment regime, the removal efficiencies were reported as follows:

1. $COD_{\text{total soluble}} = 60.8\ \%$
2. $TSS = 80\ \%$
3. Turbidity $= 10.9\ \%$

For the biological treatment process, higher $COD_{\text{soluble, total}}$ efficiencies were reported:

1. $COD_{\text{total soluble}} = 90\ \%$
2. $TSS = 40\ \%$

The characterisation of a textile effluent based on stabilisation investigations was proposed by Zgajnar and Zagorc-Koncan (2004) and the objective was to evaluate the biological treatability of a textile wastewater through the activated sludge process and probable toxicity effects on the microbial populations.

Residence time requirements and extents of biodegradability of the textile effluent were assessed through open respirometry techniques and OUR measurements. In the study, the textile effluent is reported to have exhibited 76 % biodegradability although toxicity effects on the activated sludge were also observed.

Both toxicity and open respirometry assessments confirmed acclimation of the activated sludge to the textile effluent and the activated sludge process was concluded to be a potentially efficient method of treating textile effluents.

Estimating the treatability of textile effluents amongst a range of other industrial effluents through OUR measurements in activated sludge has also been reported by Orupõld et al. (1999).

The textile effluent together with other industrial effluents were analysed and their individual and treatabilities were compared through $OUR_{\text{exo}}\, vs. t$ measurements through which the kinetic parameters of the biodegradation processes for each effluent were computed from monitoring the associated oxygen consumption for each test with different amounts of the textile effluent. From the study, it is reported that the short-term oxygen demands in the tests accounted for 25– 45 % of the BOD_5 of the textile effluent.

In a more recent study by Iqbal et al. (2007), biological treatment of a textile effluent in an activated sludge bioreactor significantly reduced the magnitudes of the pollutant parameters to such an extent that the treated effluent's composition conformed to the required national industrial effluent discharge limits.

Under experimental conditions in which temperature and pH were respectively kept constant at 25 ℃ and pH = 7 , the following removal efficiencies were attained after contacting the textile effluent with activated sludge for 240 h:

1. $COD_{\text{soluble, total}} = 90\ \%$
2. $BOD_5 = 88.2\ \%$
3. $TSS = 79\ \%$
4. $TDS = 48.5\ \%$

Although activated sludge treatment technologies are effective in reducing the amount of $COD_{\text{soluble, total}}$ in textile effluents, the activated sludge system has been reported to be ineffective in the decolourisation of textile effluents and their failure to effectively remove colour from these effluents has been attributed to the non-biodegradability of stable dyestuffs by Ghosh et al. (1978).

This has been further confirmed by study of Beydilli et al. (2000) which investigated the decolourisation of the Reactive Red 2 (RR2) dye under aerobic, anoxic, and methanogenic conditions. The study reports that the dye was not decolourised by an aerobic culture kept under aerobic conditions for 7 days.

In the study by Judkins (1978), it is reported that whilst biological treatment processes such as aerated lagoons and conventional activated sludge processes are frequently used to treat textile effluents, aerobic wastewater treatment technologies are only effective for BOD_5 and TSS removal but they are quite ineffective in removing colour from textile effluents.

Other investigations on the biodegradability of soluble azo dyes in activated systems have also reported that the dyes are not degraded under aerobic conditions (Michaels and Lewis, 1986; Pagga and Brown, 1986 and Nigam et al., 1996).

A more expository investigation on the treatability of textile effluents through the activated sludge process is provided by Orhon et al. (1992). In the study, the different chemical components of a textile effluent were identified and their respective biodegradability characteristics were estimated through an analytical protocol in which the initial $COD_{\text{soluble, inert}}$ and the $COD_{\text{soluble, residual}}$ generated through microbial metabolism during contact with the activated sludge are determined experimentally together with the kinetic and stoichiometric parameters associated with the biodegradation process.

The residual components of the effluent, together with the kinetic information about biodegradable fractions, were then used to simulate the performance of the activated sludge system through a correlation between $COD_{\text{soluble, total}}$ and the sludge age. The conclusion from the study reported that the residual components formed the larger part of textile effluent's $COD_{\text{soluble, total}}$ and this implied that full treatability of textile effluents through the activated sludge process could not be attained.

Kim et al (2007) studied methods of enhancing Biodegradability of Surfactant Effluents through electron beam irradiation prior to contacting the effluent load with activated sludge. In the study, refractory compounds from textile effluents, notably soluble dye compounds, were identified as the organic compounds that were not readily biodegradable and required electron beam irradiation as a form of pre-treatment to decompose them into compounds with a lower molecular weight which are more biodegradable.

The studies by Chiang et al. (1997) and Kapdan et al. (2000) also reported that full treatability of textile effluents through a single stage activated sludge process was not attainable without the application of physico-chemical pre-treatment methods such as electrochemical oxidation to the wastewater to decompose refractory organic components such as soluble dyes compounds.

The activated sludge process

The activated sludge process is a continuous aerobic biological wastewater treatment process which makes use of active microbial populations suspended in the wastewater to absorb and biodegrade the organic components of the wastewater and such processes take place in an aerated tank as described by Bailey and Ollis (1986).

A schematic of the conventional activated sludge process according to Bailey and Ollis (1986) is shown in Fig.5:

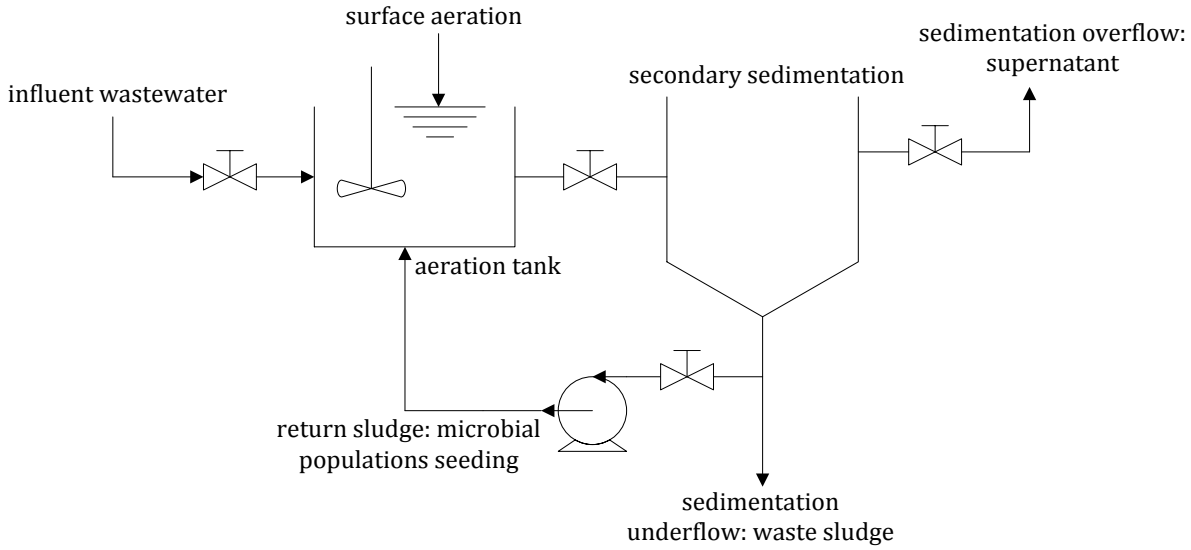

Fig.5: Process flow diagram for the activated sludge process

Active microbial populations in the aeration tank are kept in suspension by air blown from the bottom of the aeration tank through diffused aerators or by air blown from the top of the aeration tank through surface aerators and the dissolved oxygen concentration (C_{DO}) in the aeration tank should be maintained at values of $C_{\mathrm{DO}} \geq 2$ mg/dm^3 according to Smith and Scott (2005).

The biodegradation processes in the activated sludge system can be represented by a general reaction according to Metcalf and Eddy Inc. (2003):

$$a[\mathrm{C}] + b[\mathrm{O_2}] + c[\mathrm{NH_3}] + d[\mathrm{PO_4^{3-}}] \xrightarrow{\text{active biomass}} e[\text{active biomass}] + f[\mathrm{CO_2}] + g[\mathrm{H_2O}] \quad (2.1)$$

where

$\mathrm{C} =$ organic carbon

$a, b, \ldots, g =$ stoichiometric coefficients

$\mathrm{NH_3} =$ source of N as a nutrient for the active biomass

$\mathrm{PO_4^{3-}} =$ source of P as a nutrient for the active biomass

$\mathrm{H_2O}$ and $\mathrm{CO_2} =$ products of the biodegradation process

active biomass = new microbial populations from aerobic growth

Through aerobic oxidation, $\mathrm{NH_3}$ is broken down into $\mathrm{NO_3^-}$ and $\mathrm{NO_2^-}$ and organic compounds are oxidised into $\mathrm{CO_2}$ and $\mathrm{H_2O}$.

Smith and Scott (2005) reported that the active biomass in the aeration tank consists of the following bacterial species:

1. aerobic bacteria – micro-organisms which require free or dissolved oxygen to survive and grow

2. anoxic bacteria – micro-organisms which survive and grow in conditions without free or dissolved oxygen and yet biological oxidation still takes place as a result of oxygen being made available by dissolved inorganic components such as $\mathrm{NO_3^-}$ ions

3. autotrophic bacteria – micro-organisms which do not use organic carbon but rather use $\mathrm{CO_2}$ as a source of the carbon needed for growth and survival

4. heterotrophic bacteria – micro-organisms which use organic carbon for survival and growth

The typical design variables and parameters for the activated sludge process have been reported by Eckenfelder (1989), Eckenfelder et al. (1995), Eckenfelder and Grau (1998), van Haandel and van der Lubbe (2007), Von Sperling (2007), Nielsen et al. (2009) and Orhon et al. (2009).

Let the variables and parameters entailing the activated sludge process be represented by the symbology in Fig. 6:

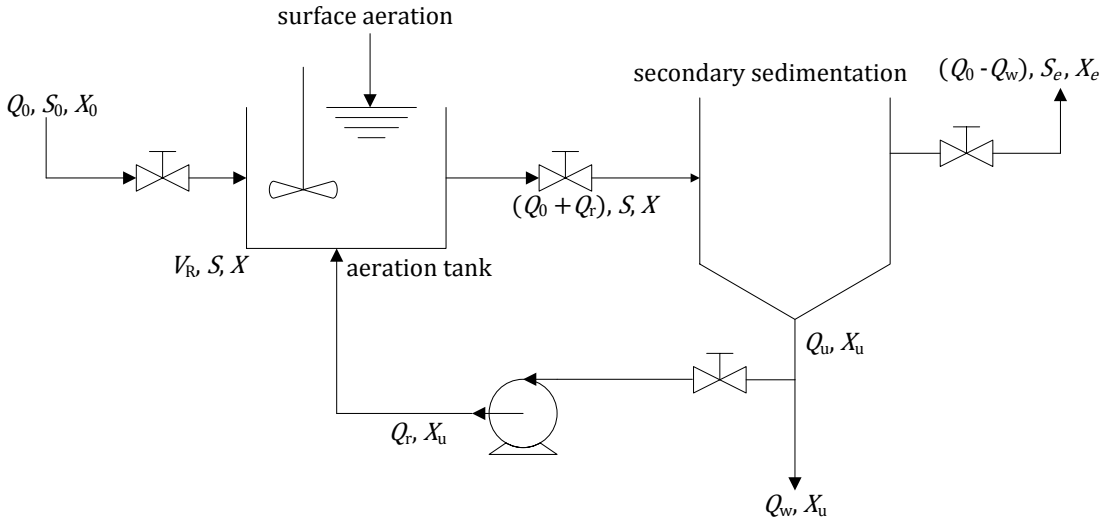

Fig.6: Activated sludge process design variables

Nomenclature:

$Q_0 =$ influent flow rate, (L^3/T)

$Q_r =$ return sludge flow rate, (L^3/T)

$Q_w =$ waste sludge flow rate, (L^3/T)

$S_0 =$ soluble biodegradable substrate concentration in the influent, (M/L^3)

$S =$ soluble biodegradable substrate concentration in the bioreactor, (M/L^3)

$X_0 =$ influent wastewater biomass concentration, (M/L^3)

$X =$ bioreactor biomass concentration, (M/L^3)

$X_\mathrm{e} =$ secondary sedimentation overflow biomass concentration, (M/L^3)

$X_\mathrm{u} =$ secondary sedimentation underflow biomass concentration, (M/L^3)

$V_\mathrm{R} =$ bioreactor volume, (L^3)

$K_\mathrm{S} =$ half saturation constant, (M/L^3)

$k_0 =$ maximum growth rate constant, $(1/T)$

$k_\mathrm{d} =$ endogenous decay rate constant, $(1/T)$

$Y =$ yield coefficient, $(dimensionless)$

$t_{\text{hydraulic retention}} =$ hydraulic retention time (T)

$t_{\text{solids retention}} =$ solids retention time (T)

Mass balances for the completely-mixed bioreactor:

1. biomass:

$$Q_0 X_0 + V_\mathrm{R}(k_0 XS/K_\mathrm{S} + S) - k_\mathrm{d} X = (Q_0 - Q_\mathrm{w})X_\mathrm{e} + Q_\mathrm{w} X_\mathrm{u} \tag{2.1}$$

2. biodegradable substrate:

$$Q_0 S_0 + V_\mathrm{R}(k_0 XS/Y(K_\mathrm{S} + S)) = (Q_0 - Q_\mathrm{w})S + Q_\mathrm{w} S \tag{2.2}$$

$$k_0 S/(K_\mathrm{S} + S) = (Q_0/V_\mathrm{R})(Y/X)(S_0 - S) \tag{2.3}$$

Combining the biomass and biodegradable substrate mass balances:

$$Q_\mathrm{w} X_\mathrm{u}/V_\mathrm{R} X = (Q_0/V_\mathrm{R})(Y/X)(S_0 - S) - k_\mathrm{d} \tag{2.4}$$

hydraulic retention time:

$$t_{\text{hydraulic retention}} = V_{\text{R}}/Q_0 \tag{2.5}$$

solids retention time:

$$t_{\text{solids retention}} = V_{\text{R}}X/Q_{\text{w}}X_{\text{u}} \tag{2.6}$$

mixed liquor suspended solids concentration:

$$X = t_{\text{solids retention}}(S_0 - S)Y/t_{\text{hydraulic retention}}(1 + k_{\text{d}}t_{\text{solids retention}}) \tag{2.7}$$

food-to-microorganism ratio:

$$F/M = Q_0S_0/V_{\text{R}}X \tag{2.8}$$

where

F/M = food-to-microorganism ratio

oxygen requirements:

$$\text{O}_2\ required = Q_0(S_0 - S)/(BOD_5/BOD_{\text{ultimate}}) - 1.42Q_{\text{w}}X_{\text{u}} \tag{2.9}$$

where

BOD_{ultimate} = ultimate BOD and this is equivalent to the total amount dissolved oxygen consumed by the biomass when biochemical reactions in the activated sludge system are allowed to proceed to completion, (M/L^3)

1.42 = biomass theoretical COD, (M/L^3)

2.1 Soluble Dye Effluents Decolourisation

Textile dyeing processes require the prior removal of impurities on the textiles which inhibit the fixation of the dyes onto the textile material. The removal of such impurities involves the use of chemical compounds such as alkalis, acids, salts, surfactants, solvents and bleaching compounds prior to the dyeing process.

Depending on the type of fabric, the different types of dyes used in the textile industry have been comprehensively described by Kulkarni et al. (1985), Carr (1995), American Association of Textile Chemists and Colorists (1997), American Association of Textile Chemists and Colorists (1999), Christie, Royal Society of Chemistry (2001), Lacasse and Baumann (2004), Choudhury (2006) and Ullmann (2008):

1. acid dyes – these are synthetic dyes that are applied from acidic solutions (pH ≤ 4) to polyamide fibres and would be typically used to dye fabrics such as wool, silk and nylon at contact temperatures $\cong 100$ °C. Bonding between the dye and fibre is some strong form of ionic bonds between basic functional groups of the fibre and acid functional groups of the dye molecule

2. direct dyes - these are dyes whose name is derived from their method of being applied onto fabrics, which is essentially the immersion of the textile into a dye solution without the necessity for other chemicals to bond the dye onto the fabric. Whilst direct dyes have high magnitudes of substantivity, their bonding to fibres is weak and thus have relatively inferior wash-fastness

3. azoic dyes - they are also known as Naphthol dyes and they are actually chemically synthesised inside the fibre and as such, are insoluble pigments and not necessarily true dyes. The soluble Naphthol functional group is contacted with the fabric and a diazo salt solution is then used to develop the colour of the textile. The functional groups of such dyes are usually toxic before prior to the reaction to form the pigment

4. disperse dyes - these dyes have extremely low solubility in water and during the dyeing process, they exist in the dye bath as a dispersion of microscopic particles. Disperse dyes are usually applied to fabrics such as polyester, nylon and acetate. Polyester is contacted with disperse dyes by heating the dye bath to temperatures ≅ 130 ℃ under an elevated pressure. The thermosol dyeing process is also used to dye textiles such as polyester, where the fabric is coated with dye bath and heated to 200 °C for about 90 seconds. Disperse dyes on polyester exhibit high magnitudes of wash-fastness and are and resistant to chemical oxidation or bleaching

5. sulphur dyes – they are synthesised from the reaction of sulphur with organic compounds and most sulphur dyes are of an unknown chemical structure. Sulphur dyes have low solubility in water and have to be converted to a soluble form for contacting with textiles. The dyeing process is similar to that used for vat dyes. Sulphur dyes exhibit high susceptibility to chemical oxidation and when contacted with certain fabrics, they decompose under high temperatures and humidity to form an acidic solution

6. reactive dyes – these are dyes which fix to the fibres of the textile by forming a covalent bond. Reactive dyes exhibit high magnitudes of light-fastness and wash-fastness and high susceptibility to chemical oxidation. Reactive dyes are usually contacted with cellulose fibres and sometimes they are applied to wool. Typical examples include Procion® MX, Procion® H, Procion® H-E, Remazol®, and Cibacron® F. Reactive dyes have varying reactivities and this means that some reactive dyes are easily applied at room temperature and others at temperatures ≅ 100 ℃. The dyeing process requires large amounts of electrolyte and there is cold rinsing and hot washing after the dyeing process to remove unfixed dye molecules

   Elvers et al. (1993) also described reactive dyes and in their study, they reported that reactive dyes are used in the dyeing of cellulosic fibres and the molecular structure of the dyes is made up of a reactive group, which is usually an activated double bond or a haloheterocycle, so that when the dye is contacted with some textile material, it forms a covalent bond with fibres on the textile material.

7. basic dyes – also known as cationic dyes, they have a functional group which reacts with acidic functional groups on fabrics and are usually contacted with acrylic fibres and seldomly applied onto some types of polyester, nylon and occasionally onto protein fibres

8. vat dyes – using a reducing agent, the vat dyeing process requires some of conversion from pigments with low water solubility to soluble leuco dyes (dyes whose molecules have two forms: colourless form and visible colour form) which are then applied onto the fabric by immersion and converted back to the insoluble form by oxidation. Vat dyes exhibit high resistance to chemical oxidation

9. Azo dye dyes have a molecular structure which contains the azo functional group (R– N = N– R'), where R and R' are either alkyl or aryl functional groups. The dye solutions are very brightly coloured as a result of the interactions between the delocalised $\pi -$ electrons and the aryl functional groups on the azo dye molecule as reported by Zollinger (2003).

The impact assessments on the effect of the dyes on human health and the receiving environment after discharge is described by Kulkarni et al. (1985).

The most critical parameters of the dyeing processes that contributed to estimating the amounts of dyes released to the environment were rinse time, rinse volume and dye exhaustion. The assessments concluded that fibre-reactive and disperse dyes were found to exhibit the lowest toxicity to the environment and as such, have since replaced most of the dyes.

Typical components of textile dye effluents included heavy metals, ammonia, alkali salts, toxic solids and large amounts of pigments and most of these compounds were found to be highly toxic.

Most of the dye effluents were also found to contain organically bound chlorine which is carcinogenic. Natural dyes were found to exhibit low environmental toxicity impacts but this was dependent on the specific mordant used in the dyeing processes. Dyeing processes which used mordants such as chromium were found to be highly toxic and exhibited high environmental impacts.

Previously, water-soluble azo dyes used in textile dyeing processes exhibited high toxicity to fresh water microbial populations as reported by Michaels and Lewis (1985).

The dark colouration imparted onto receiving fresh water streams by treated textile effluents is reported to cause disruption of photosynthetic processes of phytoplankton in the water bodies but nothing is reported on the impact of these effluents on the microbial activity in wastewater plants by Cunningham and Siago (2001).

The dyeing of textiles has since evolved and newer dyes used in the textile industry have low toxicity to water microbial populations according to the study by Cunningham and Siago (2001).

The most commonly used types of dyes in textile dyeing operations are reactive dyes as reported by Zollinger (1991) and Beydilli et al. (2000).

Newer soluble dyes in general, are reported to exhibit low toxicity to the environment by Loyd et al. (1992) and Churchley (1998) and therefore limits for colour discharges in industrial effluents are established for aesthetic reasons and not much for the prevention of environmental toxicity according to O'Neill et al. (1999).

Conventional wastewater treatment methods for textile effluents such as the activated sludge process have been described in the study by Kim et al. (2008) in which they attribute the non-treatability of textile effluents in the activated sludge system to the presence of refractory compounds such as dyes and compounds from textile dyeing processes.

The treatment of textile effluents involves the removal of colour and reduction of organic strength (COD) and generally, the treatment processes involve the use of both biological and physico−chemical treatment technologies. Although activated sludge treatment technologies are effective in reducing the amount of COD in these effluents, the activated sludge system has been reported to be ineffective in the decolourisation of textile effluents and their failure to effectively remove colour from these effluents has been attributed to the non-biodegradability of stable dyestuffs according to Ghosh et al. (1978).

This has been further confirmed in the study by Beydilli et al. (2000) who investigated the decolourisation of the Reactive Red 2 (RR2) dye under aerobic, anoxic, and methanogenic conditions.

The study reports that the dye was not decolourised by an aerobic culture kept under aerobic conditions for 7 days. According to Judkins and Hornsby (1978), it is reported that whilst biological treatment processes such as aerated lagoons and conventional activated sludge processes are frequently used to treat textile effluents, aerobic wastewater treatment technologies are only effective for BOD_5 and TSS removal but they are quite ineffective in removing colour from textile effluents.

Investigations on the biodegradability of dye effluents in the activated system have also reported that the textile effluent dyes are not degraded under aerobic conditions as reported by Michaels and Lewis (1986), Pagga and Brown (1986) and Nigam et al. (1996).

Other investigations on the possible mechanisms of decolourisation of textile effluents through conventional wastewater treatment methods such as the activated sludge process have shown that biosorption is the most likely mechanism through which the concentration of dyes is lowered in textile effluents as reported by Gupta et al. (2007), Al-Ghouti et al. (2003) and Dizge et al. (2008).

More comprehensive investigations by Aksu (2001), Alam (2004), Gulnaz et al. (2004), Chu and Chen (2004) and Ju et al. (2008) have also attributed the decolourisation of dye effluents in activated sludge to biosorption, a process where the dye molecules (adsorbates) attach themselves onto activated sludge (adsorbent).

Aksu (2001) investigated the biosorption of reactive dyes (Reactive Blue 2 and Reactive Yellow 2) onto dried activated sludge in a study which evaluated dye binding capacity of the activated sludge as a function of initial pH, initial dye concentration and type of dye. The equilibrium adsorption data was fitted onto linearised forms of the Freundlich and Langmuir adsorption models and the fits gave nearly perfect linear fits with linear correlation coefficients greater than 0.90.

According to Alam (2004), Gulnaz et al. (2004) and Chu and Chen (2004), the biosorption process involves the simultaneous depletion of dye molecules from solution and accumulation of the dye molecules at the dye effluent – activated sludge interface. The basis of separation of the dye from solution is the equilibrium between the amount of dye at the dye effluent – activated sludge interface and the amount of dye in solution.

Experimental procedures for investigating the biosorption of soluble dye effluents by activated sludge have been described by Gulnaz et al. (2004) and Alam (2004). In both studies, batch adsorption experiments were conducted on dried activated sludge which was contacted with a dye effluent which synthesised in the laboratory so that the composition and initial concentration of the dye effluent were known.

Alam (2004) evaluated the adsorptive capacity of the activated sludge as a function of initial dye concentration, contact time between adsorbent and dye solution, pH, amount of adsorbent contacted with dye, temperature and the rate of agitation of the batch mixture of the activated sludge and dye solution.

The batch experiments involved contacting a quantified volume of the dye solution (adsorbate) at a known initial concentration with a fixed volume of activated sludge (adsorbent) at a uniform concentration and agitating the mixture at a constant speed. Samples were then withdrawn from the batch mixture at 5 minute intervals for analysis and the analysis involved centrifuging the withdrawn samples at a constant speed for a fixed amount of time and analysing the resulting supernatant fraction for the dye remaining in solution.

The analysis to determine the remaining amount of dye in solution after contacting the dye solution with activated sludge for a specified amount of time involved the use of spectrophotometric methods to determine the light absorbance of the dye remaining in solution after biosorption.

In the study by Alam (2004), the equilibrium concentration of the dye in solution after biosorption and the sorption capacity of the activated sludge at equilibrium were determined and fits of the biosorption data were made onto the linearised form of the Langmuir adsorption model.

The mass of dye adsorbed per unit mass of activated sludge was computed from the difference between the initial and equilibrium dye concentration:

$$q = (C_{\text{dye, initial}} - C_{\text{dye, solution}})/m_{\text{sludge}} \times V_{\text{dye}} \quad (2.1.1)$$

where

$C_{\text{dye, initial}}$ = initial concentration of dye effluent, (g/dm^3)

$C_{\text{dye, solution}}$ = concentration of dye effluent after contact with activated sludge, (g/dm^3)

m_{sludge} = mass of activated sludge contacted with dye effluent, (g)

V_{dye} = volume of dye effluent, (dm^3)

Adsorption models are often used to give a mathematical characterisation of the adsorption equilibrium and for a single adsorbate in solution, the simplest relationship between adsorbate concentration at the solution – adsorbent interface and adsorbate concentration in solution is reported as a linear isotherm by LeVan et al. (1999):

$$q = KC \quad (2.1.2)$$

where

q = mass of adsorbate that is adsorbed per unit mass of adsorbent, (g adsorbate/g adsorbent)

C = concentration of adsorbate solution, (g/dm^3)

K = adsorption parameter, (dm^3/g adsorbent)

The mostly commonly used adsorption model to describe the biosorption of dyes effluents onto activated sludge is the Langmuir adsorption model according to Langmuir (1916). The model assumes monolayer adsorption and the model also assumes that there is negligible interaction between adsorbed molecules on different adsorption sites as described by LeVan et al. (1999):

$$q = q_{\infty}K_{\text{L}}C/1 + K_{\text{L}}C \quad (2.1.3)$$

where

q_{∞} = maximum mass of adsorbate that is adsorbed per unit mass of adsorbent to form a complete monolayer on the adsorbent surface, (g adsorbate/g adsorbent)

K_{L} = Langmuir adsorption parameter, (dm^3/g adsorbent)

The Langmuir constant (K_L) is reported by Aksu (2001) to be related to the affinity of the binding sites on the adsorbent surface.

In general, adsorption models describe the amount of adsorbate that is adsorbed by the adsorbent as a function of adsorbate concentration at a constant temperature according to LeVan et al. (1999).

Biosorption of dye effluents in terms of the mass of adsorbate, temperature, concentration of the adsorbate solution is also described by the Freundlich adsorption model according to Freundlich (1926). According to Suzuki (1990), the model assumes infinite adsorption capacity of the adsorbent thus making the mass of adsorbate adsorbed approach infinity when the concentration of the adsorbate increases:

$$q = K_F C^{1/n_F} \quad (2.1.4)$$

where

K_F = Freundlich adsorption constant, (dm^3/g adsorbent)

n_F = Freundlich adsorption parameter, ($dimensionless$)

K_F and n_F are constant for a given adsorbate – adsorbent system at a specified temperature

For both the Langmuir and Freundlich adsorption models, the adsorption parameters: q_∞, K_L, K_F and n_F are computed from best fits of q vs. C experimental data onto the respective adsorption models using the non-linear least squares estimation method.

Studies on adsorption kinetics have been conducted in order to describe adsorbate uptake rates since these rates determine the residence time of adsorbate particles at the adsorbent – adsorbate interface as reported by Augustine et al. (2007).

Gulnaz et al. (2004) also evaluated the kinetics of the biosorption processes in order to determine the adsorbate uptake rate-controlling steps from which they would then provide predictions on the mechanism of biosorption process.

Investigations by Brusatori and van Tassel (1999) and Qiu et al. (2009) have respectively reported that the kinetics of the adsorption process strongly influence the saturation of the adsorbent surface and the adsorbate uptake rate which is described by the kinetics determines the residence time required for completion of adsorption reaction.

According to Qiu et al. (2009), adsorption kinetics models are derived either from adsorption reaction models or adsorption diffusion models. The difference between the two is that adsorption diffusion models are formulated using the following steps according to Lazaridis and Asouhidou (2003):

1. diffusion across the adsorbate film surrounding the adsorbent particles

2. diffusion in the adsorbate contained in the adsorbent sites and along the adsorbent sites' walls and this termed as internal diffusion or intra-particle diffusion

3. adsorption and desorption between the adsorbate and active adsorbent sites

Conversely, adsorption reaction models derived from chemical reaction kinetics are formulated on the basis of the whole process of adsorption without considering the steps described by to Lazaridis and Asouhidou (2003).

According to Qiu et al. (2009), recent adsorption studies have employed only adsorption reaction models as reported by Aksu (2001), Gulnaz et al. (2004), Alam (2004), Chu and Chen (2004) and Ju et al. (2008).

The biggest shortcoming with most of these studies is that pseudo-second order adsorption kinetic model based on chemisorption was inappropriately applied to describe physisorption processes.

Some of the commonly used adsorption kinetics models derived from adsorption reaction models include:

1. pseudo-first order rate equation derived from Lagergren (1898) by Ho (2004): the model best describes the kinetic processes of liquid adsorbate – solid adsorbent phase adsorption:

$$\frac{dq}{dt} = k_1(q_\infty - q) \tag{2.1.5}$$

Integrating the model between the boundary conditions according to Ho (2004):

$$\int_0^q 1/(q_\infty - q)\, dq = \int_0^t k_1\, dt$$

$$\log_{10}(q_\infty - q) = \log_{10}(q_\infty - (k_1/2.303)t)$$

According to Qiu et al. (2009), in order to distinguish adsorption kinetic models based on adsorption capacity from solution concentration, the first-order rate equation has been termed the pseudo-first-order adsorption kinetics model by Ho and McKay (1998a).

In recent investigations, the pseudo-first-order adsorption kinetics model has been used to describe the adsorption kinetics of pollutants from effluents by Hameed and El-Khaiary (2008b).

2. pseudo-second order rate equation according to Ho and McKay (1999): which is based on the assumptions that adsorption process is second-order and the rate-limiting step is chemical adsorption involving the exchange of electrons between the adsorbent and adsorbate ions in solutions. Furthermore, the adsorption process follows the Langmuir equation according to Ho and McKay (1999) and the rate of adsorption depends on the number adsorbate particles occupying adsorbent sites and the total number of adsorbate particles occupying adsorbent sites at equilibrium:

$$\frac{dq}{(q_\infty - q)^2} = k_2 dt \tag{2.1.6}$$

Integrating the model between the boundary conditions according to Ho and McKay (1999):

$$\int_0^q 1/(q_\infty - q)^2\, dq = \int_0^t (k_2)\, dt$$

$$t/q = (1/k_2 q_\infty^2) + (1/q_\infty)t$$

According to Qiu et al. (2009), in order to distinguish adsorption kinetic models based on adsorption capacity from solution concentration, the second-order rate equation has been termed the pseudo-second-order adsorption kinetics model by Ho (2006).

In recent investigations, the pseudo-second-order adsorption kinetics model has been applied to describe the adsorption kinetics of metal ions and dyes from aqueous solutions by Cheng et al. (2008).

Qiu (2009) reported that for kinetics models derived from adsorption diffusion models, either liquid film diffusion or intra-particle diffusion is the rate limiting step. As such, kinetics models derived from adsorption diffusion models are formulated principally to describe film diffusion or intra-particle diffusion processes.

Typical models that apply to biosorption processes include:

1. linear driving force rate equation according to Cooney (1999): this is a typical model that is applied to liquid adsorbate - solid adsorbent systems, where the rate of adsorbate accumulation on the adsorbent sites is equal to rate of adsorbate mass transfer across the liquid film according to the law of conservation of mass.

   The model is represented mathematically as follows:

   $$\frac{d\bar{q}}{dt} = k_{\mathrm{L}} A_{\mathrm{s}} / V_{\mathrm{p}} (C - C_{\mathrm{i}}) \qquad (2.1.7)$$

   where

   $\bar{q}$ = average adsorbate concentration in the adsorbent

   k_{L} = film mass transfer coefficient

   V_{p} = volume of adsorbent particle

   A_{s} = surface area of adsorbent particle

   C = bulk adsorbate concentration in the liquid phase

   C_{i} = adsorbate concentration at the liquid adsorbate – solid adsorbent interface

2. film diffusion mass transfer rate equation according to Boyd et al. (1947): kinetics model also applicable to liquid adsorbate – solid adsorbent systems and is represented by a system of equations:

$$\ln(1-(q/q_\infty)) = -Rt \quad (2.1.8)$$

$$R = 3D_\infty/r_a\delta r_a k_\infty \quad (2.1.9)$$

where

$R =$ adsorbate film diffusion constant, $(1/\mathrm{h})$

$D_\infty =$ effective adsorbate film diffusion constant, $(\mathrm{m}^2/\mathrm{h})$

$r_a =$ adsorbent particle radius, (m)

$\delta r_a =$ adsorbate film thickness, (m)

$k_\infty =$ adsorption equilibrium constant, $(dimensionless)$

The adsorbate film diffusion constant , R, was the computed from a straight line plot of $\ln(1-(q/q_\infty))$ vs. t with a slope of $-R$.

Synopsis

With respect to the removal of colour in receiving municipal wastewater treatment plants, not much has been discussed in existing literature on the decolourisation of soluble dye effluents through the conventional activated sludge process.

The only form of treatability of textile dye effluents through the activated sludge process as discussed by Ghosh et al. (1978) is the reduction of soluble COD in textile effluents however the process has been reported not to be able to remove colour in textile effluents through biodegradation under aerobic conditions as confirmed by Nigam et al. (1996).

However removal of colour from textile effluents has been historically attained through use of biosorption methods as discussed by various authors: Al-Ghouti et al. (2003), Gupta et al. (2007) and Dizge et al. (2008). In their investigations, by contacting the effluents with various types of organic material and from both linear and non-linear fits of the decolourisation data onto adsorption models, the high conformity of the data onto the models showed that the most probable mechanisms through which the concentration of dyes in textile effluents was lowered was through biosorption.

The use of activated sludge as an adsorbent for the biosorption of soluble dyes from textile effluents has been comprehensively studied by Gulnaz et al. (2004) and Alam (2004). However in both studies, activated sludge was used only in dried pulverised form as opposed to the conventional wet activated sludge in bioreactors constituting the of municipal wastewater treatment plants.

Whilst dried pulverised activated sludge has been shown to be an effective adsorbent for the removal of colour in soluble dye effluents, the removal of soluble dyes from textile effluents in receiving municipal wastewater treatment plants has been observed to occur at the consisting of the bioreactor vessels with wet activated sludge and secondary sedimentation vessels.

In all of the receiving municipal wastewater treatment plants that were selected as cases for the study (Umbilo, Mariannridge and Verulam wastewater treatment plants), the measure or count of influent soluble colour into the bioreactor vessels containing wet activated sludge was always higher than of the effluent soluble colour in the supernatant exiting the secondary sedimentation vessels and remaining activated sludge in the bioreactor vessels had the same colour as the influent soluble dyes in the received textile effluents.

In the Verulam wastewater treatment plant, the soluble colour decolourisation through the conventional activated sludge process is completed in much less time than the hydraulic residence time of the plant $\left(t_{\text{hydraulic retention}} = 6\,\text{h}\right)$. Similar findings have also been historically observed for the Umbilo and Mariannridge plants and it was then hypothesised that soluble colour is imparted onto the wet activated sludge and this results in the remaining activated sludge having the same colouration as the received textile effluent and inevitably measures of soluble colour in the bioreactor influent that are higher than those logged for the bioreactor effluent.

The most probable mechanism that was hypothesised for the decolourisation of soluble dye effluents observed at the receiving municipal wastewater treatment plants was biosorption and the non-existence of historical publications and studies on the biosorption of soluble dyes through wet activated sludge in receiving municipal wastewater treatment plants thus provided the impetus for undertaking the study and investigating the decolourisation of soluble dye effluents through the conventional activated sludge process.

2.2 Effect of Surfactant Effluents on Oxygen Transfer

The foaming occurrences observed in wastewater treatment plants treating industrial effluents have been attributed to the presence of surfactants from textile effluents by Karsa and Porter (1995), Punmia et al. (1998), OECD (2001), Mara and Horan (2003), Lacasse and Baumann (2004), Tsoler (2004), Wang et al. (2004), Lehr et al. (2005), Myers (2006) and Ruzicka et al. (2009).

The different types of surfactants used in the processing of textile fabrics have been described by Ash and Ash (1997), McCutcheon Division (2001), Elsner (2003), Flick (2003), Ash and Ash (2004), Showell (2005), Myers (2006) and Rosen and Kunjappu (2012):

1. anionic surfactants: the hydrophilic part of the surfactant molecule consists of negatively-charged functional groups such sulphonates ($R-SO_2-O^-$), sulphates (SO_4^{2-}) or carboxylates ($R-CO_2^-$). Anionic surfactants sensitive to water hardness

2. cationic surfactants: the hydrophilic part of the surfactant molecule consists of positively-charged functional groups such quaternary ammonium ions (NR_4^+). Cationic surfactants fasten to the surfaces where they provide softening attributes and anti-static effects

3. non-ionic surfactants: the hydrophilic part of the surfactant molecule does not have any ionic charge. These surfactants find major use in cleaning processes and exhibit high resistance to water hardness.

4. amphoteric surfactants: the ionic charge on the hydrophilic part of the surfactant molecule is controlled by the pH of the bulk liquid phase in which the surfactant is existing. At $pH \geq 7$, they can act as an anionic surfactant and at $pH \leq 7$, the can act as a cationic surfactant

Conflicting findings on the overall effects of foaming attributed to surfactants on O_2 transfer in both fresh and wastewater systems have been reported in previous studies.

According to Judd and Judd (2011), the composition of wastewater, specifically the presence of surfactants, has adverse effects on the size, shape and stability of aeration bubbles. At high concentration, the surfactant molecules are reported to build up on the exterior surface of aeration bubbles thus attenuating the diffusion of O_2 from the gas phase to the liquid phase whilst also decreasing the surface tension. Whilst decreasing the surface tensions translates to an increment in the air – H_2O interfacial area (a), this does not do much to aid O_2 transfer in fine bubble diffusion aeration system since the aeration bubbles are already of a minuscule size and the increase in air – H_2O interfacial area will not have much of a positive effect on O_2 transfer.

Experiments with a plunging jet loop system with a perforated downcomer were conducted to investigate oxygen transfer rate in aqueous solutions of glucose and a low foam surfactant by Fakeeha et al. (1999). At normal temperature and pressure, it is reported that the volumetric O_2 coefficient ($k_L a$) decreases with increasing loading of glucose while it increases with increasing the surfactant concentration.

Masutani (1988) also reported that whilst the increase in surfactant concentration at the air – H_2O interface might result in an increment in the value of a, the adsorption of the surfactants onto the air – H_2O interface results in a greater decrement in the liquid film mass transfer coefficient (k_L) which outweighs the increment in the interfacial area so that the net or overall effect on the volumetric O_2 coefficient ($k_L a$) is a decrement.

Furthermore according to Masutani (1988), the presence of surfactants on the air – H_2O interface results in a decrement in the available surface area for molecular diffusion and also results in the formation of a hydration layer on the interface. Consequently this translates to higher surface viscosity and increased thickness of the interfacial layer, thus increasing the resistance to O_2 transfer.

This is also similar to the findings in the study by Mancy and Okun (1960) and Mancy and Okun (1965) who attempted to describe the decrease in oxygen transfer due the presence of surfactants by stating that:

1. whilst surfactants do not physically compound any resistance to mass transfer, they inhibit hydrodynamic activities on the gas – liquid interface

2. the interfacial film of surfactant molecules forms a viscous hydration layer which decreases the number of sites available for O_2 molecules to diffuse to the water phase

Studies on the effects of surfactants on $k_L a$ in clean water systems by Wagner and Pöpel (1996) state that non-ionic surfactants decreased O_2 transfer more strongly than anionic surfactants and the presence of surfactants reduced the value of $k_L a$ by as much as 55 % of the initial value.

Hebrard (2008) investigated the influence of anionic surfactants on k_L in a clean water system and they observed that k_L decreases with increasing surfactant concentration in which the value of k_L decreased with increasing surfactant concentration until the value of k_L reached asymptotic value.

Conversely for activated sludge systems, different findings have been reported by Sundararajan and Ju (1995) who stated that in activated sludge systems, the adsorption of surfactants on bubble surfaces is a spontaneous process where the surface tension is greatly decreased thus resulting in finer bubbles and values of a interface and in such a way that overall effect was a significant increment in the values of $k_L a$.

The same observations were also reported in the studies by Lynch and Sawyer (1954), Downing et al. (1957) and Eckenfelder (1959), where the computed air – water interfacial area (a) increased with increasing surfactant concentration in such a way this resulted in an overall increment in the values of $k_L a$.

The two-film mass transfer model according to Lewis and Whitman (1924) has been applied to describe gas – liquid interfacial mass transfer in studies by Masutani (1988), Hangos and Cameron (2001), Mueller et al. (2002), Asano (2006), Jakobsen (2008), Clark (2009), Gottschalk et al. (2010) and Theodore and Ricci (2011):

$$\frac{dC}{dt} = k_{\mathrm{L}}a(C^* - C) \tag{2.2.1}$$

where

$\frac{dC}{dt} =$ rate of change in dissolved O_2 concentration, (mg/dm^3/h)

$k_{\mathrm{L}}a =$ volumetric O_2 transfer coefficient, (1/h)

$C^* =$ saturation concentration of dissolved O_2, (mg/dm^3)

$C =$ concentration of dissolved O_2 in the bulk liquid phase, (mg/dm^3)

The saturation concentration of dissolved O_2 (C^*) is the value of the dissolved O_2 in H_2O which at $t = \infty$ h, is in equilibrium with the O_2 concentration in the bulk gas phase (air) as defined by Henry's law:

$$C^* = C_{\text{air phase}}/\mathrm{H} \tag{2.2.2}$$

where

$C_{\text{air phase}} =$ concentration of O_2 in the bulk air phase, (mg/dm^3)

H = Henry's constant, ($dimensionless$)

To compute for $k_{\mathrm{L}}a$, the two-film mass transfer model was integrated between the boundary conditions described by Asano (2006), Jakobsen (2008), Clark (2009), Gottschalk et al. (2010) and Theodore and Ricci (2011):

$$\int_{C_0}^{C} 1/(C^* - C)\, dC = \int_0^t (k_{\mathrm{L}}a)\, dt \tag{2.2.3}$$

This resulted in an integrated form of the model:

$$(C^* - C)/(C^* - C_0) = exp[(-k_{\mathrm{L}}a)t] \tag{2.2.4}$$

where

$C_0 =$ dissolved O_2 in the bulk liquid water phase at $t = 0$ h, (mg/dm^3)

$C =$ dissolved O_2 in the bulk liquid water phase at $t = t$ h, (mg/dm^3)

Through the non-linear least squares estimation method, $C_0, k_L a$ and C^* are estimated as parameters of the best fits of C_{DO} vs. t measurements onto the integrated form of the two-film mass transfer model as described by the American Society of Civil Engineers - Oxygen Transfer Standards Subcommittee (1983).

For wastewater or activated sludge systems where there is dissolved O_2 consumption by microbial populations, the two-film mass transfer model was modified to include an Oxygen Uptake Rate (OUR) parameter by Eckenfelder (1959). This resulted in an unsteady-state dissolved O_2 mass balance:

$$\frac{dC}{dt} = k_L a(C^* - C) - OUR \tag{2.2.5}$$

where

OUR = Oxygen Uptake Rate, (mg/dm^3/h)

Eckenfelder (1959) estimated $k_L a$ through a non-steady-state method under stabilised operating conditions which involved the withdrawal of samples from an activated sludge system at 1 min intervals during periods of aeration (oxygenation) and measuring the dissolved O_2 concentration.

Sampling was continued until a steady-state condition was approached and $k_L a$ was computed through a graphical method involving the unsteady-state dissolved O_2 mass balance. This method involved the drawing of tangents to several points on the curve produced by a plot of C_{DO} vs. t measurements. From these tangents, the value of dC/dt at a corresponding value of C_{DO} was computed.

For batch activated sludge systems, Sundararajan and Ju (1995) described a method to determine $k_L a$ through the dynamic method previously reported by Dang et al. (1977) and Ruchti et al. (1981).

The computed value of $k_L a$ was corrected for the gas residence time, serial resistances of O_2 transfer through liquid diffusion film and the C_{DO} vs. t measurements sensor to yield the true $k_L a$:

$$1/(k_{\mathrm{L}}a\,)_{\mathrm{corrected}} = (1/k_{\mathrm{L}}a\,) - \left(\tau_e - \tau_f - \tau_g\right) \quad (2.2.6)$$

where

$(k_{\mathrm{L}}a\,)_{\mathrm{corrected}}$ = corrected $k_{\mathrm{L}}a$, (1/h)

τ_e = parameter representing the resistance to dissolved O_2 transfer across the measuring dissolved O_2, (h)

τ_f = parameter representing the resistance to dissolved O_2 transfer through the liquid diffusion film, (h)

τ_g = gas residence time, (h)

The YSI 5700 series Dissolved Oxygen (DO) probes have been utilised to conduct C_{DO} vs. t measurements in activated sludge systems by Sundararajan and Ju (1995) and Leung et al. (2006).

The DO probe has inherent response dynamics errors associated with it which are attributed to the design of the instrument and such errors can lead to inaccurate computations of the O_2 $k_{\mathrm{L}}a$ from C_{DO} vs. t data as reported by Kok and Zajic (1975) and Spanjers and Olsson (1992).

Philichi and Stenstrom (1989) have modelled the response time delay of DO probes as a first order dynamic response:

$$\frac{dC_{\mathrm{p}}}{dt} = (C - C_{\mathrm{p}})/\tau \quad (2.2.7)$$

where

C_{p} = dissolved O_2 concentration reading recorded by the DO probe, (M/L^3)

C = actual dissolved O_2 concentration, (M/L^3)

t = time, (T)

τ = first-order time constant (T)

The first order time constant (τ) is described by Spanjers and Olsson (1992) as a measure of the time delay of the DO probe in its dynamic response to changes in dissolved O_2 concentration and serves as an indicator for the fouling of the DO probe membrane or other defects on the dissolved O_2 sensor.

Synopsis

With respect to the mathematical quantification of the effect of surfactant effluents on oxygen transfer in receiving municipal activated sludge systems, not much has been discussed in existing literature, specifically on the use and calibration of Clark dissolved oxygen instrumentation to accurately measure C_{DO} vs. t data and quantifying the extent of oxygen transfer through gas – liquid interfacial mass transfer models.

Whilst the foaming occurrences that have been observed in the aeration basins vessels of municipal activated sludge receiving textile effluents have been attributed to the presence of surfactants by various authors: Lehr et al. (2005), Myers (2006) and Ruzicka et al. (2009), not much was discussed on measurements of C_{DO} vs. t in the presence of the observed foaming and there were no subsequent predictions on the effect the foam had on oxygen transfer from the gas phase (air) to the liquid phase (H_2O).

The conflicting views on the effect of surfactants on oxygen transfer in fresh and wastewater systems by Judd and Judd (2011) and Fakeeha et al. (1999), only provide qualitative speculations on the effect of increasing surfactant concentration on volumetric O_2 coefficient ($k_L a$) but they do not provide descriptions on the systematic measurement of C_{DO} vs. t data and computation of $k_L a$ in the presence of varying concentrations of surfactants.

The limited number of publications on the effect of surfactants on $k_L a$ mostly made use of clean or fresh water systems and analysed the effects of increasing anionic and non-ionic surfactant concentrations on both k_L and a as separate entities as opposed to taking measurements of C_{DO} vs. t data sets and predicting $k_L a$ as a single entity from interfacial mass transfer models as exhibited in the studies by Masutani (1988), Wagner and Pöpel (1996) and Hebrard et al. (2008).

The few existing studies in which there was the employment of the methodology of utilising Clark dissolved oxygen instrumentation for C_{DO} vs. t and computing $k_L a$ as a parameter of mass transfer model through non-linear least squares regression methodology as prescribed by the American Society of Civil Engineers - Oxygen Transfer Standards Subcommittee (1983) have been published historically by Masutani (1988), Hangos and Cameron (2001), and more recently, by Gottschalk et al. (2010) and Theodore and Ricci (2011).

However in all these studies, the estimates of $k_L a$ that were computed from non-linear fits of C_{DO} vs. t data sets onto the Lewis-Whitman interfacial mass transfer model were only confined to clean and fresh water systems and did not extend to municipal activated sludge systems where there is dissolved oxygen consumption by active microbial populations.

The only study in which the estimation of $k_L a$ was extended to activated sludge systems was reported by Eckenfelder (1959) and this study, there was the incorporation of dissolved oxygen uptake by active microbial populations into the the Lewis-Whitman two-film mass transfer model so that the modified form includes Oxygen Uptake Rate (OUR) as a parameter.

In as much as the study by incorporated OUR as a parameter of the Lewis-Whitman interfacial mass transfer model, it did not compute estimates of $k_L a$ through non-linear fits of C_{DO} vs. t data sets onto the Lewis-Whitman interfacial mass transfer model as prescribed by the American Society of Civil Engineers - Oxygen Transfer Standards Subcommittee (1983).

In all of the receiving municipal wastewater treatment plants that were selected as cases for the study (Umbilo, Mariannridge and Verulam wastewater treatment plants), the foaming occurrences attributed to the presence surfactants in textile effluents were observed in all of the aerated bioreactors constituting the activated sludge processes and the proliferation of foam occurred during the oxygenation phases of the aeration processes.

The limited existence of exhaustive historical publications and studies on the use and calibration of Clark dissolved oxygen instrumentation to accurately measure C_{DO} vs. t data and extending the modified form of the Lewis-Whitman interfacial mass transfer model according to Eckenfelder (1959) to activated sludge systems for the computation of $k_L a$ estimates through the non-linear least squares regression method led to the undertaking of this study.

The investigation required the development of an analytical protocol through which attempts would be undertaken to mathematically quantify the effects of surfactant effluents on oxygen transfer through non-linear least squares regression methods.

This would then shape the principal thrust of the study which was concentrated on the application and examination of the developed analytical protocol to evaluate if indeed the protocol could be utilised to provide an accurate and precise methodology which mathematically quantifies the effects of surfactant effluents on oxygen transfer in receiving municipal activated sludge systems.

2.3 Biodegradability of Surfactant Effluents

Fairly uniform extents of biodegradability of pure surfactants have been reported in Material Safety Data sheets provided by the surfactant manufacturers.

A non-ionic secondary alcohol ethoxylate surfactant branded TERGITOL™ 15-S-15 by the Dow® Chemical Company has a reported general structural formula of $C_{12-14}H_{25-29}O[CH_2CH_2O]_xH$ and the biodegradability assessed through the Soap and Detergent Association's semi-continuous activated sludge test method is $\geq$ 90 % (The Dow® Chemical Company, 2009).

A detergent synthesised from a blend of sodium capryl sulphonate and linear alcohol ethoxylates is manufactured by Parish Supply Corp. has proprietary structural formula and has a reported biodegradability of $\cong$ 100 % (Parish Supply Corp., 2012)

Biodegradability assessments reported for a proprietary blend of non-ionic surfactants branded Ivey-sol® by Ivey International Inc. resulted in $\cong$ 90 % biodegradation of the product after 28 days using the Modified OECD Screening Test (OECD Test No.301 E) and $\cong$ 70 % biodegradation of the product after 28 days using CO_2 Evolution Test (Modified Sturm Test, OECD Test No. 301 B) (Ivey International Inc., 2011).

A more expository assessment on the biodegradability of pure surfactants was conducted by Talmage (1994) through a study on the environmental and human safety of alcohol ethoxylates and alkylphenol ethoxylates surfactants.

The study reported that alcohol ethoxylate surfactants underwent rapid primary and ultimate biodegradation in activated sludge systems and the test methods employed in the assessment involved addition of a specific quantity of surfactant to an activated sludge medium and biodegradation of the surfactant was computed from the final substrate concentration at the of the experiment. The initial and final surfactant concentrations were estimated through the Chemical Oxygen Demand (COD) test according to the Standard Methods described by the American Public Health Association, American Water Works Association (1995).

The study also reported on the extent of surfactant removal in municipal activated sludge plants presumably through both adsorption and onto the sludge and biodegradation and for influent surfactant concentrations of up to 10 mg/dm^3, the removal estimates were between 90% and 94%.

Investigations on the biodegradability of surfactants from textile effluents have been previously conducted by Goudar et al. (1999) and this study assessed the biodegradability of Sorbitan Monooleate (non-ionic surfactant) and Sodium Dodecyl Sulphate (anionic surfactant), in an activated sludge system.

A previous study by Sykes et al. (1979) was based on a primary linear alkyl ethoxylate non-ionic surfactant branded Neodol 45-7 and the investigation reported that after an activated sludge plant had become acclimatised to the surfactant effluent, $COD_{\text{soluble, total}}$ removal efficiencies were approximately 80%.

Reemtsma and Jekel (2007) describe the biodegradation of surfactants under aerobic conditions as a step-wise process in which the first stage of biodegradation is termed the primary biodegradation process in which the surfactant effluents lose their surface active and environmental toxicity properties. The same is reported by Knepper et al. (2003) who also describe the aerobic biodegradation of surfactants

According to Karsa and Porter (1995) and Lichtfouse (2009), most surfactant effluents are biodegradable under aerobic conditions and the biodegradation pathway of typical industrial surfactants such as linear alkylbenzene sulphonates (LAS) is described by four stages:

1. oxidative conversion of the methyl groups (CH_3-) of the alkyl chain into a carboxyl group through a process termed $\omega -$ oxidation

2. oxidative shortening of the alkyl chain by two carbon units through a process termed $\beta -$ oxidation

3. oxidative ring splitting

4. splitting of the carbon-sulphur bond (sulphate liberation)

Respirometry has been applied by Mohan et al. (2006) to investigate the biodegradability of two surfactants branded Triton X-100 and Rhamnolipid under aerobic, nitrate-reducing, sulphate-reducing, and anaerobic conditions. Further investigations by Mohan et al. (2006) also used respirometry to estimate the biodegradation coefficients (biokinetics) of Triton X-100 and Rhamnolipid under aerobic, nitrate-reducing, sulphate-reducing, and anaerobic conditions and both studies showed that surfactants were biodegradable under aerobic conditions.

Carvalho et al. (2000) evaluated the oxygen uptake response of activated sludge to the presence of non-ionic synthetic surfactants using closed respirometry techniques which were complemented with titrimetric surfactant measurements and Total Organic Carbon (TOC) experiments to assess the primary and ultimate biodegradation of the surfactant.

The findings from the study showed respirograms which had multiple peaks for non-acclimatised active biomass. For acclimatised sludge, shorter biodegradation times and the respirograms with single oxygen uptake rate peaks were observed.

Consequently, the findings from the study by Carvalho et al. (2000) led to the development of a model to describe activated sludge acclimatisation to a non-ionic surfactant by Carvalho et al. (2001). The fitting of respirometric experimental data from experiments was fitted onto the model was using a wastewater dynamic modelling and simulation platform through which the model's kinetic and stoichiometric parameters were estimated and the platform was also used to calibrate the model.

Respirometry experiments have been previously used in the analysis of activated sludge processes to describe the kinetics of the biochemical reactions which take place in aerated wastewater treatment systems by Spanjers and Vanrolleghem (1995) and Vanrolleghem et al. (1999).

According to Suschka and Ferreira (1986) and Hagman and Jansen (2007) respirometry experiments provide useful kinetics and stoichiometry data on biodegradation of organic substrates by activated sludge systems. The respirograms generated from such experiments show the variation of the oxygen uptake rate (OUR) of microbial species in the activated sludge with time.

As reported by van Haandel and van der Lubbe (2007), the endogenous respiration rate (OUR_{end}) represents oxygen uptake by the microbial species in the absence of biodegradable substrates and under these aerobic conditions, a reduction in the volatile solids concentration (VSS) with a concurrent consumption of oxygen is observed and these processes are attributed to the oxidation of microbial protoplasm so that there is a release of the energy required to sustain aerobic cell functions.

The exogenous oxygen uptake rate (OUR_{exo}) is a direct representation of rate of soluble substrate degradation and subsequent microbial growth. As such, respirometry finds extensive use in evaluating the behaviour of activated sludge systems in the presence of organic substrates as described Spanjers et al., (1998).

The kinetics of the biochemical processes which take place in the activated sludge system during the consumption and degradation of organic substrates by the active biomass have been described in activated sludge models by Henze et al. (1987), Gujer et al. (1999) and Henze et al. (2000).

Previous studies by Spanjers and Vanrolleghem (1995) combined respirometry experiments with the IAWQ Activated Sludge Model No. 1 (ASM1) according to Henze et al. (1987) to formulate a procedure to estimate wastewater characteristics, compute biodegradation kinetic parameters for heterotrophic and autotrophic processes and simultaneous compute decay coefficients for heterotrophic and autotrophic microbial populations.

Brouwer et al. (1998) also applied respirometry experiments to obtain activated sludge kinetics and wastewater characteristics and a modified version of the ASM1 that describes the oxygen uptake rate of the nitrification process to identify the state variables and model parameters for the activated sludge process.

Damayanti et al. (2010) assessed the biodegradability of a palm oil effluent in a continuous stirred tank reactor (CSTR) using open respirometry methods and the ASM1 to compute the kinetic parameters of the biodegradation processes.

More recently, Mhlanga (2009) combined batch respirometry experiments with the IAWQ Activated Sludge Model No.3 (ASM3) according to Gujer et al. (1999) to model and predict the control parameters for eThekwini Municipality's Mariannridge wastewater treatment plant.

Schwarz et al. (2003) and Oliveira et al. (2009) also applied the combination of batch respirometry experiments and dynamic modelling of activated sludge processes through the ASM3 to predict the consumption of organic carbon in a batch activated sludge system.

According to Cokgor et al. (2006), the area under the curve during exogenous respiration in a respirogram represents the amount of oxygen consumed by the respiring microbial cells and this directly represents the different fractions of substrate that are consumed by the biomass. The ASM3 is then applied to interpret the respirogram and make estimates of the stoichiometric and kinetic coefficients for the biodegradation process.

More elaborate interpretations of respirometry experiments for estimating biodegradability of an effluent have been provided by Vanrolleghem et al. (2003) and in their study, they report that from the same respirogram (plot of OUR vs. t), the following can estimated from the area under the curve as shown in Fig 7.:

1. the amount of the readily biodegradable substrate consumed: $S_S(1 - Y_H)$

   provided the following conditions are satisfied prior to the running of the experiment:

   (a) heterotrophic yield coefficient (Y_H) is known

   (b) the initial substrate to biomass ratio (S_0/X_0) is known

   (c) suppression of nitrification processes

2. the amount of the slowly biodegradable substrate consumed: $X_S(1 - Y_H)$

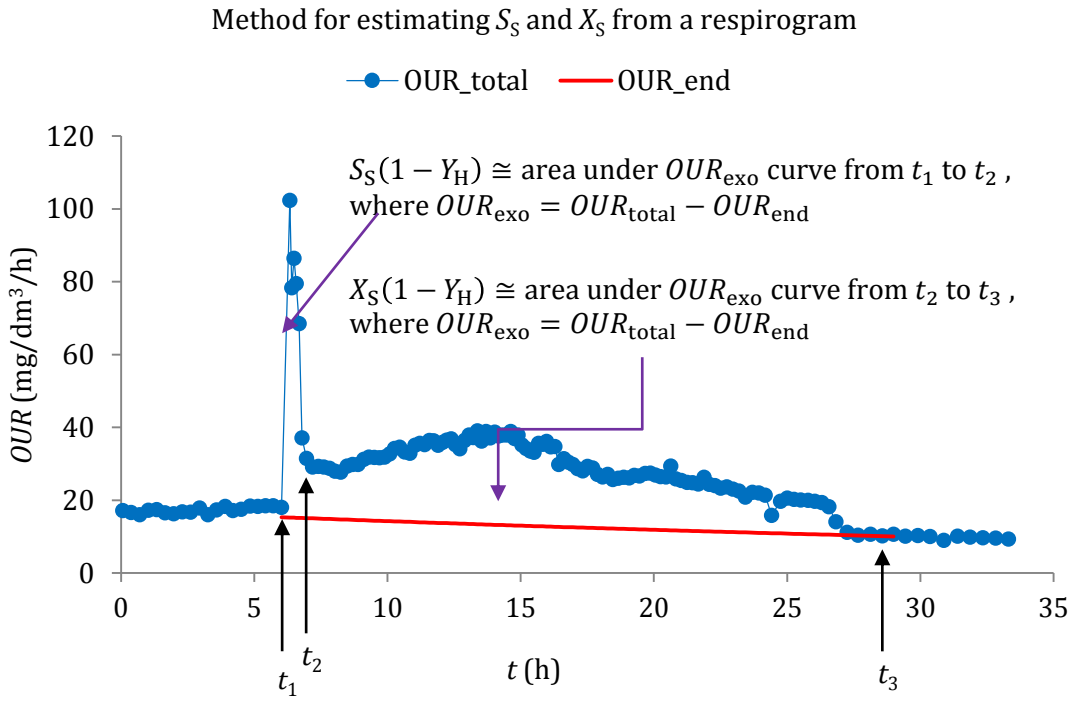

Fig.7: Method for computing S_S and X_S from the area under a respirogram

The same method was employed by Fall et al. (2011) to assess the divergence between respirometry experiments and physicochemical methods in determining the COD fractions in municipal wastewater. In their study, the area under the OUR_{exo} vs. t curve took into account dilution effects from the addition of the substrate and amount of readily biodegradable substrate consumed by the activated sludge was determined as shown in Fig.7.

Vollertsen and Hvitved-Jacobsen (2002) assessed the biodegradability of a wastewater through respirometry experiments and the COD fractionation method and their study computed the amounts of readily and slowly biodegradable substrates consumed in a bioreactor by identifying the areas under the respirogram representing the endogenous and exogenous respiration phases of the experiment.

The exogenous respiration phase was further segmented into the readily biodegradable substrate consumption phase and slowly biodegradable substrate consumption phase and respective amounts of substrate consumed were computed as shown in Fig.7, where $Y_H = 0.70$.

Approximating material balances in which OUR was correlated to the rate of soluble biodegradable substrate consumption (dS_S/dt) and biomass growth rate (dX_H/dt) was reported by Young (1999):

$$OUR = dS_S/dt - dX_H/dt \quad (4.1.3.4.5)$$

$$\because dX_H/dt = Y_H\, dS_S/dt$$

$$\Rightarrow OUR = dS_S/dt - Y_H\, dS_S/dt$$

$$OUR = dS_S/dt(1 - Y_H)$$

$$OUR = dS_S/dt(1 - Y_H)$$

$$\therefore OUR\ dt = dS_S(1 - Y_H)$$

where

$OUR\ dt \cong$ area under the OUR_{exo} vs. t curve

Numerical integration methods are employed to compute the area under the curve and the various methods available have been discussed by Abramowitz and Stegun (1972) and their algorithmic implementation was encoded by Press et al. (1992) and Press et al. (1996).

Synopsis

With respect to the biodegradability of surfactant effluents under aerobic conditions, the various manufacturers of surfactants provide numerical estimates of the extent to which their products are biodegradable as described by The Dow® Chemical Company (2009) and Parish Supply Corp. (2012) but there are limited discussions on the methodologies that are employed to compute the reported biodegradability. The few notable methodologies that are employed compute biodegradability of proprietary surfactant products are cited by Ivey International Inc. (2011) and these are the Modified OECD Screening Test (OECD Test No.301 E) and the using CO_2 Evolution Test (Modified Sturm Test, OECD Test No. 301 B) but the shortcomings of both methodologies are that they result in markedly different computed extents of biodegradability and for both methods, biodegradability is reported after 28 days.

Since the hydraulic residence time of the Verulam municipal wastewater treatment plant selected as a case for this study is far less than 28 days $\left(t_{\text{hydraulic retention}} = 6\ \text{h}\right)$, both the Modified OECD Screening Test (OECD Test No.301 E) and the using CO_2 Evolution Test (Modified Sturm Test, OECD Test No. 301 B) reported by Ivey International Inc. (2011) are not suitable for assessing the biodegradability of surfactant effluents in receiving municipal activated sludge systems.

A much more fitting and suitable analytical protocol for determining biodegradability of surfactants in an activated sludge system was discussed by Talmage (1994) and the study computed the biodegradability of pure surfactant products contacted with activated sludge through measurements of the initial and final soluble COD composition of a surfactant load prior to and after contacting the surfactant load with an activated sludge medium.

In the study by Talmage (1994), all measurements of soluble COD were computed according to the Standard Methods described by the American Public Health Association, American Water Works Association (1995) and whilst this is prescribed methodology for measuring s soluble COD, this analytical protocol has limitations in fully assessing biodegradability because it does not compute the corresponding microbial growth resulting from the assimilation of the substrates that are biodegraded.

More expository methods for investigating the biodegradability of surfactants under aerobic conditions through the use of Clark dissolved oxygen instrumentation to measure C_{DO} vs. t data in the activated sludge systems and computing the variation of oxygen uptake rate (OUR) of the microbial species in the activated sludge with time and correlating that to the assimilation of the substrates that are biodegraded and the resulting microbial growth have been described by Carvalho et al. (2000), Carvalho et al. (2001) and Mohan et al. (2006).

This methodology of computing the variation of oxygen uptake rate OUR vs. t in activated sludge systems has been termed respirometry and is fully described by Spanjers and Vanrolleghem (1995) and Vanrolleghem et al. (1999) and has found extensive use in computing the biodegradability of various types of effluents in activated sludge systems as described and discussed by Spanjers and Vanrolleghem (1995), Brouwer et al. (1998), Schwarz et al. (2003), Cokgor et al. (2006), Oliveira et al. (2009) and Mhlanga (2009).

However in most of the studies in which respirometry was employed to compute biodegradability, the analytical protocol involved the combination of computing OUR vs. t measurements and fitting the data onto various forms of according to Henze et al. (1987), Gujer et al. (1999) and Henze and International Water Association Task Group on Mathematical Modelling for Design and Operation of Biological Wastewater Treatment (2000).

Whilst the technique of computing OUR vs. t data makes use of Clark dissolved oxygen instrumentation and is inevitably in synchrony with the thrust of the preceding study intending to develop an analytical protocol and examining the method to determine if indeed it can provide reliable means of quantifying the effects of surfactant effluents on oxygen transfer in receiving municipal activated sludge systems, predicting the resulting biodegradability of such effluents through the use of activated sludge models as described in existing literature was outside the scope of this study.

Instead, other methods were to be developed and examined to determine if the developed analytical protocol could precisely and accurately predict the biodegradability of surfactant effluents in receiving municipal activated sludge systems from Clark dissolved oxygen instrumentation measurements of OUR vs. t data only without the use of activated sludge models.

Since comprehensive interpretations of OUR vs. t data for estimating biodegradability of any effluent received by an activated sludge system without involving the use of activated sludge models have been described by Young (1999) and Vanrolleghem et al. (2003), the main thrust of this study was shaped by need to make use of such methods in developing and testing the analytical protocol to determine if through the same respirometry experiment, the methodology would provide accurate and precise mathematical quantifications of the effects of surfactant effluents on oxygen transfer in receiving municipal activated sludge systems and simultaneously provide predictions of the subsequent extents of biodegradability of such effluents.

3. OBJECTIVES

The principal objective of the study was to formulate an analytical protocol and evaluate the aptness or the appropriateness of the formulated methodologies in predicting the treatability of industrial effluents received by municipal wastewater treatment plants.

The various methodologies constituting the analytical protocol were to be designed around the use of open respirometry apparatus employing the UCT DO/OUR meter because this was the instrument of choice selected by eThekwini Municipality. This implied that the scope of this study neither required evaluating the suitability of other kinds of apparatus or nor did it require the designing of new apparatus to evaluate the treatability of industrial effluents received by municipal wastewater treatment plants.

A textile effluent with a known composition was selected as a case for the investigation.

Based on the scope of the project defined in the Introduction section of this study (Section 1.), specific objectives of the individual segments of the study described in Sections 1.1, 1.2 and 1.3 are respectively provided in Sections 3.1, 3.2 and 3.3.

3.1 Soluble Dye Effluents Decolourisation

The primary objective of the investigation was to develop methodologies and evaluate the suitability of the formulated methods in accurately quantifying the extent to which a laboratory-scale activated sludge system would be capable of decolourising a soluble dye effluent with a known initial concentration.

From the hypothesised mechanism through which the soluble dye effluent would be decolourised (biosorption), the realisation of the overall objective of the study was dependent on the establishment of a calibration curve correlating $C_{\text{dye, solution}} = f(A)$, where $A =$ light absorbance of the dye solution measured by a UV-Vis spectrophotometer at the dominant wavelength ($\lambda_{\max}$) computed from the light absorbance spectra of the stock dye effluent solution prior to contacting with activated sludge and $C_{\text{dye, solution}} =$ soluble dye concentration remaining in solution after adsorption of the dye onto the activated sludge with which is it contacted with.

With the aid of the calibration curve, subsequent estimates of $C_{\text{dye, solution}}$ vs. t after contacting the dye effluent with the activated sludge system would then be computed from the equivalent measurements of A vs. t

3.2 Effect of Surfactant Effluents on Oxygen Transfer

The primary objective of the investigation was the development of an analytical protocol and evaluating if the developed analytical methods could be employed to accurately provide a mathematical quantification of the effects of a surfactant effluent on oxygen transfer in a laboratory-scale activated sludge system.

Quantification of the effects of the surfactant effluent on oxygen transfer would be described by computed estimates of $k_{\text{L}}a$ from C_{DO} vs. t, where $k_{\text{L}}a =$ volumetric O_2 transfer coefficient, $(1/\text{h})$ and $C_{\text{DO}} =$ dissolved oxygen concentration, (mg/dm^3).

From the designed analytical protocol, the realisation of the overall objective of the study was dependent on the following factors:

1. synthesising the surfactant so that its composition and concentration approximates the actual textile effluent at the point of discharge to the receiving municipal activated sludge system

2. applying standard titrimetric procedures to characterise the synthetic textile effluent in terms of total soluble COD concentration ($COD_{\text{soluble, total}}$)

3. applying the prescribed methodologies according to the Standard Methods described by the American Public Health Association, American Water Works Association (1995) for the estimation of the VSS concentration of the activated sludge prior to contacting with the surfactant effluent

4. use the operating data from the receiving municipal activated sludge system to design the laboratory experiment

5. pre-conditioning the laboratory-scale activated sludge system so that:

(a) all residual organic substrates present in the sludge at the time of sampling are biodegraded prior to contacting with the surfactant effluent

(b) all nitrification processes are suppressed since they tend to elevate the overall uptake of dissolved O_2 thus distorting the C_{DO} vs. t measurements from which $k_{\mathrm{L}}a$ estimates are computed

6. setting up and calibrating instrumentation through which accurate C_{DO} vs. t measurements would be logged without disrupting the activated sludge processes prior to and after dosing the activated sludge system with a load of surfactant effluent

7. formulating robust numerical methods through which $k_{\mathrm{L}}a$ estimates would computed from C_{DO} vs. t measurements

3.3 Biodegradability of Surfactant Effluents

The primary objective of the investigation involved extending the experimental apparatus and methods constituting the analytical protocol designed in Section 3.2 in combination with suitable numerical methods and evaluating if the amalgamation could be employed to accurately estimate the biodegradability in a laboratory-scale activated sludge system of the same surfactant effluent load whose effects on oxygen transfer are evaluated in Section 3.2.

Since assessments on biodegradability were inferred from OUR vs. t measurements which were simultaneously logged together with C_{DO} vs. t measurements through the same experimental run, realisation of the overall objective of this study was dependent on similar factors described in Section 3.2.

The computation of biodegradability required quantifying the mass of total soluble COD $\left(m_{COD_{\mathrm{soluble,\ total}}}\right)$ in the surfactant effluent and estimating the mass of soluble biodegradable substrate $\left(m_{S_{\mathrm{S}}}\right)$ consumed by the activated sludge:

$$biodegradability = \left(\frac{m_{S_{\mathrm{S}}}}{m_{COD_{\mathrm{soluble,\ total}}}}\right) \times 100\%$$

4. METHODOLOGY

For all three segments of the study described in Sections 1.1, 1.2 and 1.3, the activated sludge contacted with the soluble dye and surfactant effluents was sampled from the same wastewater treatment plant and a uniform volume of activated sludge ($V_{\text{sludge}} = 1.5\ \text{dm}^3$) was employed for all experiments so that comparable evaluations on the suitability and appropriateness of the analytical methods that were employed in assessing the capabilities of the same activated sludge system in treating different components of the same effluent could be established.

With respect to the investigation on the decolourisation of soluble dye (Section 1.1), the same soluble dye effluent volume ($V_{\text{dye}} = 0.5\ \text{dm}^3$) and stock soluble dye effluent concentration ($C_{\text{dye, stock}} = 0.06\ \text{g/dm}^3$) were respectively contacted with an activated sludge system for the same residence time ($t_{\text{R}} = 2\ \text{h}$) in the absence and presence of a readily biodegradable substrate to effectively assess the effects of microbial growth process on the decolourisation of the dye effluent.

With respect to the investigations described in Sections 1.2 and 1.3 of the study, the respective experimental data sets (C_{DO} vs. t and OUR vs. t measurements) were simultaneously logged from the same experiment.

Mathematical quantification of the effects of the surfactant effluent on oxygen transfer required computing estimates of the volumetric oxygen transfer coefficient ($k_{\text{L}}a$) as a measure of the transfer of oxygen from air to the water phase of an activated sludge system and this required the use of the Levenberg-Marquardt algorithm to estimate respective best fit values of $k_{\text{L}}a$ as parameter from non-linear fits of C_{DO} vs. t data onto a modified form of the Lewis-Whitman two-film interfacial mass transfer model.

Estimates of the biodegradability of the textile effluent as described in Section 1.3 were computed as a function of the difference between the mass of total soluble COD in the surfactant effluent load $\left(m_{COD_{\text{soluble, total}}}\right)$ and the mass of soluble biodegradable substrate in the surfactant load consumed by the activated sludge $\left(m_{S_{\text{S}}}\right)$ after contacting the surfactant effluent load with activated sludge for $t = t_{\text{R}}$ h.

Estimating both $m_{COD_{\text{soluble, total}}}$ and $m_{S_{\text{S}}}$ required a methodology which combined:

1. standard laboratory titrimetric analytical methods

2. respirometric experiments in which OUR vs. t measurements were logged in the absence and presence of the surfactant effluent for OUR_{end} vs. t and OUR_{exo} vs. t measurements respectively

3. computing estimates of m_{S_S} from the area under the OUR_{exo} vs. t curve

The specific hypotheses, materials and methods and analytical methods employed in each segment of the study as described in Sections 1.1, 1.2 and 1.3 are respectively provided in Sections 4.1, 4.2 and 4.3.

With respect to the study on investigating the decolourisation of the soluble dye effluent s in the activated sludge system, the materials and apparatus consisted of:

1. a synthesised reactive dye effluent discharged to a selected receiving municipal wastewater treatment plant and of a known mass concentration

2. a laboratory-scale activated sludge system, where the sludge was sampled from municipal activated sludge system to which the dye effluent was discharged

3. a centrifuge system which separated the sludge solids from the dye effluent remaining in solution after contacting the laboratory-scale activated sludge system with the soluble dye effluent

4. UV−Vis spectrophotometer for estimating the amount dye remaining in solution after contacting the laboratory-scale activated sludge system with the soluble dye effluent

5. a readily biodegradable substrate was dosed into the laboratory-scale activated sludge system to simulate microbial growth processes as it would have been at the actual municipal wastewater treatment plant

The study on assessing the effect of surfactants on oxygen transfer and their subsequent biodegradability in the activated system made use of the following materials and apparatus:

1. a synthesised surfactant effluent discharged to a selected receiving municipal wastewater treatment plant and of a known mass concentration

2. a laboratory-scale activated sludge system, where the sludge was sampled from municipal activated sludge system to which the surfactant effluent was discharged

3. an open respirometry system employing the use of the UCT DO/OUR meter to simultaneously make measurements of C_{DO} vs. t and compute corresponding estimates of OUR vs. t through the same experiment

4. suitable mathematical methods for quantifying:

   (a) the extent of oxygen transfer into the activated sludge system through analyses of C_{DO} vs. t measurements

   (b) subsequent biodegradability of the surfactant effluent through computations of oxygen uptake rate (OUR) of the active microbial species in activated sludge system after contacting with the surfactant effluent

The major analytical methodologies that would be employed in the various segments constituting the overall study included:

1. characterisation of the activated sludge through quantifications of the mass of solids per unit volume of sludge by computing estimates of the volatile suspended solids (VSS) concentration in the activated sludge

2. computing food-to-micro-organism (F/M) ratio for the receiving municipal wastewater treatment plant

3. computing the mass concentration of soluble biodegradable substrates dosed into the activated sludge system through measurements of soluble COD concentration

4.1 Soluble Dye Effluents Decolourisation

4.1.1 Hypothesis

With respect to this study, it was hypothesised that analytical protocol developed for the investigation was adequately suitable in exhibiting that soluble dye effluent decolourisation does take place in the activated sludge system and biosorption was the postulated decolourisation mechanism. It was further proposed that batch adsorption tests in which samples of the soluble dye effluent were contacted with activated sludge were adequate to determine equilibria and kinetic parameters for predicting decolourisation of the soluble dye effluent in a receiving wastewater treatment plant.

It was also postulated that since the composition of the synthesised soluble dye effluent was known and the dye effluent only contained a single dye compound in solution (single adsorbate in solution system), the adsorption mechanism through which decolourisation would take place could be described with an adsorption model to give a mathematical characterisation of the adsorption equilibrium.

For the single adsorbate in solution system, it was hypothesised that the relationship between the interfacial adsorbate concentration on the solution – adsorbent interface and adsorbate concentration in solution would follow the linear adsorption isotherm defined in Equation 2.1.2 according to LeVan et al. (1999).

From the postulated decolourisation mechanism, it was further hypothesised that since microbial growth processes occur in the activated sludge system in the presence of biodegradable substrates, the cumulative mass of soluble dye absorbed would increase with the occurrence of microbial growth and contact time.

4.1.2 Materials and apparatus

4.1.2.1 Dye effluent

Procion Red H−E7B reactive dye effluent discharged to the Umbilo wastewater treatment plant by Dyefin Textile Factory was selected for the study. The molecular structure of Procion Red H-E7B dye has been previously illustrated by García-Montaño et al. (2006).

A stock dye effluent concentration of $C_{\text{dye, stock}} = 0.06\ \text{g/dm}^3$ was selected for the study and the synthesis of the dye effluent is provided in Appendix A.1.1.

4.1.2.2 Activated sludge system

The laboratory-scale activated sludge system consisted of a $2\ \text{dm}^3$ glass vessel in which $1.5\ \text{dm}^3$ of activated sludge was contacted with $0.5\ \text{dm}^3$ of dye effluent.

The sludge contacted with the dye effluent was sampled on the 24th of January 2009 from the aeration tank at eThekwini Municipality's Umbilo wastewater treatment plant. At the time of sampling of activated sludge, the local textile industry was at full production capacity.

The bioreactor was an extended aeration activated sludge system under continuous agitation by a magnetic stirrer. As it would be at the actual municipal wastewater treatment, the laboratory-scale activated sludge system was operated at ambient temperature without any form of temperature control applied to it and the pH of the reactor contents was monitored during each experimental run and maintained at 7 pH units.

4.1.2.3 Centrifuge

Samples withdrawn from the activated sludge system were centrifuged to separate the sludge solids from the dye effluent remaining in solution prior to spectrophotometric analysis. For such a purpose, the Z 323 table-top centrifuge manufactured by HERMLE Labortechnik was utilised.

4.1.2.4 Spectrophotometer

Analyses for the amount dye remaining in solution after biosorption were conducted using the Merck Spectroquant® UV−Vis Pharo™ 300 spectrophotometer. The spectrophotometer measured visible light absorbance of a sample through a 10 mm cuvette over a wavelength range of 190 nm $\leq \lambda \leq$ 1 000 nm.

4.1.2.5 Readily biodegradable substrate

To simulate microbial growth processes in the laboratory-scale activated sludge system as it would have been at the actual municipal wastewater treatment plant (where there is a continuous flow of biodegradable organic substrates which translate to growth of microbial species), a readily biodegradable substrate was dosed into the activated sludge system.

The readily biodegradable substrate was synthesised from dissolving $CH_3COONa_{(s)}$ in distilled H_2O as described in Appendix A.1.2.

4.1.3 Analytical protocol

4.1.3.1 Activated sludge characterisation

The mass of solids per unit volume of sludge were quantified through estimates of the volatile suspended solids (VSS) concentration according to the Standard Methods described by the American Public Health Association, American Water Works Association (1995).

The procedures for computing VSS estimates for the activated sludge used in the investigation are provided in Appendix A.2.1.

4.1.3.2 Determination of the dominant wavelength

The dominant wavelength ($\lambda_{\max}$) was computed from the light absorbance spectra generated by the spectrophotometer for analyses of the Procion Red H-E7B dye effluent at the concentration of the stock dye effluent, $C_{\text{dye, stock}} = 0.06$ g/dm^3.

The value of λ corresponding to the maximum light absorbance peak observed over a wavelength range of 190 nm $\leq \lambda \leq$ 1 000 nm in the visible spectrum was equivalent to ($\lambda_{\max}$).

The light absorbance spectrum from which ($\lambda_{\max}$) was computed is provided in Appendix A.2.2.

4.1.3.3 Calibration curve for the correlation between dye effluent concentration and light absorbance

A calibration curve quantifying $C_{\text{dye, solution}} = f(A)$ was constructed from light absorbance measurements that were made for initial dye effluent concentrations at the instant when a known volume of the stock dye solution was contacted with the activated sludge system.

The initial dye solution concentration after being charged into the activated sludge system was estimated from diluting a selected volume of the stock dye solution with the resulting volume of supernatant $(V_{\text{supernatant}})$ extracted from the volume of activated sludge (V_{sludge}) which the stock dye solution would be contacted with to result in $V_{\text{R}} = 2$ dm^3.

For the construction of the calibration curve, the volumes of the stock dye effluent and the corresponding volumes of activated sludge which the dye effluent was contacted with are shown in Table 1:

Table 1: Volumes of the stock dye effluent contacted with corresponding volumes of activated sludge

V_{dye} (dm^3)	V_{sludge} (dm^3)
0.20	1.80
0.30	1.70
0.40	1.60
0.50	1.50
0.60	1.40
0.70	1.30
0.80	1.20

The initial dye effluent concentration after dilution was computed as follows:

$$C_{\text{dye, initial}} = m_{\text{dye, initial}}/V_{\text{total}} \qquad (4.1.3.3.1)$$

where

$C_{\text{dye, initial}}$ = dye effluent concentration after dilution with supernatant, (g/dm^3)

$m_{\text{dye, initial}} = C_{\text{dye, stock}} \times V_{\text{dye}}$ = mass of dye in stock dye effluent prior to dilution with supernatant, (g)

$C_{\text{dye, stock}}$ = concentration of the stock dye effluent = $0.06\ \text{g/dm}^3$

V_{dye} = volume of stock dye effluent prior to dilution with supernatant from the activated sludge, (dm^3)

$V_{\text{total}} = V_{\text{dye}} + V_{\text{supernatant}}$ = total volume of liquid in the activated sludge system, (dm^3)

From the plot of $C_{\text{dye, initial}}$ vs. A, where A = light absorbance of the dye effluent after dilution with supernatant, the correlation between $C_{\text{dye, solution}}$ vs. A was computed through the least squares linear regression method.

4.1.3.4 Dosing of activated sludge system with readily biodegradable substrate

To approximate the actual conditions at the municipal wastewater treatment plant where there is continuous loading of biodegradable organic substrates which result in microbial growth, the laboratory activated sludge system was continuously dosed with CH_3COOH.

The concentration of the CH_3COOH dosed into the batch activated sludge system was derived from:

1. food-to-micro-organism (F/M) ratio estimated for the receiving municipal wastewater treatment plant

2. COD of the CH_3COOH substrate

The stoichiometric equation representing the biodegradation of CH_3COOH by activated sludge is as follows:

$$CH_3COOH + 2O_2 \xrightarrow{aerobic\ biodegradation} 2CO_2 + 2H_2O \qquad (4.1.3.4.1)$$

Since the readily biodegradable substrate was a pure compound with a known molecular structure, the COD of $CH_3COOH_{(aq)}$ was computed from the stoichiometry of the biodegradation of $CH_3COOH_{(aq)}$:

$$\text{g } COD_{CH_3COOH} = \left[\left(C_{CH_3COOH} \times t_R \times Q_{CH_3COOH}\right)/M_{r,\ CH_3COOH}\right] \times m_{ratio} \times M_{r,\ O_2} \quad (4.1.3.4.2)$$

Where

$\text{g } COD_{CH_3COOH}$ = mass of COD from CH_3COOH, (g COD)

C_{CH_3COOH} = mass concentration of CH_3COOH , (g/dm^3)

t_R = contact time, (h)

Q_{CH_3COOH} = volumetric flow rate of CH_3COOH dosing , (dm^3/h)

$M_{r,\ CH_3COOH}$ = molar mass of $CH_3COOH = 60$ g/mol

m_{ratio} = stoichiometric molar ratio of O_2 moles to CH_3COOH moles, ($dimensionless$)

$M_{r,\ O_2}$ = molar mass of $O_2 = 32$ g/mol

For the receiving municipal wastewater treatment plant, $F/M = 0.7\ \text{g } COD/\text{g } VSS$ and from experimental computations, $VSS = 3.0125$ g/dm^3.

Since $V_{sludge} = 1.5$ dm^3, the equivalent $\text{g } COD_{CH_3COOH}$ that was fed into the batch bioreactor was thus computed as follows:

$$\text{g } COD_{CH_3COOH} = (F/M) \times VSS \times V_{sludge}) = (0.7 \times 3.0125 \times 1.5) = 3.16 \text{ g COD} \quad (4.1.3.4.3)$$

The following variables were selected for contacting the dye effluent with the activated sludge system:

1. $t_R = 2$ h
2. $Q_{CH_3COOH} = 0.012$ dm^3/h

The required mass concentration of CH_3COOH was thus computed as follows:

$$\because \text{g } COD_{CH_3COOH} = \left[\left(C_{CH_3COOH} \times t_R \times Q_{CH_3COOH}\right)/M_{r,\ CH_3COOH}\right] \times m_{ratio} \times M_{r,\ O_2} \quad (4.1.3.4.4)$$

$$\Longrightarrow C_{CH_3COOH} = \left(\text{g } COD_{CH_3COOH} \times M_{r,\ CH_3COOH}\right)/\left(m_{ratio} \times M_{r,\ O_2} \times t_R \times Q_{CH_3COOH}\right)$$

$$C_{CH_3COOH} = (3.16 \times 60)/(2 \times 32 \times 2 \times 0.012)\ \text{g/dm}^3$$

$$C_{CH_3COOH} = 123.44\ \text{g/dm}^3$$

Assuming that the death rate of the microbial populations in the activated sludge was negligible, the rate of biomass growth (dX_H/dt) was computed from the product of heterotrophic yield coefficient (Y_H) and the rate of substrate consumption(dS/dt) as reported by Najafpour (2006), Katoh and Yoshida (2009):

$$dX_H/dt = -Y_H\, dS_S/dt \quad (4.1.3.4.5)$$

where

dX_H/dt = biomass growth rate, (g COD/dm^3/h)

$-dS_S/dt$ = rate of substrate consumption, (g COD/dm^3/h)

Y_H = heterotrophic yield coefficient, (g X_H/g X_{STO})

For CH_3COOH, $Y_H = 0.63$ g X_H/g X_{STO} according Gujer et al. (1999).

4.1.3.5 Dye effluent decolourisation in the absence of CH_3COOH dosing

A volumetric load of 0.5 dm^3 of the stock dye effluent at $C_{dye,\ stock} = 0.06\ g/dm^3$ was contacted with 1.5 dm^3 of activated sludge for 2 h in an extended aeration activated sludge system under continuous agitation.

From $t = 0$ h to $t = 2$ h, a 0.02 dm^3 sample was withdrawn from the activated sludge system unit after every 0.25 h interval and centrifuged at 10000 rpm for 0.13 h and the resulting supernatant was filtered through a 0.45 μm fibre glass filter medium and analysed in the spectrophotometer for light absorbance.

Since adsorption was the hypothesised dye effluent decolourisation mechanism, the spectrophotometric measurements estimated the mass dye remaining in solution.

The mass balance between the initial mass of dye charged into the activated sludge system, the mass of dye adsorbed and mass of dye remaining in solution:

$$m_{dye,adsorbed} = m_{dye,\ initial} - m_{dye,\ solution} \quad (4.1.3.5.1)$$

where

$m_{dye,adsorbed}$ = mass of soluble dye adsorbed, (g)

$m_{dye,\ solution}$ = mass of soluble dye remaining in solution, (g)

$m_{dye,\ initial}$ = initial mass of soluble dye charged into the activated sludge system, (g)

Estimates of $m_{dye,\ solution}$ were computed from measurements of $C_{dye,\ solution}$ and V_{total}:

$$m_{dye,\ solution} = \left(C_{dye,\ solution} \times V_{total}\right)g \quad (4.1.3.5.2)$$

where

$C_{dye,\ solution}$ = mass concentration of soluble dye remaining in solution, (g/dm^3)

Estimates of $C_{\text{dye, solution}}$ were computed from light absorbance measurements using the correlation computed by the linear least squares algorithm to quantify $C_{\text{dye, solution}} = f(A)$ for the calibration curve provided in Appendix A.2.3.

The adsorption process was quantified from:

1. plots of:

   (a) $m_{\text{dye, adsorbed}} = f(t)$

   (b) $q = f(t)$

   (c) $q = f(C_{\text{dye, solution}})$

   where

   $$q = (m_{\text{dye,adsorbed}})/(VSS \times V_{\text{sludge}}) \quad (4.1.3.5.3)$$

   $$\Longrightarrow q = \left(m_{\text{dye, initial}} - m_{\text{dye, solution}}\right)/\left(VSS \times V_{\text{sludge}}\right)$$

2. estimates of:

   (a) q_{∞}

   (b) $\%\ decolourisation$

   where

   $$q_{\infty} = m_{\text{dye, adsorbed, }\infty}/\left(VSS \times V_{\text{sludge}}\right) \quad (4.1.3.5.4)$$

   $$\Longrightarrow q_{\infty} = \left(m_{\text{dye, initial}} - m_{\text{dye, solution, }\infty}\right)/\left(VSS \times V_{\text{sludge}}\right)$$

   $$\therefore q_{\infty} = \left[\left(C_{\text{dye, initial}} \times V_{\text{dye}}\right) - \left(C_{\text{dye, solution, }\infty} \times V_{\text{total}}\right)\right]/(VSS \times V_{\text{sludge}})$$

   $$\%\ decolourisation = \left[\left(C_{\text{dye, initial}} - C_{\text{dye, solution, }\infty}\right)/C_{\text{dye, initial}}\right] \times 100\ \% \quad (4.1.3.5.5)$$

4.1.3.6 Dye effluent decolourisation in the presence of CH_3COOH dosing

$V_{dye} = 0.5\ dm^3$ was contacted with $V_{sludge} = 1.5\ dm^3$ for $t_R = 2$ h in the presence of CH_3COOH dosing which brought with it dilution effects and this was accounted for by the computed V_{total}:

$$V_{total} = V_{supernatant} + V_{dye} + V_{CH_3COOH} \quad (4.1.3.6.1)$$

where

V_{CH_3COOH} = cumulative volume of CH_3COOH dosed to the activated sludge system, (dm^3)

For $Q_{CH_3COOH} = 0.012\ dm^3/h$, the resulting cumulative volumes of CH_3COOH added to the activated sludge system in the successive 0.25 h intervals are provided in Appendix A.2.4.

The COD mass flow rate from CH_3COOH dosing at $C_{CH_3COOH} = 123.44\ g/dm^3$ and $Q_{CH_3COOH} = 0.012\ dm^3/h$ was computed as follows:

$$dS_S/dt = \left[\left(C_{CH_3COOH} \times Q_{CH_3COOH}\right)/M_{r,\ CH_3COOH}\right] \times m_{ratio} \times M_{r,\ O_2} \quad (4.1.3.6.2)$$

$$\Rightarrow dS_S/dt = [(123.44 \times 0.012/60) \times 2 \times 32]\ g\ COD/h$$

$$\therefore dS_S/dt = 1.58\ g\ COD/h$$

The cumulative mass of biomass from growth processes at every $t = 0.25$ h interval when a sample was withdrawn from the activated sludge system for analysis was computed as follows:

$$\text{microbial growth} = Y_H \times dS_S/dt \times t \quad (4.1.3.6.3)$$

$$\therefore \text{microbial growth} = (0.63\ g\ X_H/g\ X_{STO}) \times (1.58\ g\ COD/h) \times t\ h$$

Using a conversion factor of $1.42\ g\ COD/g\ VSS$ reported by Metcalf and Eddy (2003), the microbial growth estimates initially computed in terms of g COD were expressed in terms of VSS in Appendix A.2.5.

The addition of biomass from microbial growth process to the initial mass of VSS present in the activated sludge system at $t = 0$ h increased the total mass of VSS:

$$\text{g } VSS_{\text{total}} = \left(V_{\text{sludge}} \times VSS\right) + [(0.63 \times 1.58 \text{ g } COD/\text{h} \times t \text{ h})/1.42 \text{ g } COD/\text{g } VS)] \quad (4.1.3.6.4)$$

where

$\text{g } VSS_{\text{total}}$ = total mass of VSS at $t = t$ h, (g VSS)

In the presence of CH_3COOH dosing, the adsorption process was quantified from:

1. plots of:

   (a) $m_{\text{dye, adsorbed}} = f(t)$

   (b) $q = f(t)$

   where

   $$q = m_{\text{dye, adsorbed}}/\text{g } VSS_{\text{total}} \quad (4.1.3.6.5)$$

   $$\Longrightarrow q = \left(m_{\text{dye, initial}} - m_{\text{dye,adsorbed}}\right)/\text{g } VSS_{\text{total}}$$

   $$\therefore q = \left[\left(C_{\text{dye, initial}} \times V_{\text{dye}}\right) - \left(C_{\text{dye,adsorbed}} \times V_{\text{total}}\right)\right]/\text{g } VSS_{\text{total}}$$

2. estimates of:

   (c) q_∞

   (d) $extent\ of\ decolourisation$

   where

   $$q_\infty = m_{\text{dye,adsorbed},\infty}/\text{g } VSS_{\text{total}} \quad (4.1.3.6.6)$$

   $$\Longrightarrow q_\infty = \left(m_{\text{dye, initial}} - m_{\text{dye, solution},\infty}\right)/\text{g } VSS_{\text{total}}$$

   $$\therefore q_\infty = \left[\left(C_{\text{dye, initial}} \times V_{\text{dye}}\right) - \left(C_{\text{dye, solution},\infty} \times V_{\text{total}}\right)\right]/\text{g } VSS_{\text{total}}$$

$$\%\ decolourisation = \left[\left(C_{\text{dye, initial}} - C_{\text{dye, solution}, \infty}\right)/C_{\text{dye, initial}}\right] \times 100\ \% \quad (4.1.3.6.7)$$

4.2 Effect of Surfactant Effluents on Oxygen Transfer

4.2.1 Hypothesis

With respect to this study, it was hypothesised that analytical protocol developed for the investigation was adequately suitable in accurately providing a mathematical quantification of the effects of a surfactant effluent on oxygen transfer in a laboratory-scale activated sludge system.

Quantification of the effects of the surfactant effluent on oxygen transfer from air to the waster phase of the activated sludge system would be described by estimates of $k_{\mathrm{L}}a$ prior to and after loading the activated sludge system with a surfactant effluent and it was further postulated that estimates of $k_{\mathrm{L}}a$ could be computed C_{DO} vs. t data measurements systematically logged in the activated sludge system during aeration.

4.2.2 Materials and apparatus

4.2.2.1 Synthetic surfactant effluent

The surfactant effluent selected for the study was representation of a typical effluent discharged by a textile factory to the Verulam wastewater treatment plant. The effluent was synthesised from a pure surfactant reagent branded Tritec™ obtained from local textile factory called JMV Textiles.

From the product specifications described in the surfactant reagent's Material Safety Data Sheet, the compound reported to be a transparent liquid with high $\mathrm{H_2O}$ solubility and the chemical composition is a synergetic blend of non-ionic surfactants combined with biodegradable solvents.

The synthesis involved diluting the pure surfactant reagent with fresh $\mathrm{H_2O}$ and the process of synthesising the surfactant effluent and computations to estimate the effluent's final concentration at the point of discharge to the Verulam wastewater treatment plant are provided in Appendix B.1.1.

4.2.2.2 Activated sludge system

The laboratory-scale activated sludge system consisted of a 2 dm^3 glass vessel in which 1.5 dm^3 of activated sludge was contacted with 0.1 dm^3 of surfactant effluent.

The sludge contacted with the dye effluent was sampled on the 2nd of December 2011 from the aeration tank at eThekwini Municipality's Verulam wastewater treatment plant. At the time of sampling of activated sludge, the local textile industry was at full production capacity.

The bioreactor was an batch activated sludge system under continuous agitation by a magnetic stirrer. As it would be at the actual municipal wastewater treatment, the laboratory-scale activated sludge system was operated at ambient temperature without any form of temperature control applied to it and the pH of the reactor contents was monitored during each experimental run and maintained at 7 pH units.

4.2.2.3 DO/OUR meter

The UCT DO/OUR meter was employed to simultaneously make measurements of C_{DO} vs. t and compute corresponding estimates of OUR vs. t through the same experiment.

The equipment was designed by the Departments of Chemical Engineering, Electrical Engineering and Civil Engineering at the University of Cape Town. The operating principles of the UCT DO/OUR meter have been reported by Randall et al. (1991).

The UCT DO/OUR meter is equipped with an YSI (Yellow Springs Instruments) 5739 DO probe for making C_{DO} vs. t measurements and an integrated self-calibrating temperature. The DO probe is a Clark dissolved oxygen electrode with a signal proportional to O_2 partial pressure at a constant temperature.

The probe has a Teflon® gas permeable membrane enclosing some $KCl_{(aq)}$ electrolyte and the difference in O_2 partial pressure across the gas permeable membrane establishes the O_2 flux. This will then result in a flow of electric current in the probe and this electric current is directly proportional to the membrane flux and O_2 partial pressure. The probe current is temperature compensated to allow for the computation of C_{DO} vs. t measurements.

The calibration of the DO probe was done manually using a 0.08 mol/dm^3 $Na_2SO_{3(aq)}$ through a procedure described in the Appendix B.2.1 according to the specifications provided by the YSI 5739 DO Probe Instruction Manual.

4.2.3 Analytical protocol

4.2.3.1 Activated sludge characterisation

The mass of solids per unit volume of sludge was quantified through estimates of the volatile suspended solids (VSS) concentration according to the Standard Methods described by the American Public Health Association, American Water Works Association (1995).

The procedures for computing VSS estimates for the activated sludge used in the investigation are provided in Appendix A.2.1.

4.2.3.2 Surfactant effluent characterisation

The mass of soluble biodegradable substrate per unit volume of the surfactant effluent was computed from estimates of the total soluble Chemical Oxygen Demand ($COD_{\text{total soluble}}$) for the effluent according to the Standard Methods described by the American Public Health Association, American Water Works Association (1995).

The procedures for computing $COD_{\text{total soluble}}$ estimates for the surfactant effluent are provided in Appendix B.3.1.

4.2.3.3 Surfactant effluent contact volume

The volume of the surfactant effluent (V_{effluent}) contacted with the activated sludge system was computed as a function of:

1. F/M ratio $= 0.7$ g COD/g VSS
2. $VSS = 3.0125$ g/dm^3
3. $V_{\text{sludge}} = 1.5$ dm^3

4. surfactant effluent $COD_{\text{total soluble}} = 31.63\ \text{g/dm}^3$

$$\because F/M \text{ ratio} = (COD_{\text{total soluble}} \times V_{\text{effluent}})/(VSS \times V_{\text{sludge}}) \quad (4.2.3.3.1)$$

$$\Rightarrow V_{\text{effluent}} = (F/M \text{ ratio} \times VSS \times V_{\text{sludge}})/COD_{\text{total soluble}}$$

$$\therefore V_{\text{effluent}} = (0.7 \times 3.0125 \times 1.5)/31.63\ \text{dm}^3 = 0.1\ \text{dm}^3$$

4.2.3.4 Surfactant effluent contact time

The residence time of the surfactant (t_{R}) in the activated sludge system was computed as a function of the following wastewater treatment plant operating variables:

1. $Q_0 = 270843.345\ \text{dm}^3/\text{h}$

2. $V_{\text{R}} = 400000\ \text{dm}^3$

$$t_{\text{R}} = V_{\text{R}}/Q_0 \quad (4.2.3.3.2)$$

$$\therefore t_{\text{R}} = 400000\ \text{dm}^3/270843.345\ \text{dm}^3/\text{h} = 14.77\ \text{h} \cong 15\ \text{h}$$

4.2.3.5 Activated sludge pre-conditioning

For each experiment prior to the simultaneous logging of C_{DO} vs. t measurements and OUR vs. t estimates, the activated sludge was pre-conditioned so that the initial state of the activated sludge was uniform across all experiments.

The pre-conditioning process involved:

1. inhibiting nitrification processes by dosing the activated sludge system with 0.02 g N-allylthiourea/dm^3 sludge as specified by Spanjers H., Vanrolleghem P.A., (1995).

2. oxidising all the biodegradable substrates present in the activated sludge at the time of sampling at the wastewater treatment plant. Under conditions of controlled aeration, the process required the activated sludge system to undergo endogenous respiration whilst OUR_{end} vs. t estimates were logged.

   From plots OUR_{end} vs. t data from separate experiments respectively presented in Fig.8 and Fig.9, the minimum amount time during which the activated sludge system was supposed to undergo endogenous respiration until uniform OUR_{end} vs. t estimates were observed to indicate the absence of biodegradable substrates was ≅ 12 h.

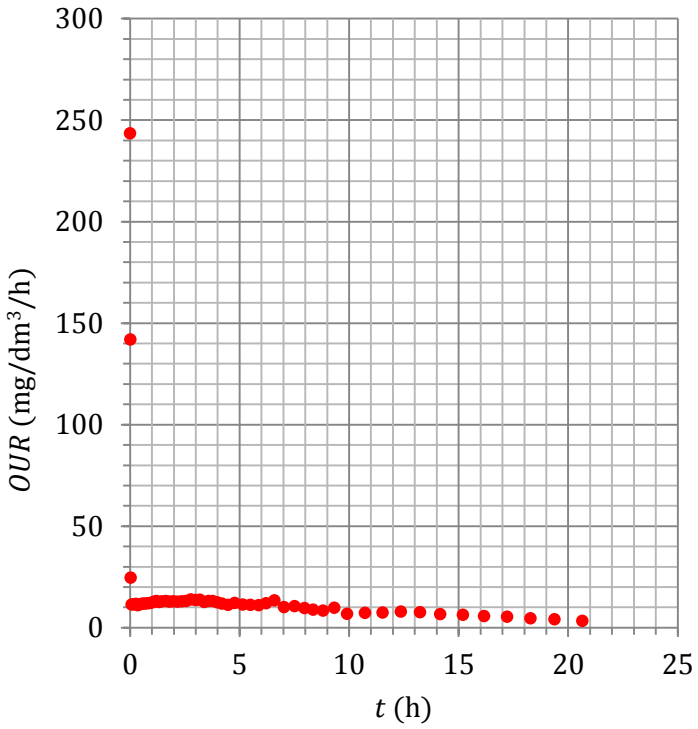

Fig.8: Experiment 1: endogenous respiration for the activated sludge pre-conditioning process

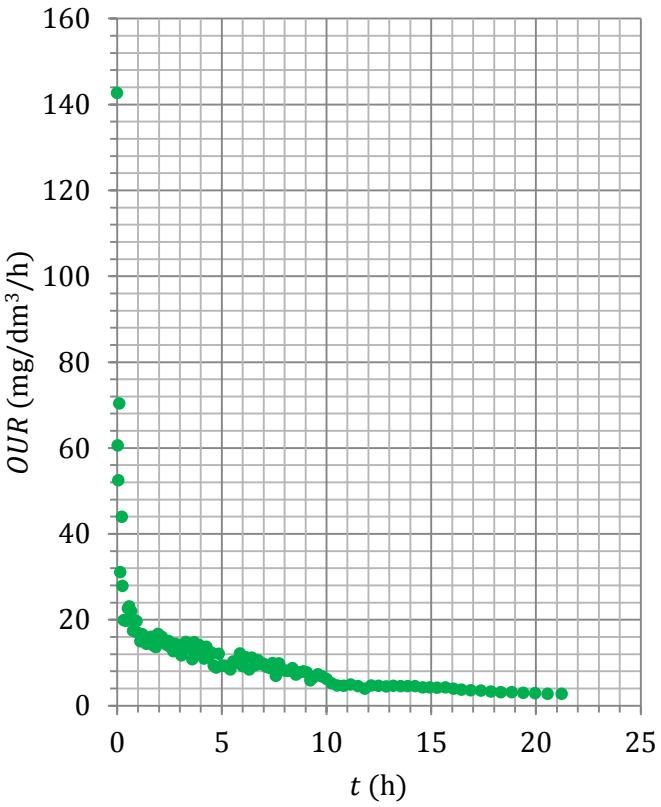

Fig. 9: Experiment 2: endogenous respiration for the activated sludge pre-conditioning process

4.2.3.6 Respirometry experiment

The accuracy in the logging of C_{DO} vs. t measurements and OUR vs. t estimates in previous respirometry studies has been counteracted by surface aeration and the entry of air into the activated sludge system such occurrences have been reported to contribute to inaccuracies in the respirometry results by Marsili-Libelli and Tabani (2002).

To lessen such inaccuracies, modifications on the laboratory activated sludge system were implemented in all respirometry experiments and the modifications involved incorporating a mixture of $N_{2(g)}$ and compressed air into the headspace between the activated sludge surface and the lid of the bioreactor vessel.

The incorporation of the blend of $N_{2(g)}$ and compressed air was done in such a way that a state of equilibrium was established in the activated sludge system where there would be no $O_{2(g)}$ entering into the activated sludge system from the headspace or $O_{2(g)}$ leaving the activated sludge system and escaping into the headspace.

This state of equilibrium required the volumetric flow rates of $N_{2(g)}$and compressed air to be measured by separate gas rotameters on separate gas flow lines prior to being blended.

The volumetric flow rate of each gas was adjusted along the gas flow line through manually-operated valves and the gas rotameters for both the $N_{2(g)}$and compressed air were of the same type and same model: Dwyer® Visi-Float® Model VFA, and the rotameters were calibrated at Dwyer® Instruments Incorporated in Michigan City, Indiana, U.S.A. according to Dwyer® Series VFA and VFB Visi-Float® (2008).

Along the gas flow lines, the rotameters were vertically mounted and the state of equilibrium was established by turning off the aeration to the activated sludge system so that only the blend of $N_{2(g)}$ and compressed air was allowed to flow into the headspace of the bioreactor unit.

The flow rates of the $N_{2(g)}$ and air into the headspace of the bioreactor unit were adjusted so that in the absence of aeration, C_{DO} in the activated sludge system was equal to the median value between the lower C_{DO} set point ($C_{DO,\ min}$) and upper C_{DO} set point ($C_{DO,\ max}$) points of dissolved concentration measurements by the UCT DO/OUR meter.

The respirometry experiment was set up as shown in Fig.10.

The upper C_{DO} set point ($C_{DO,\ max}$) on the UCT DO/OUR meter was set to 6 mg/dm^3 and the lower C_{DO} set point ($C_{DO,\ min}$) was set to 2 mg/dm^3.

Estimates of the oxygen $k_L a$ were computed from C_{DO} vs. t measurements data sets logged during the re-oxygenation phase (air on) of every aeration cycle and these occurred between $C_{DO,\ min}$ and $C_{DO,\ max}$, i.e. 2 mg/dm^3 $\leq C_{DO} \leq$ 6 mg/dm^3 as shown in Fig.11.

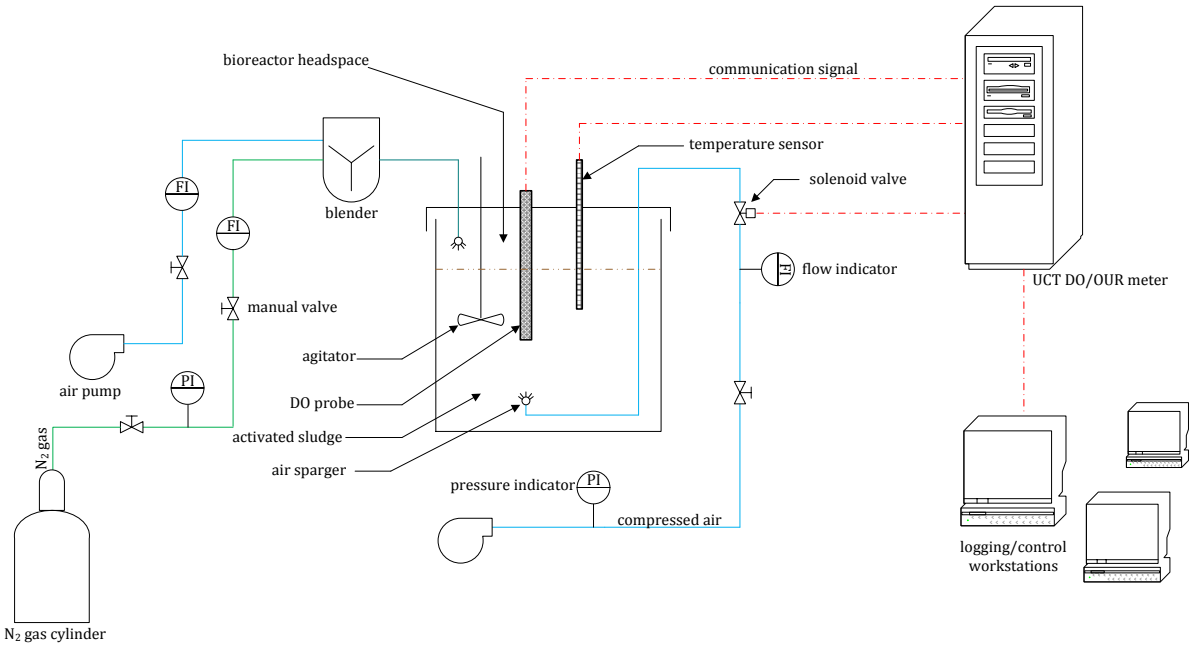

Fig.10: Set up of the respirometry experiment

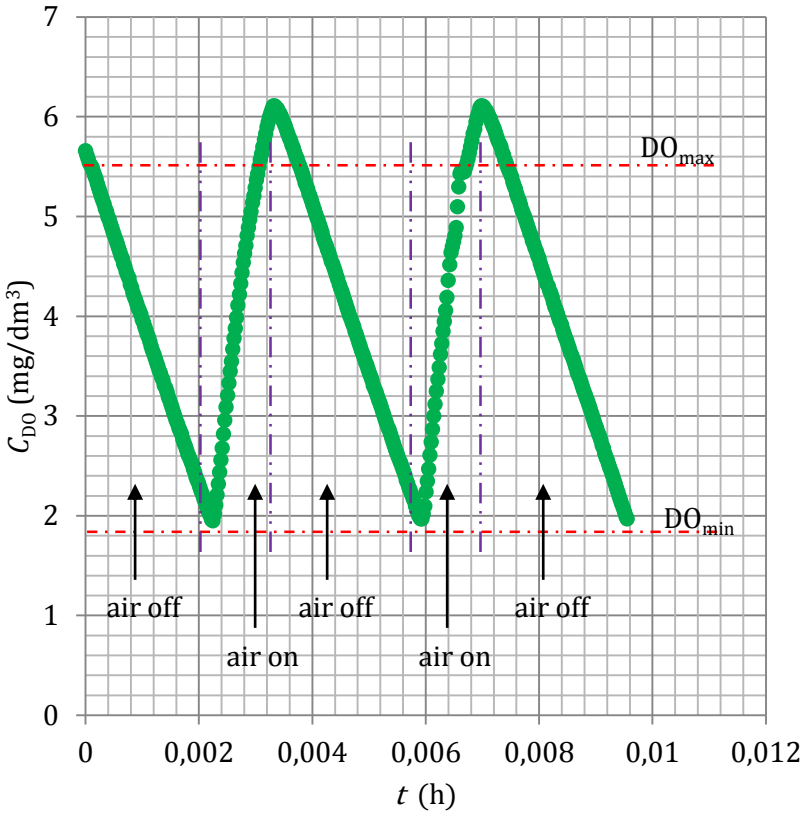

Fig.11: Aeration cycles showing the re-oxygenation phases (air on) from which $k_L a$ estimates would be computed

4.2.3.7 Computing estimates of the volumetric oxygen transfer coefficient

From C_{DO} vs. t data sets logged prior to and after dosing the activated sludge system with 0.1 dm^3 of the surfactant effluent, estimates of $k_L a$ were computed through a modified form of the Lewis-Whitman gas-liquid interfacial mass transfer model which incorporates the OUR parameter to account for oxygen consumption by the aerobic microbial species in the bioreactor:

$$\frac{dC}{dt} = k_L a(C^* - C) - OUR \qquad (4.2.3.7.1)$$

To minimise inaccuracies and imprecisions resulting from human error, the use of a Computer Algebra System was employed in solving the model defined in Equation 4.2.3.7.1.

The use of Computer Algebra Systems in solving Ordinary and Partial Differential Equations and Differential Equations has been comprehensively employed and demonstrated by Jeffrey (2002), Bronshtein et al., (2007), Stewart (2008) and Kreyszig (2011).

Integrating Equation 4.2.3.7.1 between the boundary conditions defined Asano K. (2006), Jakobsen (2008), Clark (2009), Gottschalk et al. (2010) and Theodore and Ricci (2011) and computing the solution using the Wolfram Mathematica® 8.0 Computer Algebra System according to Wolfram Research (2010):

$$\int_{C_0}^{C} (1/(k_{\mathrm{L}}a(C^* - C) - OUR))\, dC = \int_0^t dt \tag{4.2.3.7.2}$$

$$C = \frac{e^{-(k_{\mathrm{L}}a)t}\left(e^{(k_{\mathrm{L}}a)t} k_{\mathrm{L}}a\, C^* + OUR - e^{(k_{\mathrm{L}}a)t} OUR + C_0 k_{\mathrm{L}}a - C^* k_{\mathrm{L}}a\right)}{k_{\mathrm{L}}a}$$

where

$C^* = 8.2$ mg/dm^3 at the laboratory operating temperature of 25 °C and atmospheric pressure of 760 mmHg as reported in the National Field Manual for the Collection of Water-Quality Data according to the U.S. Geological Survey (2014)

$C_0 = C_{\mathrm{DO,\ min}} = 2$ mg/dm^3 as set on the UCT DO/OUR meter in Section 4.2.3.6

$$OUR = -\left(\frac{dC_{\mathrm{DO}}}{dt}\right)_{\text{deoxygenation phase}}$$

where

deoxygenation phase refers to the air off phase exhibited in Fig.11 when C_{DO} vs. t data is logged during $t_{\text{air off}} < t < t_{\text{air on}}$

Prior to the computation of each $k_{\mathrm{L}}a$ estimate, the OUR component of the model required for estimating $K_{\mathrm{L}}a$ was estimated through computations of: $-\left(\frac{dC}{dt}\right)$ from C_{DO} vs. t data sets logged during the deoxygenation phase ($t_{\text{air off}} < t < t_{\text{air on}}$).

Through the non-linear least squares regression method, $k_{\mathrm{L}}a$ was computed as a parameter of the best non-linear fits of C_{DO} vs. t data sets onto the solution of Equation 4.2.3.7.2.

The computations were performed through the Levenberg-Marquardt algorithm implemented on the Curve Fitting Toolbox™ in MATLAB® R2011a according to MathWorks, Inc. (2012) and the goodness-of-fit was described by the following statistical indicators generated by the Curve Fitting Toolbox™ and provided in regression reports in Appendix B.4:

1. $sum\ of\ squared\ residuals$ (SSE): a value of $SSE \cong 0$ indicated a good fit

2. $squared\ correlation\ coefficient$ (R^2): this was equivalent to the square of the correlation between the experimental response variables and the model's response values. A value $R^2 \cong 1$ showed that a greater portion of variance was accounted for by the model and hence a good fit

The model parameter estimates were computed with 95% confidence lower and upper bounds and the best fit plots were accompanied by their corresponding residuals scatter plots.

The estimates of $k_{\mathrm{L}}a$ computed at ambient temperature were corrected for temperature effects through a temperature correction factor derived from an exponential function which approximates the van't Hoff-Arrhenius correlation as reported by Metcalf and Eddy (2003):

$$k_{\mathrm{L}}a_{\,(\mathrm{T})} = k_{\mathrm{L}}a_{\,(20\,^{\circ}\mathrm{C})} \times 1.024^{(\mathrm{T}-20\,^{\circ}\mathrm{C})} \qquad (4.2.3.7.3)$$

where

$k_{\mathrm{L}}a_{\,(\mathrm{T})} = \mathrm{O}_2$ volumetric transfer coefficient at ambient temperature T °C, $(1/T)$

$k_{\mathrm{L}}a_{\,(20\,^{\circ}\mathrm{C})} =$ standard O_2 volumetric transfer coefficient at 20 °C, $(1/T)$

$1.024 =$ numerical value of correction factor for diffused air and mechanically aerated systems according ASCE (1991), $(dimensionless)$

The efficacy of the YSI 5739 DO Probe in logging precise and accurate C_{DO} vs. t measurements was inferred from estimates of the first order time constant (τ) computed as parameter of the first order dynamic response model according to Philichi T., Stenstrom M.K. (1989).

As reported by Spanjers H., Olsson G. (1992), estimates of τ serve a measure of the time delay of the DO probe in its dynamic response to changes in dissolved O_2 and the response dynamics were assessed through comparisons between the computed values of τ and the designed response time of the YSI 5739 DO Probe to reach 90% of its steady-state value at 25 ℃ and this was specified in the YSI 5739 DO Probe product manual to be approximately 10 seconds.

If the computed estimates of τ were less than the YSI 5739 DO Probe designed response time of 10 seconds, then YSI 5739 DO Probe's integrity was sufficient enough to log precise and accurate C_{DO} vs. t measurements. Furthermore, time constant should also be much less than the time constant of the mass transfer process. The method through which estimates of τ were computed from the best fits of C_{DO} vs. t measurements logged for a fresh H_2O system onto the the first order dynamic response model according to Philichi T., Stenstrom M.K. (1989) is provided in Appendix B.3.2.

4.3 Biodegradability of Surfactant Effluents

4.3.1 Hypothesis

With respect to this study, it was hypothesised that by extending the experimental apparatus and methods constituting the analytical protocol designed in Section 4.2 in combination with suitable numerical methods, the amalgamation could be employed to accurately estimate the biodegradability of the same surfactant effluent load whose effects on oxygen transfer were evaluated in Section 4.2.

From the chemical composition of the synthetic surfactant effluent described in Section 4.2.2.1, it was hypothesised that there were fractions of soluble components of the effluent which were biodegradable and the other fractions of soluble components were inert.

It was also further hypothesised that from the chemical composition of the surfactant effluent, the active biomass in the activated sludge system would strongly prefer the biochemical formation of storage products over direct assimilation and immediate consumption.

4.3.2 Materials and apparatus

Biodegradability assessments were inferred from OUR vs. t computations and since the UCT DO/OUR meter was employed to simultaneously make measurements of C_{DO} vs. t and compute corresponding estimates of OUR vs. t through the same experiment, the same materials and apparatus described in Section 4.2.2 was employed in this segment of the study.

4.3.3 Analytical protocol

Since the experimental data was simultaneously obtained from the same experiment described in Section 4.2.3, the same analytical methods described in Section 4.2.3.1, Section 4.2.3.2, Section 4.2.3.3, Section 4.2.3.4, Section 4.2.3.5 and Section 4.2.3.6 were also applied to this segment of the study.

The OUR vs. t estimates were computed through the respirometry experiment described in Section 4.2.3.6 and with reference to Fig.11, estimates of OUR vs. t were computed by the UCT DO/OUR meter from the slope of C_{DO} vs. t during the de-oxygenation phases (air off) of aeration cycles controlled by the C_{DO} set points of $2\ \mathrm{mg/dm^3}$(air on) $\leq\ C_{\mathrm{DO}}\ \leq\ 6\ \mathrm{mg/dm^3}$(air off).

4.3.3.1 Quantifying biodegradability

Biodegradability estimates were computed from fractions of the total soluble COD concentration of the synthetic surfactant effluent as follows:

$$biodegradability = \left(\frac{m_{S_{\mathrm{S}}}}{m_{COD_{\mathrm{soluble,\ total}}}}\right) \times 100\% \qquad (4.3.3.1.1)$$

Estimates of $m_{COD_{\mathrm{soluble,\ total}}}$ for the surfactant effluent were computed through the method described in Section 4.2.3.2 and since the surfactant effluent was synthesised from a mixture of fresh H_2O and pure surfactant, there were no particulate biodegradable substrates (X_{S}) present and estimates of $m_{S_{\mathrm{S}}}$ were computed from the total area under the OUR_{exo} vs. t curve as shown in Fig.12.

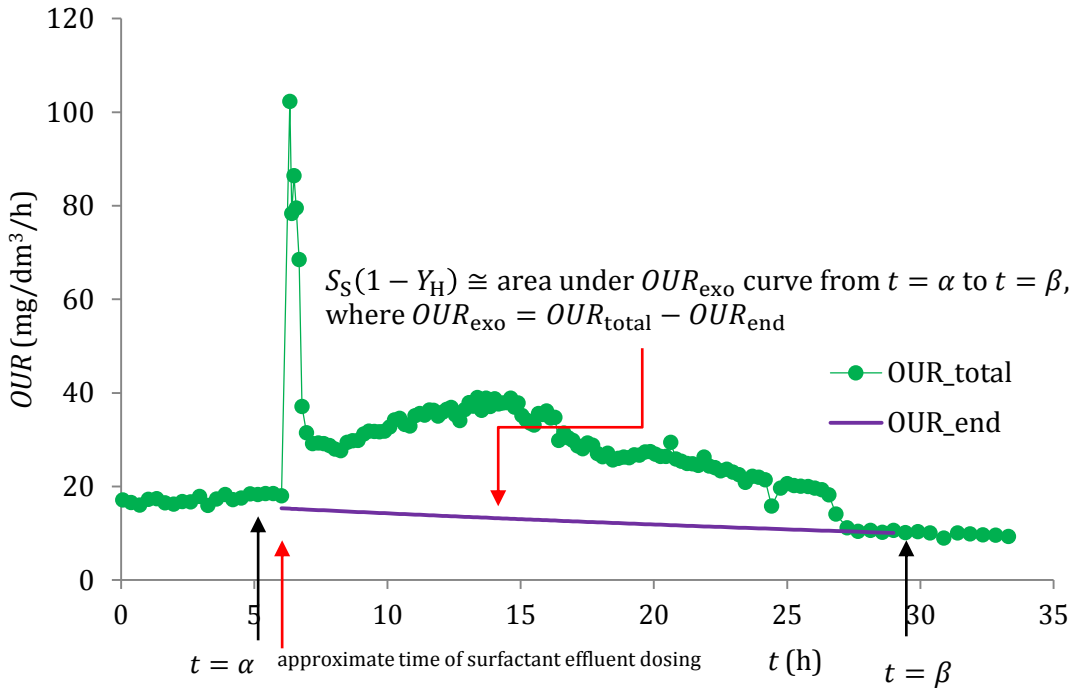

Fig.12: Method for estimating S_S from the area under a respirogram

With reference to Fig.12, the area under the OUR_{exo} vs. t curve was computed using a modified form of the Simpson's numerical integration technique:

$$\text{total area under the } OUR_{exo} \text{ vs. } t \text{ curve} \cong \int_{t=\beta}^{t=\alpha} (OUR_{exo})\, dt \qquad (4.3.3.1.2)$$

$$\int_{t=\beta}^{t=\alpha} OUR_{exo}\, dt$$

$$\cong \frac{\Delta t}{3}\left[f(\alpha) + 2\sum_{i=1}^{(n/2)-1} f(t_{2i}) + 4\sum_{i=1}^{(n/2)} f(t_{2i-1}) + f(\beta)\right]$$

where

$t_i = \alpha + (i(\Delta t))$ for $i = 0,1, \ldots n-1, n$

$\Delta t = (\beta - \alpha)/n$

$n =$ sub-intervals of equal length into which the interval $[\alpha, \beta]$ was divided

With reference to both Fig.12 and Equation 4.3.3.1.2, estimates of m_{S_S} were computed as follows:

$$m_{S_S} \cong \frac{\left[\frac{\Delta t}{3}\left(f(\alpha) + 2\sum_{i=1}^{\left(\frac{n}{2}\right)-1} f(t_{2i}) + 4\sum_{i=1}^{\left(\frac{n}{2}\right)} f(t_{2i-1}) + f(\beta)\right)\right]}{(1 - Y_H)} \times V_{total} \quad (4.3.3.1.3)$$

where

$V_{total} = V_{sludge} + V_{effluent} = 1.6\ dm^3$

$Y_H = 0.63$

Estimates for $m_{COD_{soluble,\ total}}$ were computed from the product of $COD_{soluble,\ total}$ and $V_{effluent}$:

$$m_{COD_{soluble,\ total}} = COD_{soluble,\ total} \times V_{effluent} \quad (4.3.3.1.4)$$

The Simpson's numerical integration technique was implemented in MATLAB® R2011a according to MathWorks, Inc. (2012) by Garcia (2009) and the MATLAB®source code for the implementation was provided in Appendix B.5.

5. RESULTS

Execution and assessing the suitability of the analytical methods designed for investigating the decolourisation of soluble dye effluents in an activated sludge system through the postulated mechanism of physical adsorption as described in Section 4.1.1 resulted in 2-dimensional scatter plots and computations of the following:

1. mass of soluble dye adsorbed as a function of contact time

2. ratio of the mass of dye adsorbed to the mass of adsorbent as a function of contact time

3. ratio of the mass of dye adsorbed to the mass of adsorbent as a function of the soluble dye effluent concentration remaining in solution after adsorption

4. maximum ratio of the mass of dye adsorbed to the mass of adsorbent at $t = \infty$ hours

5. extent of dye effluent decolourisation computed as a function of the initial dye effluent concentration and concentration of the dye effluent remaining in solution after adsorption at $t = \infty$ hours

Implementation and evaluating the appropriateness of the analytical protocol that was designed for examining the effects of the surfactant effluents on oxygen transfer from air to the water phase of an activated sludge system resulted in the following:

1. computation of the volumetric oxygen transfer coefficient ($k_{\mathrm{L}}a$) estimates from C_{DO} vs. t data

2. 2-dimensional scatter plots of C_{DO} vs. t measurements being plotted together with their corresponding estimates of $k_{\mathrm{L}}a$ vs. t. For both plots, an indicator on the $t - axis$ specified the time during the experiment when a 0.1 dm^3 surfactant effluent load was charged into the activated sludge system and the consequent effects the surfactant effluent were shown on both the C_{DO} vs. t and the $k_{\mathrm{L}}a$ vs. t scatter plots

Evaluation the suitability of the methodologies that were designed for the estimation of biodegradability of the surfactant effluent in an activated sludge system required the generation of OUR vs. t data sets and these were computed together with C_{DO} vs. t measurements from the same experiment.

The charging of the 0.1 dm^3 surfactant effluent load into the activated sludge system marked the onset of exogenous respiration (OUR_{exo}) as an indicator for the assimilation of the surfactant effluent by the heterotrophic microbial populations in the activated sludge and biodegradability estimates were computed numerically from the resulting respirograms (scatter plots of OUR vs. t).

Greater detail on the specific results that were generated for each segment of the study is provided in the Sections 5.1, 5.2 and 5.3 respectively.

5.1 Soluble Dye Effluents Decolourisation

5.1.1 Mass of soluble dye adsorbed as a function of contact time

The contrast between the mass of dye adsorbed by the activated sludge as a function of contact time in the absence and presence of CH_3COOH dosing is shown in Fig.13.

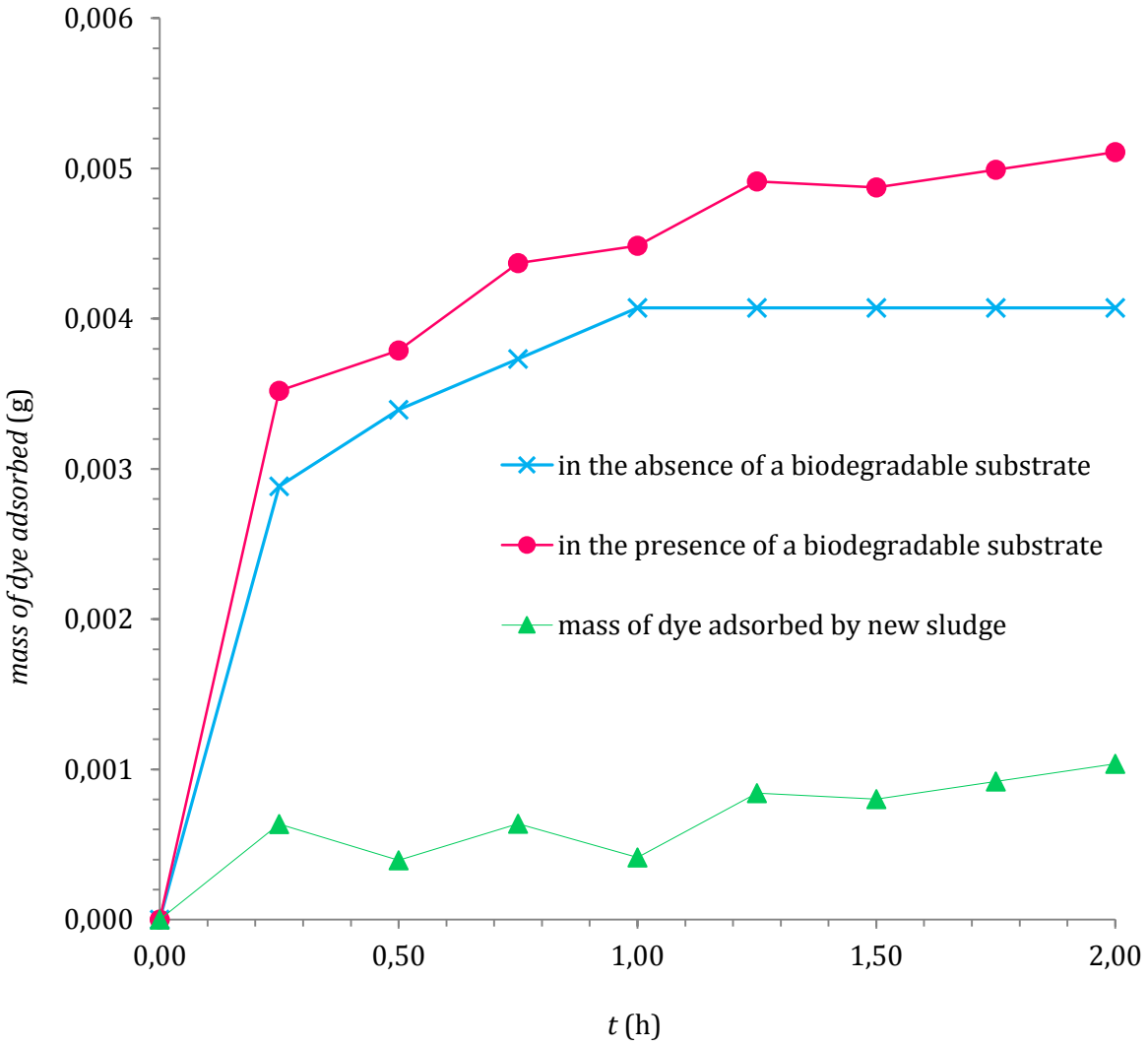

Fig.13: Mass of soluble dye adsorbed as a function of contact time

At any given time during which the soluble dye effluent was contacted with the activated sludge system ($0 \leq t \leq 2$ h), the mass of dye adsorbed by the new sludge generated by microbial growth processes resulting from the presence of a biodegradable substrate was computed from the difference between the mass of dye adsorbed in the presence of CH_3COOH dosing and the mass of dye adsorbed in the absence of CH_3COOH dosing.

5.1.2 Ratio of the mass of soluble dye adsorbed per unit mass of adsorbent as a function of contact time

As a function of contact time, the contrast between the mass of dye adsorbed per unit mass of adsorbent in the absence and presence of CH_3COOH dosing is shown in Fig.14.

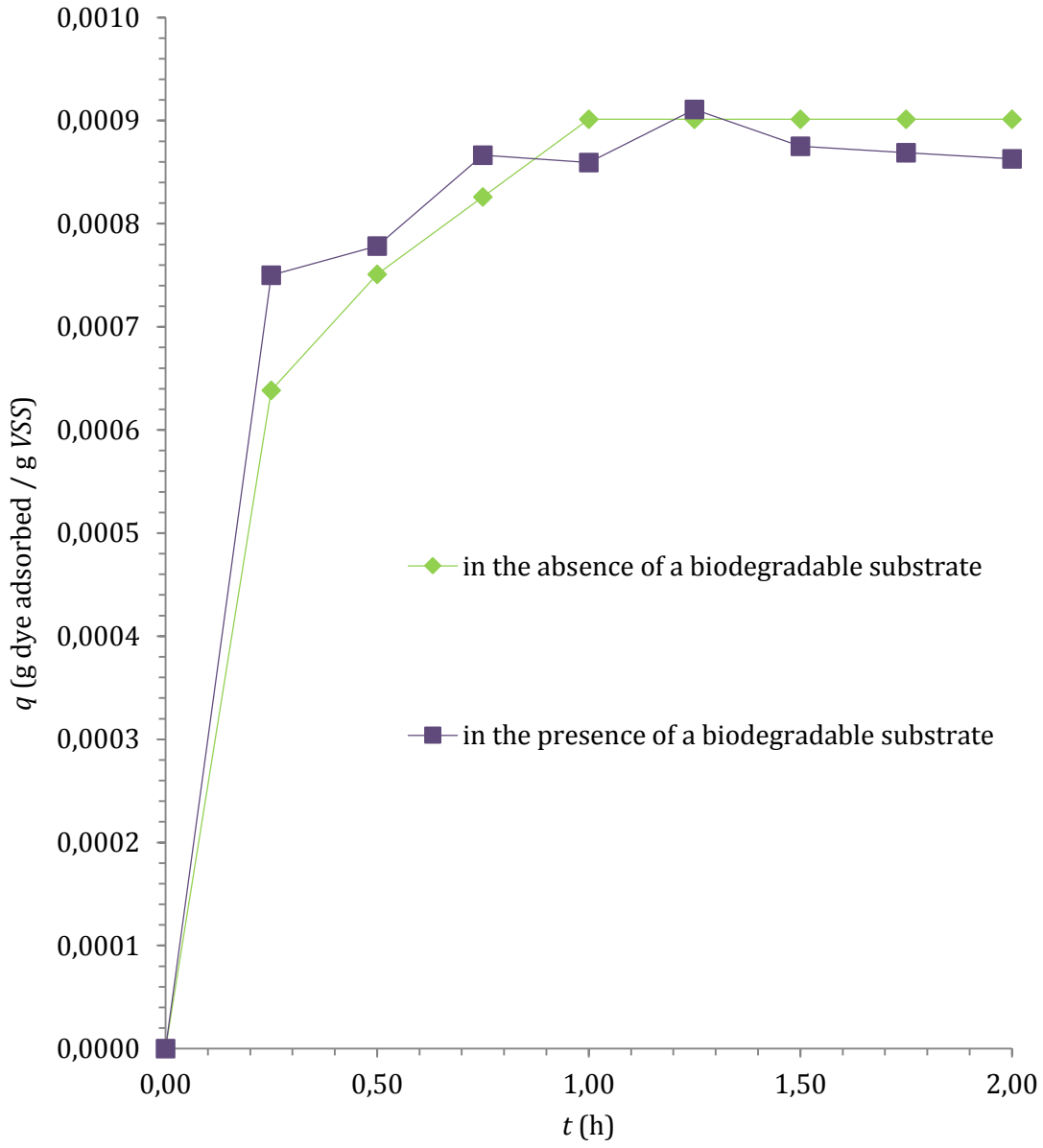

Fig.14: Ratio of the mass of soluble dye adsorbed per unit mass of adsorbent as a function of contact time

5.1.3 Relationship between the solution – adsorbent interfacial adsorbate concentration and the adsorbate concentration

For a system with a fixed mass of adsorbent (fixed amount of g VSS, in the absence of CH_3COOH dosing) and a single soluble dye adsorbate in solution, the adsorption equilibrium was represented by a scatter plot of the mass of adsorbate that is adsorbed per unit mass of adsorbent as a function of the concentration of adsorbate solution as shown in Fig.15.

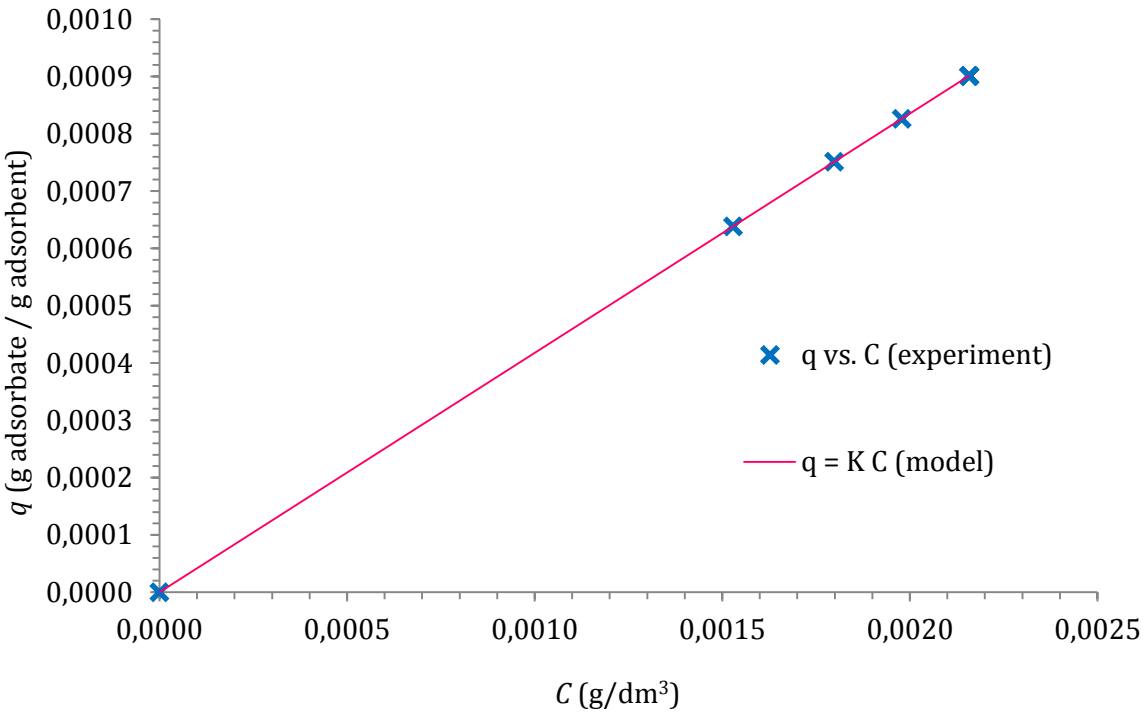

Fig.15: Mass of adsorbate is adsorbed per unit mass of adsorbent as a function of adsorbate concentration

The goodness-of-fit regression report resulting from the linear least squares fit of q vs. C data onto the adsorption model for a single adsorbate in solution system is as shown in Table 2.

Table 2: Linear least squares regression report for the best fit of q vs. C data onto the adsorption model for a single adsorbate in solution system

$Best\ fit\ estimate\ for\ adsorption\ parameter\ K$ (dm^3/g)	0.4175
95% $confidence\ level\ lower\ bound for\ adsorption\ parameter\ K$ (dm^3/g)	0.4175
95% $confidence\ level\ upper\ bound for\ adsorption\ parameter\ K$ (dm^3/g)	0.4175
$Sum\ of\ squares\ due\ to\ error\ (SSE)$	2.609e-014
r^2	0.999

From the best fit adsorption model parameter estimates, the resulting correlation between the ratio of the mass of adsorbate adsorbed per unit mass of adsorbent and the adsorbate concentration is: $q = 0.4175\ C$

5.1.4 Maximum ratio of the mass of dye adsorbed per unit mass of adsorbent

Estimates of the maximum ratio of the mass of dye adsorbed per unit mass of adsorbent at $t = \infty$ hours were computed according to Equation 4.1.3.5.4 and are as shown in Table 3:

Table 3: Maximum ratio of the mass of dye adsorbed per unit mass of adsorbent

	in the absence of CH_3COOH	in the presence of CH_3COOH
q_∞ (g dye adsorbed/g VSS)	0.00090	0.00091

5.1.5 Extent of dye effluent decolourisation

The extents of dye effluent decolourisation computed as a function of the initial dye effluent concentration and concentration of the dye effluent remaining in solution after adsorption at $t = \infty$ hours were computed according to Equation 4.1.3.5.5 and are as shown in Table 4:

Table 4: Extents of dye effluent decolourisation

	in the absence of CH_3COOH	in the presence of CH_3COOH
% $decolourisation$	13.57	18.07

5.2 Effect of Surfactant Effluents on Oxygen Transfer

For each experiment, the laboratory measurements from which $k_L a$ estimates were computed were represented by scatter plots of C_{DO} vs. t experimental data.

Along the $t - axis$ of each scatter plot, a vertical arrow was inserted to indicate the time during the execution of the experiment when a 0.1 dm^3 surfactant effluent load was dosed into the activated sludge system and the corresponding estimates of $k_L a$ were represented by scatter plots of $k_L a$ vs. t.

The goodness-of-fits for the computed $k_L a$ estimates was quantified by non-linear regression statistical indicators.

5.2.1 Experiment no.1 $k_L a$ estimates

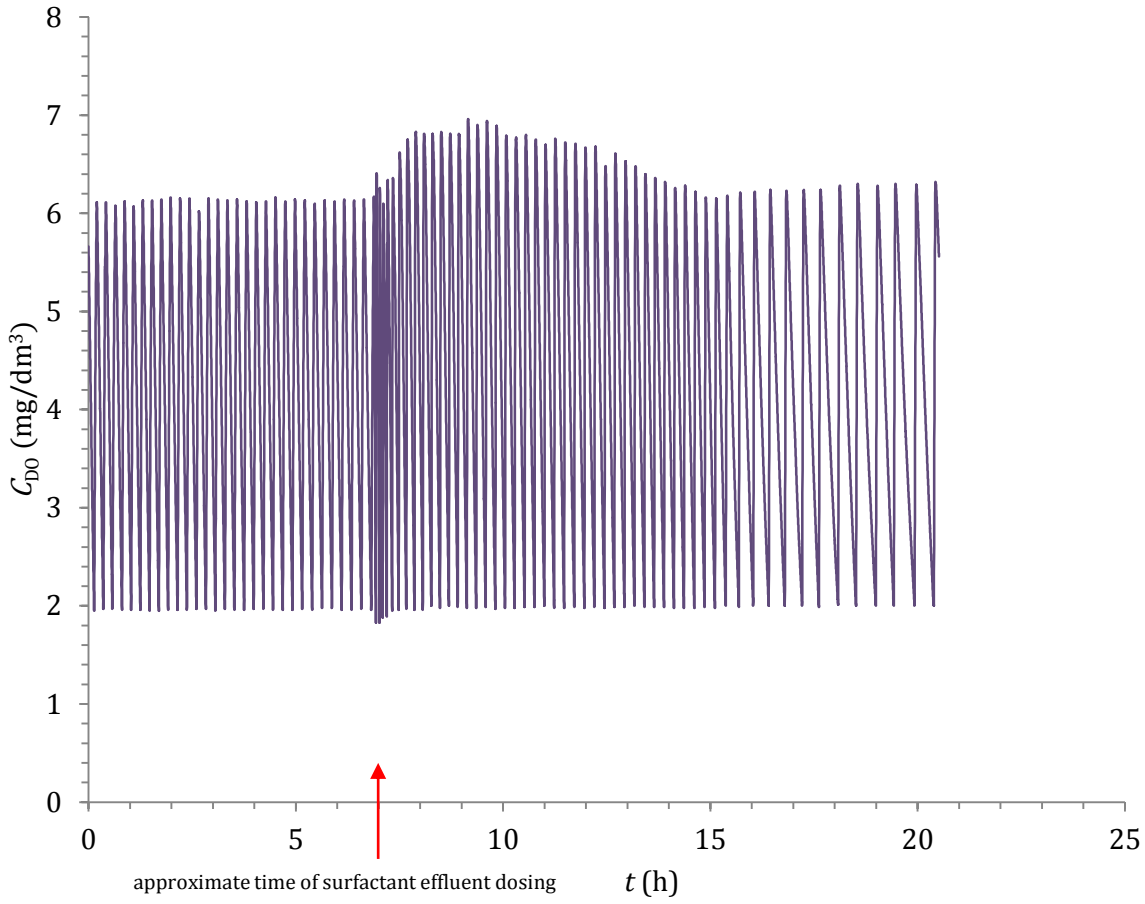

Fig.16: Scatter plot for experiment no.1 C_{DO} vs. t measurements

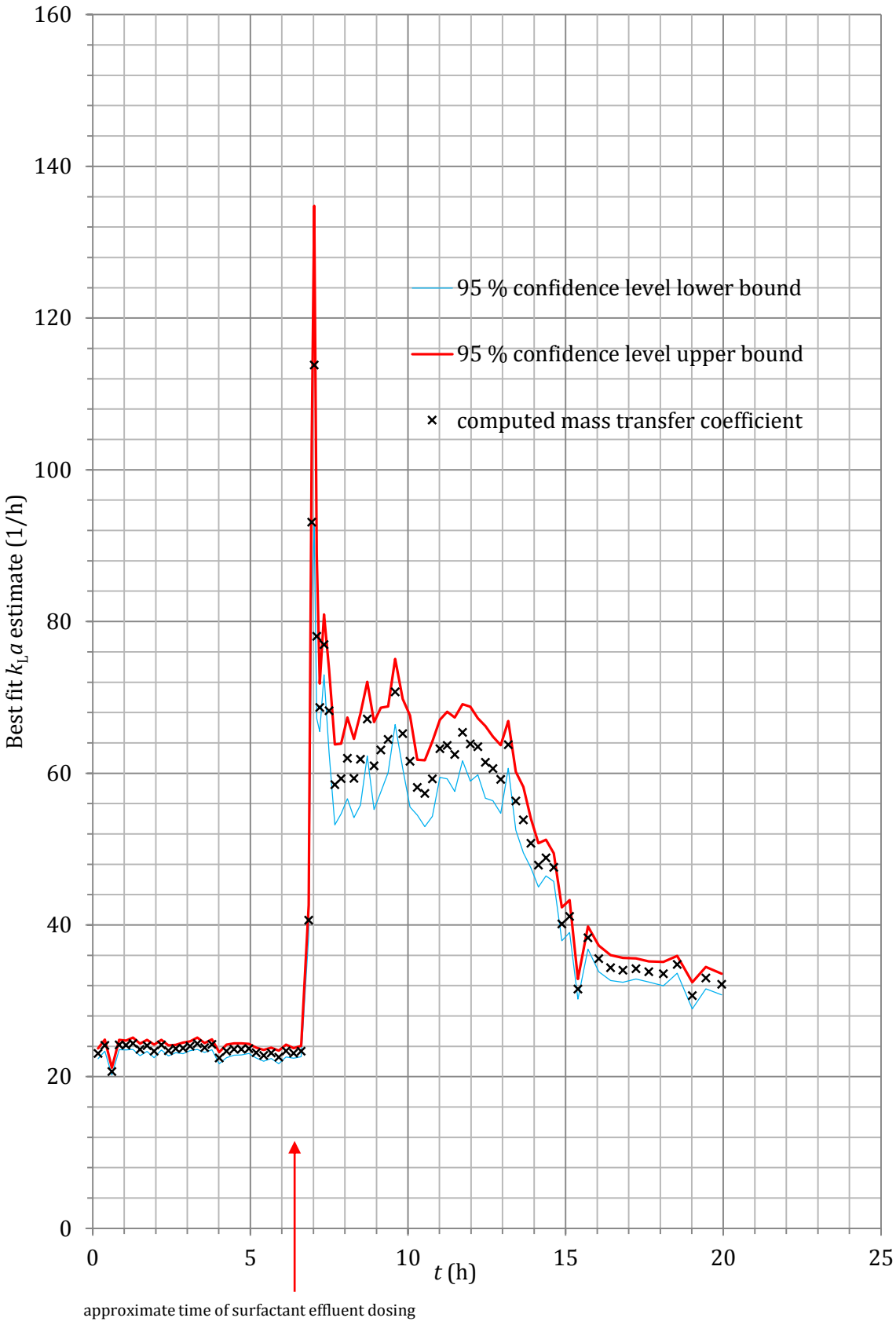

Fig.17: Scatter plot for experiment no.1 $k_L a$ vs. t estimates

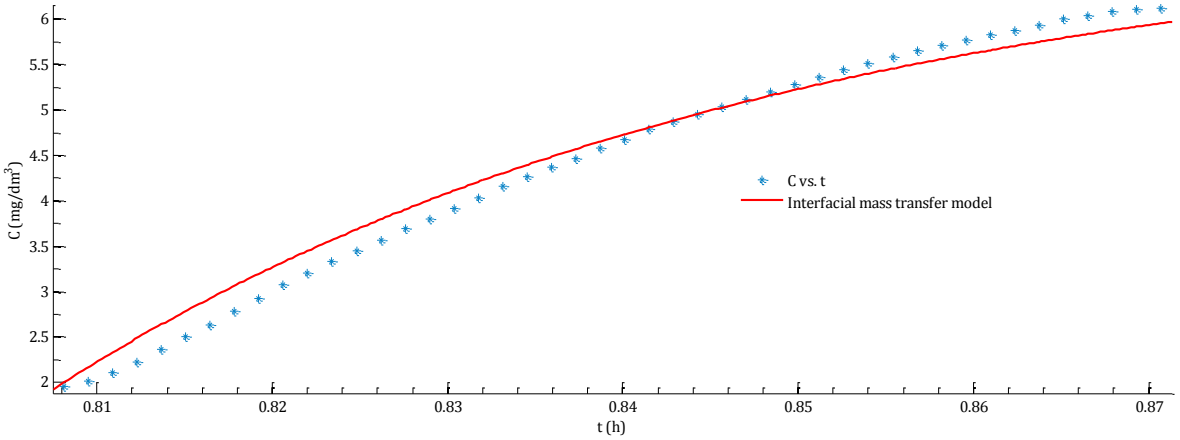

Fig.18: Experiment no.1 best non-linear fit prior to dosing of surfactant effluent: C_{DO} vs. t data set no.4

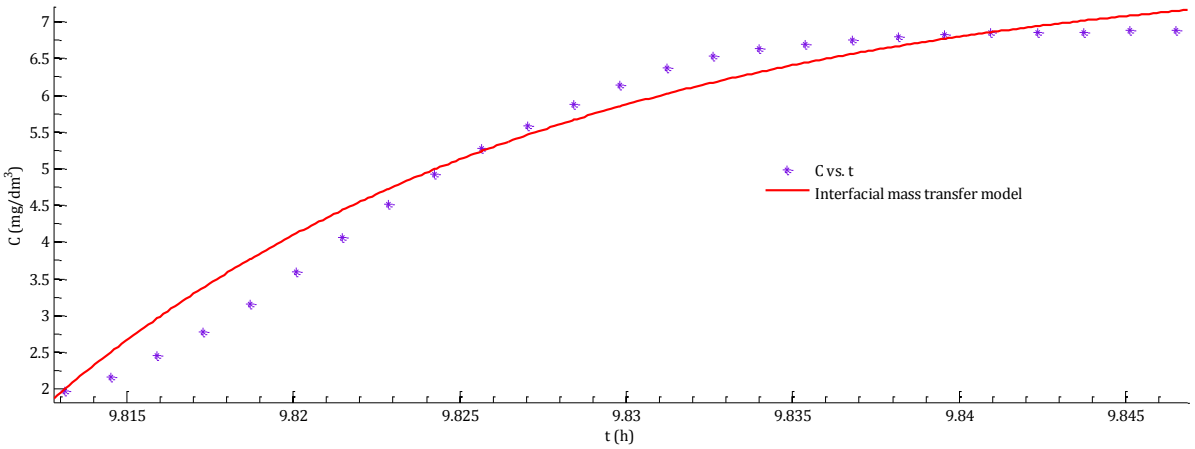

Fig.19: Experiment no.1 best non-linear fit after dosing of surfactant effluent: C_{DO} vs. t data set no.47

5.2.2 Experiment no.2 $k_L a$ estimates

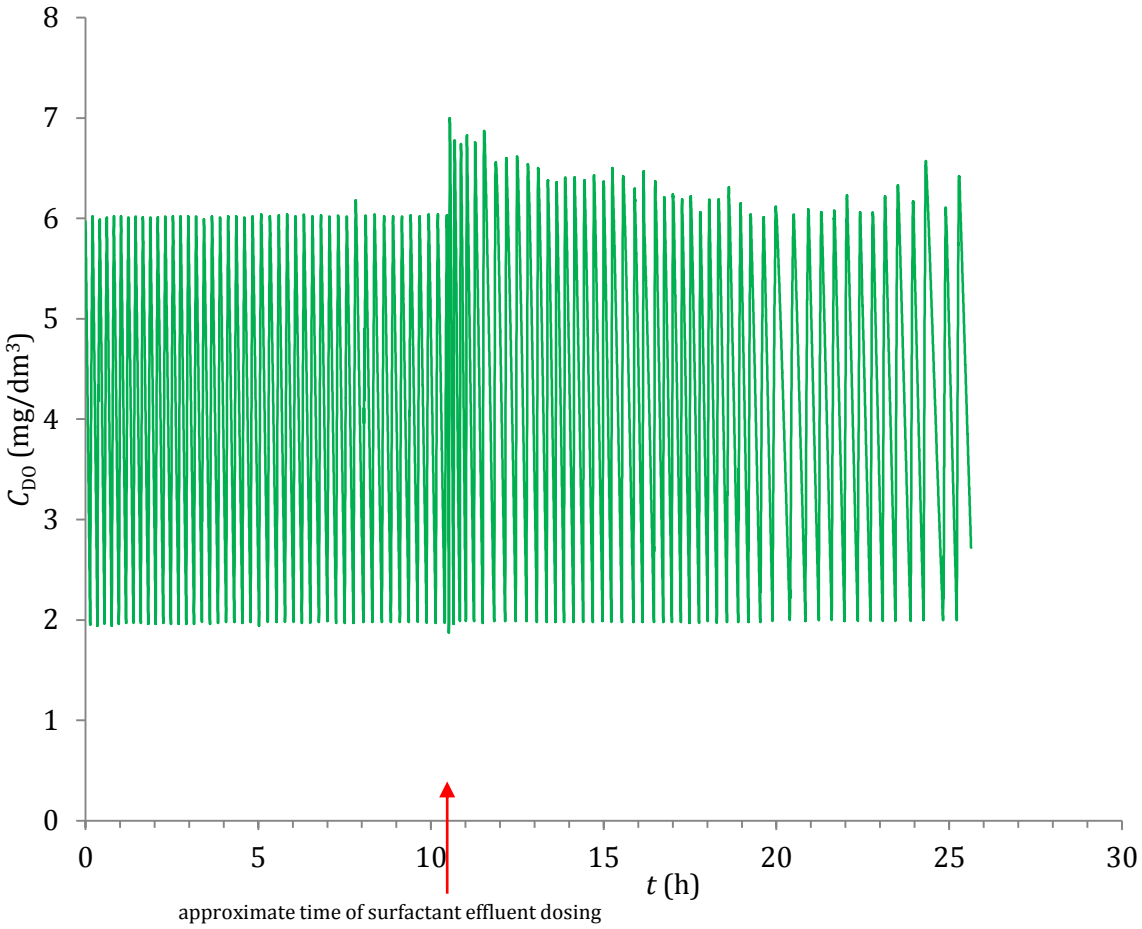

Fig.20: Scatter plot for experiment no.2 C_{DO} vs. t measurements

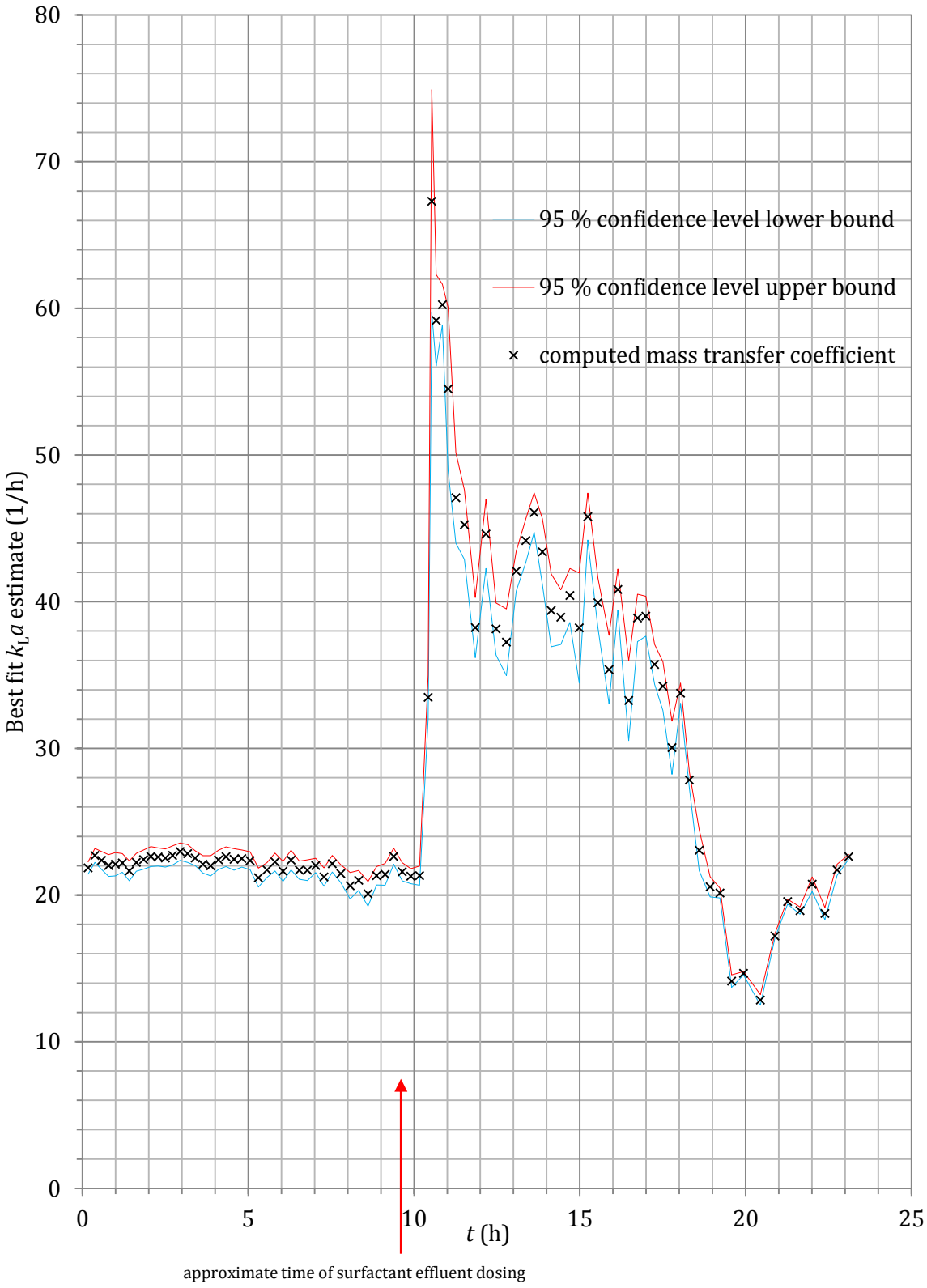

Fig.21: Scatter plot for experiment no.2 $k_L a$ vs. t estimates

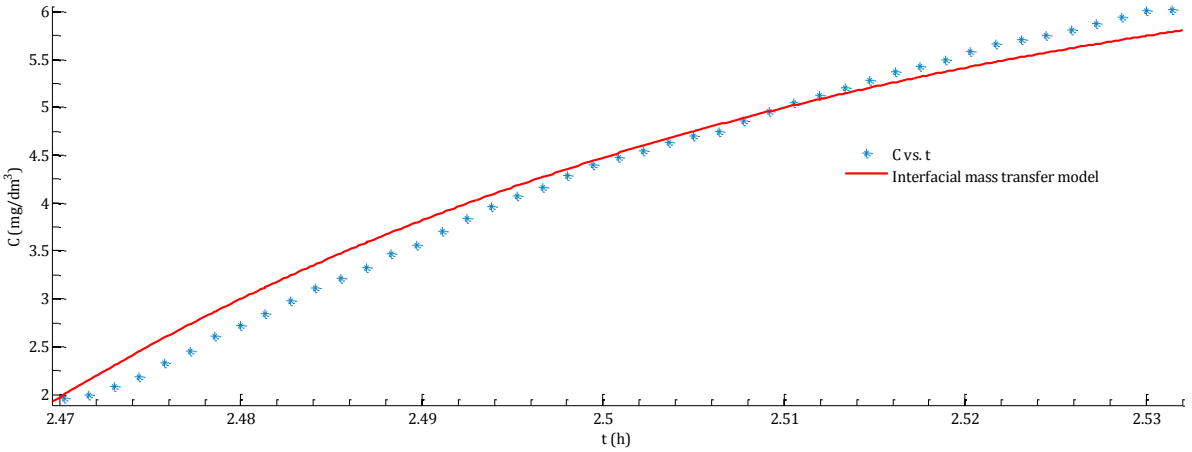

Fig.22: Experiment no.2 best non-linear fit prior to dosing of surfactant effluent: C_{DO} vs. t data set no.12

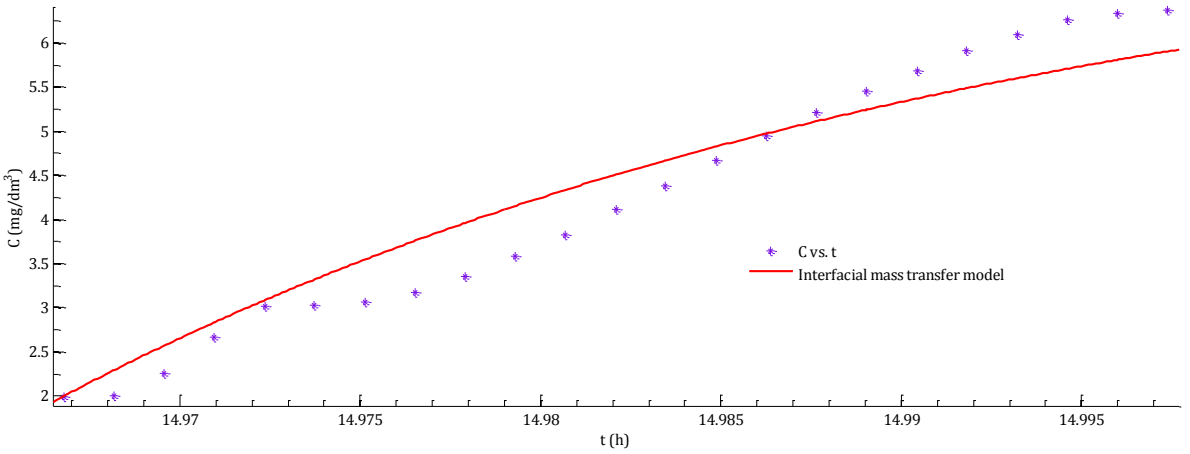

Fig.23: Experiment no.2 best non-linear fit after dosing of surfactant effluent: C_{DO} vs. t data set no.62

5.2.3 Experiment no.3 $k_L a$ estimates

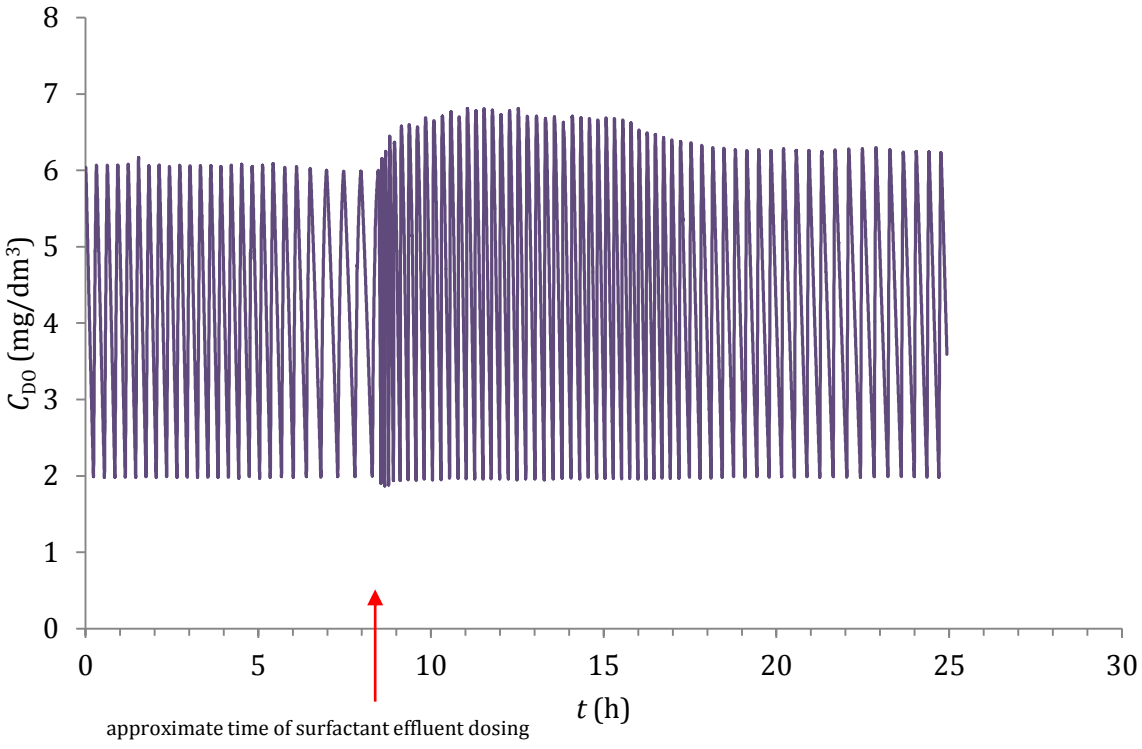

Fig.24: Scatter plot for experiment no.3 C_{DO} vs. t measurements

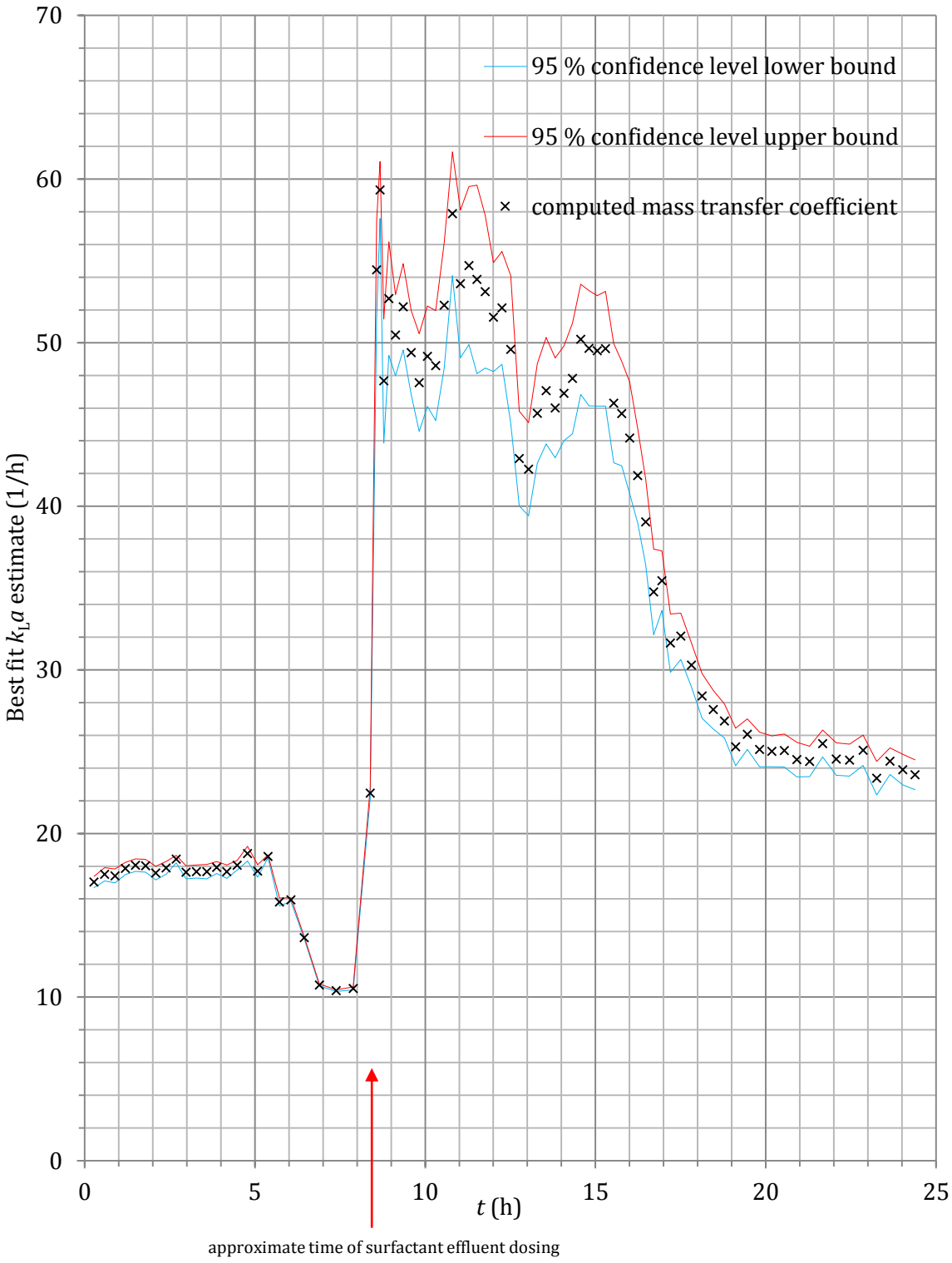

Fig. 25: Scatter plot for experiment no.3 $k_L a$ vs. t estimates

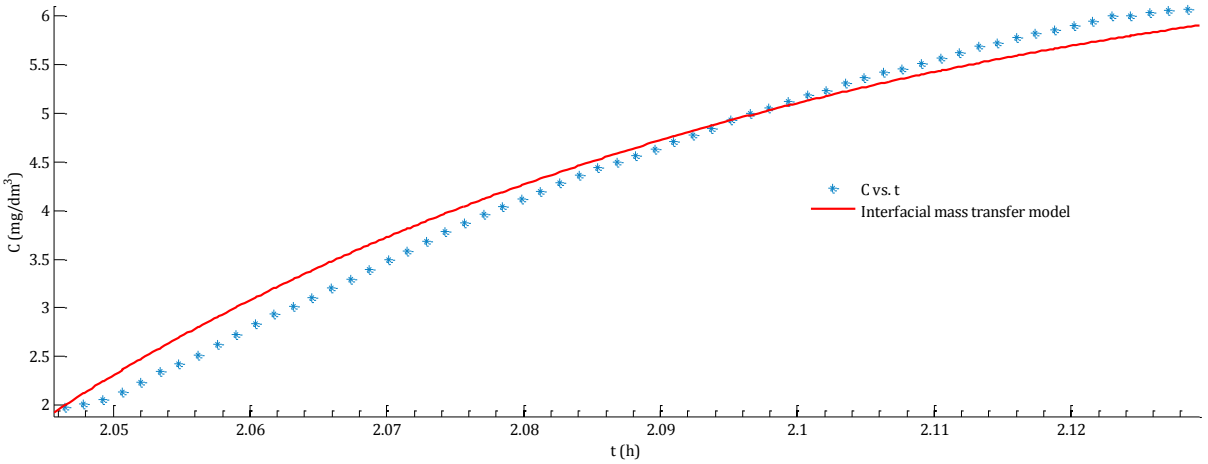

Fig.26: Experiment no3 best non-linear fit prior to dosing of surfactant effluent: C_{DO} vs. t data set no.7

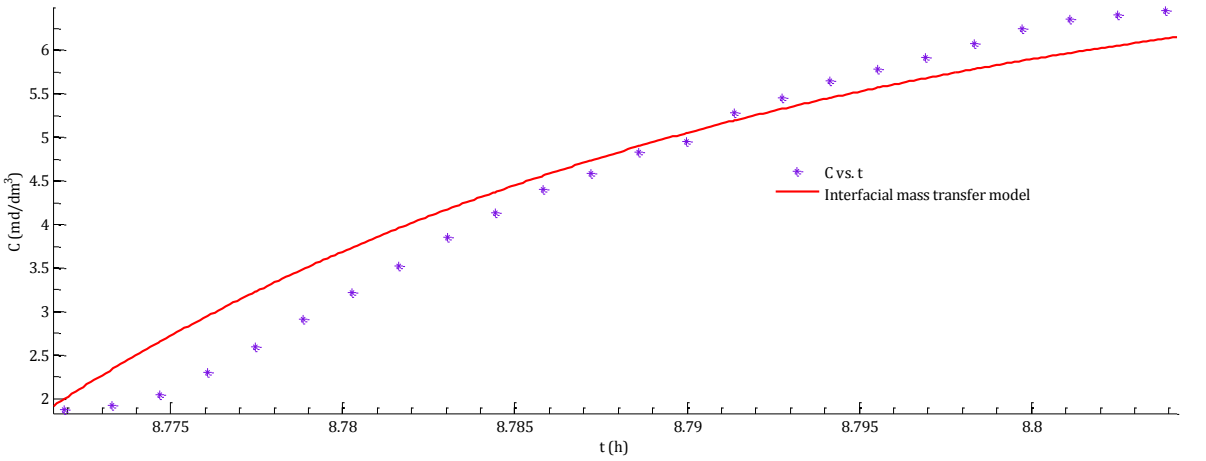

Fig.27: Experiment no.3 best non-linear fit after dosing of surfactant effluent: C_{DO} vs. t data set no.28

5.2.4 Experiment no.4 $k_L a$ estimates

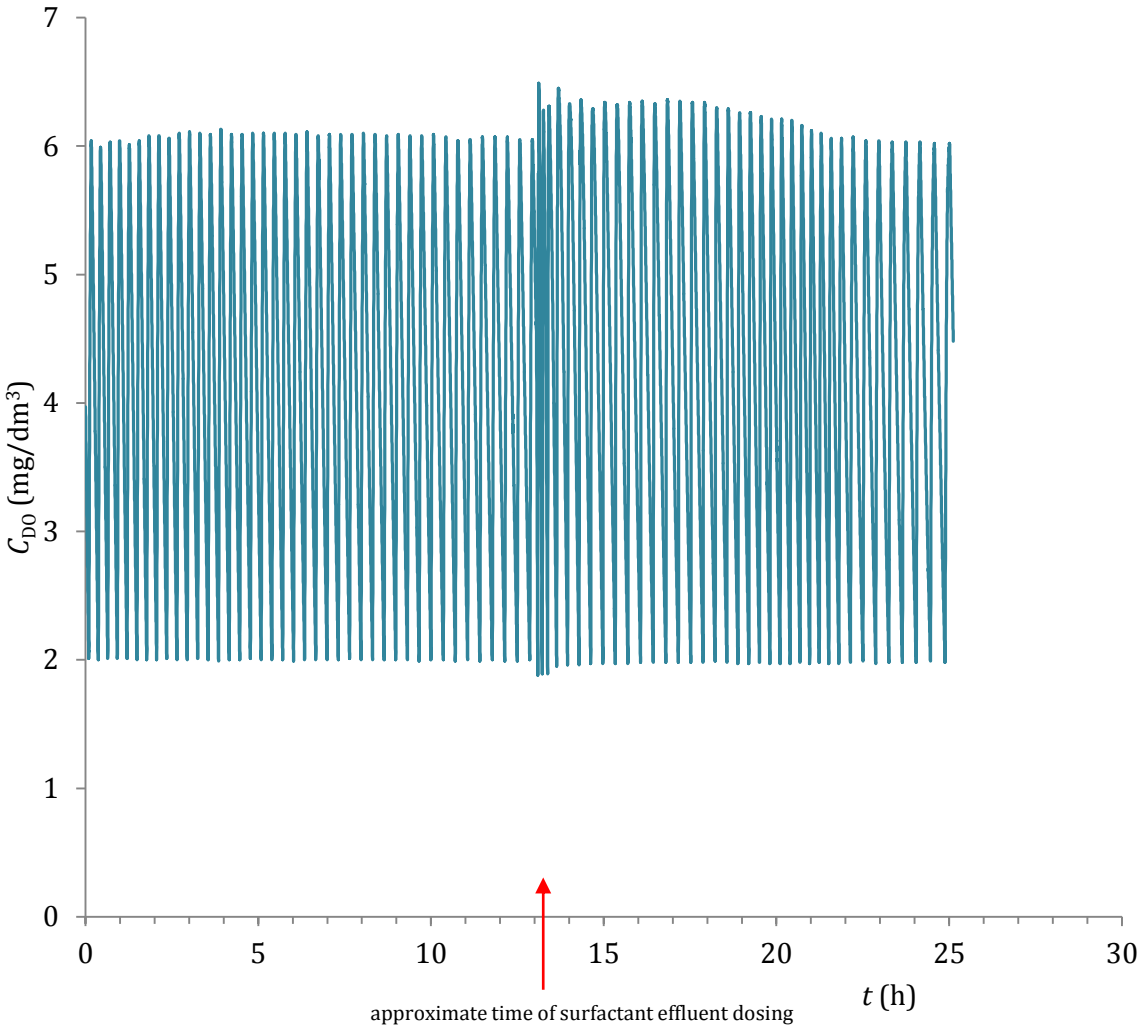

Fig.28: Scatter plot for experiment no.4 C_{DO} vs. t measurements

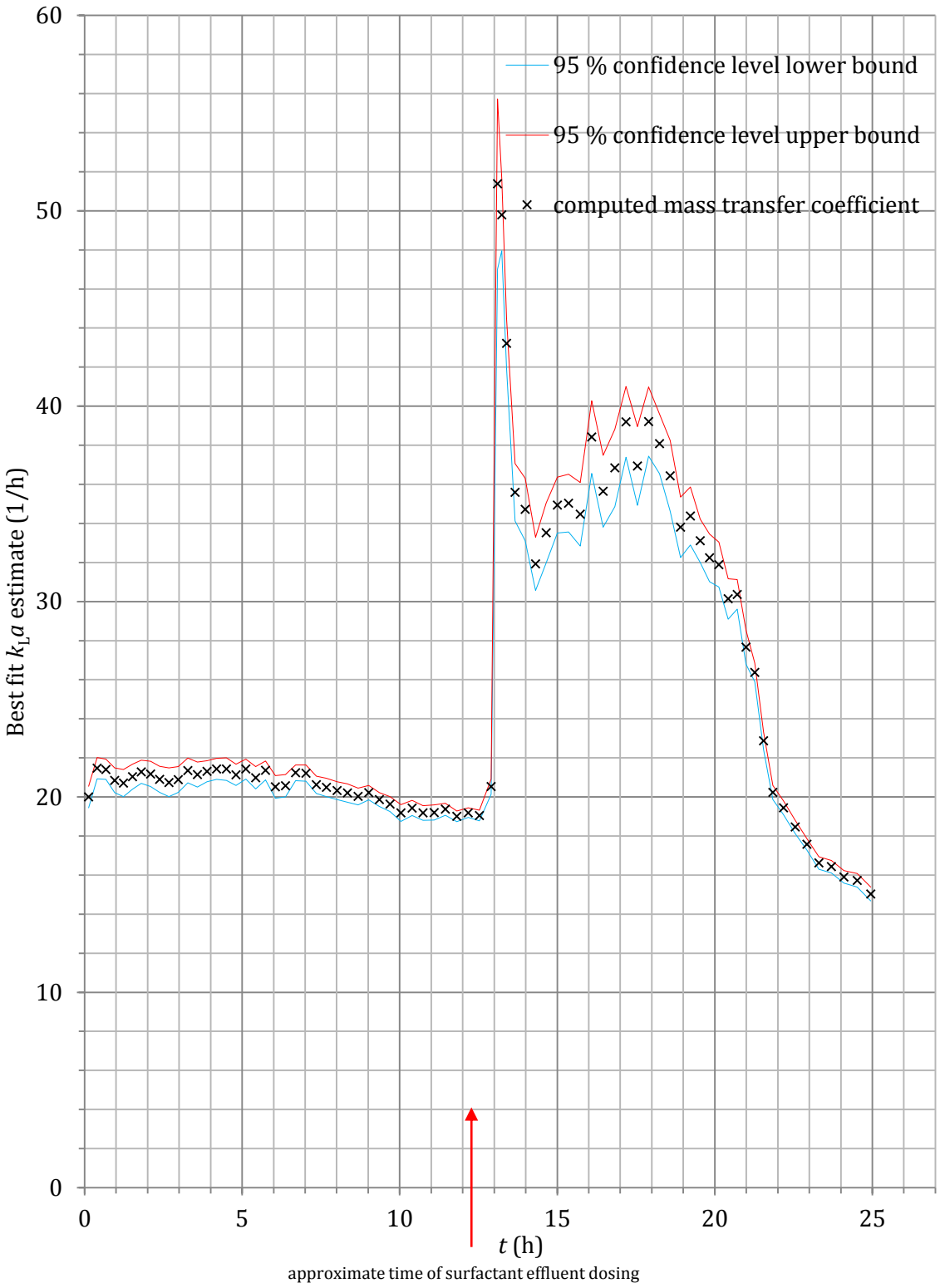

Fig.29: Scatter plot for experiment no.4 $k_L a$ vs. t estimates

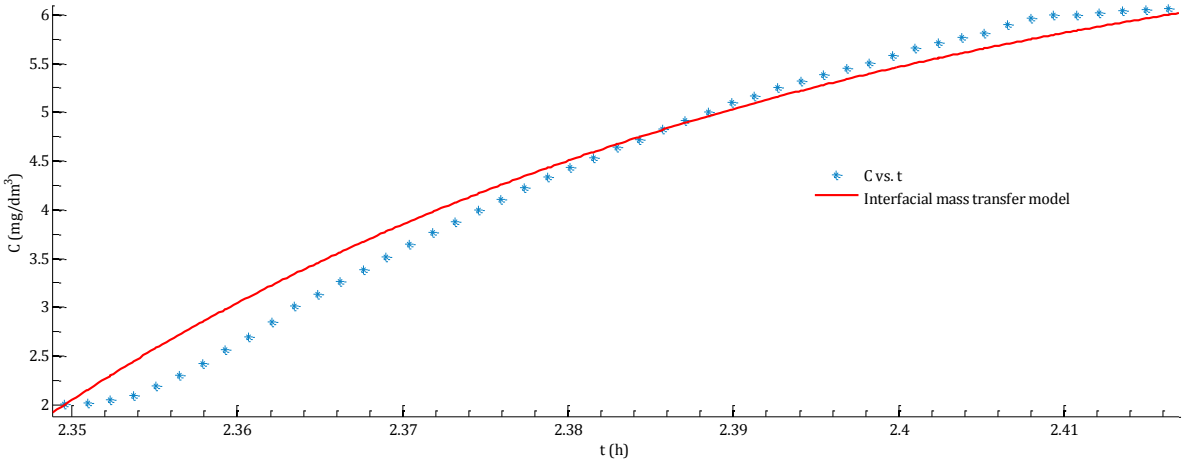

Fig.30: Experiment no.4 best non-linear fit prior to dosing of surfactant effluent: C_{DO} vs. t data set no.9

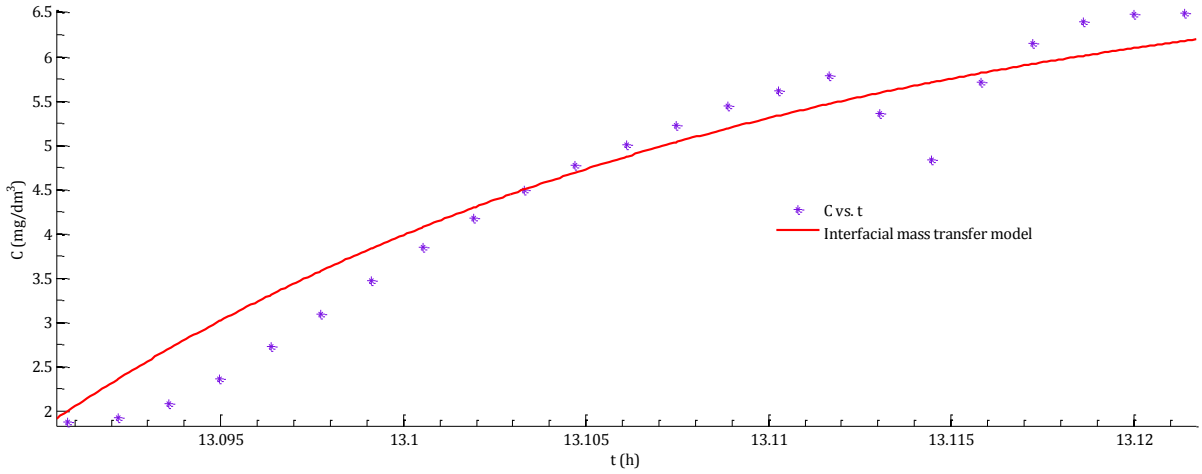

Fig.31: Experiment no.4 best non-linear fit after dosing of surfactant effluent: C_{DO} vs. t data set no.42

5.2.5 Experiment no.5 $k_L a$ estimates

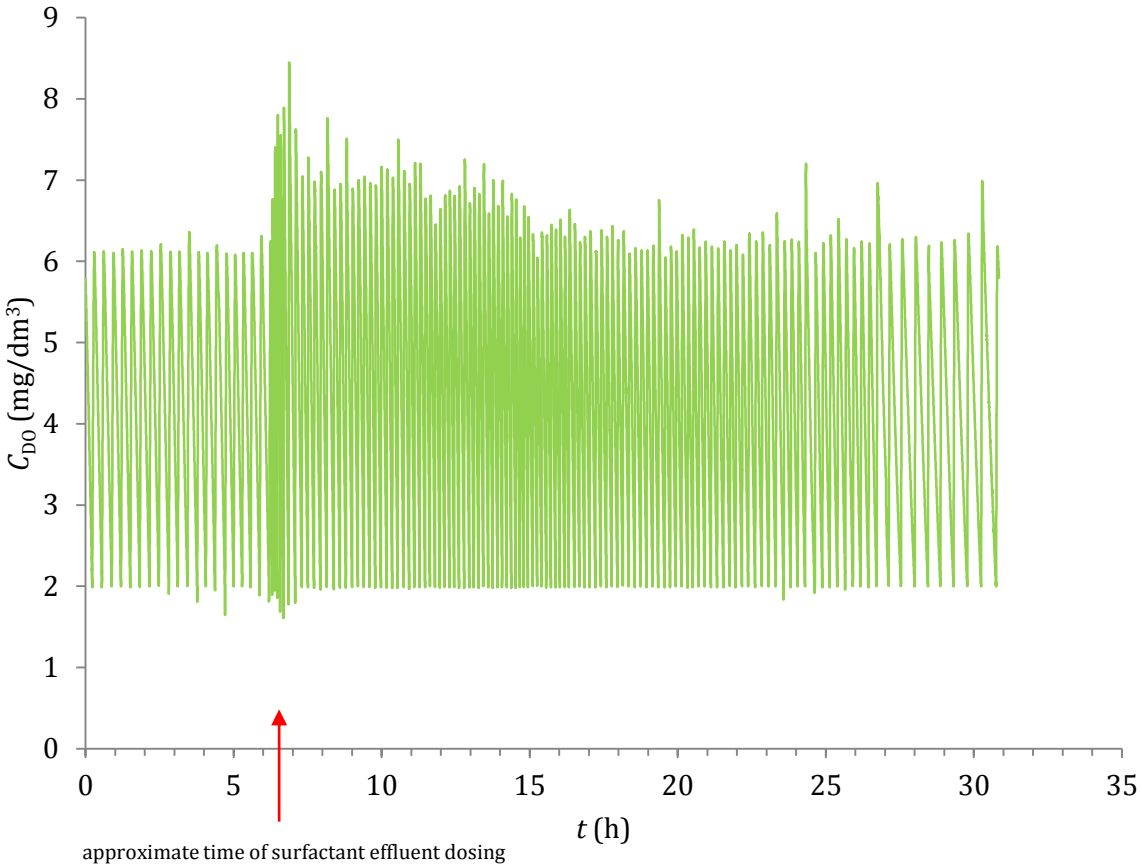

Fig.32: Scatter plot for experiment no.5 C_{DO} vs. t measurements

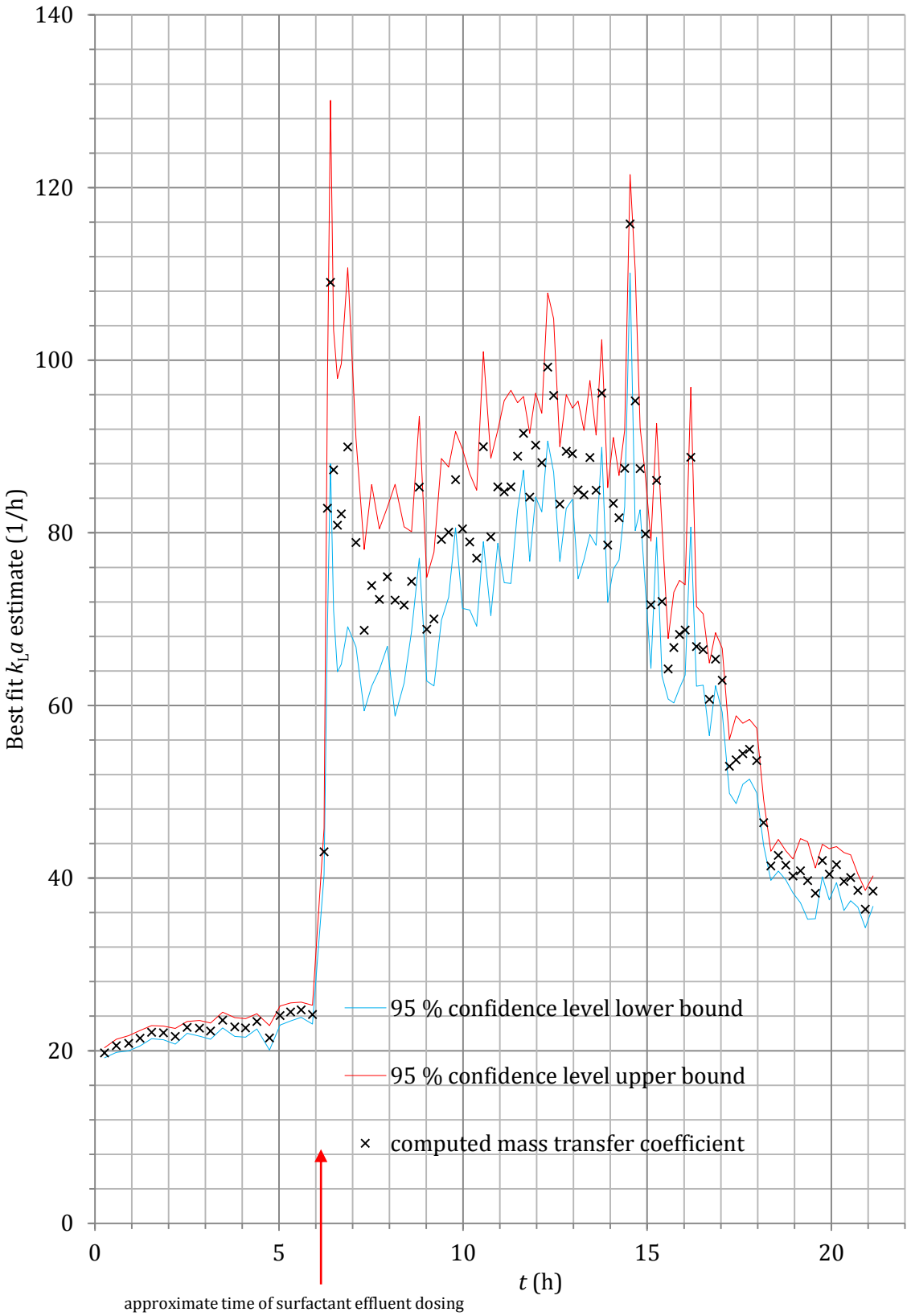

Fig.33: Scatter plot for experiment no.5 $k_L a$ vs. t estimates

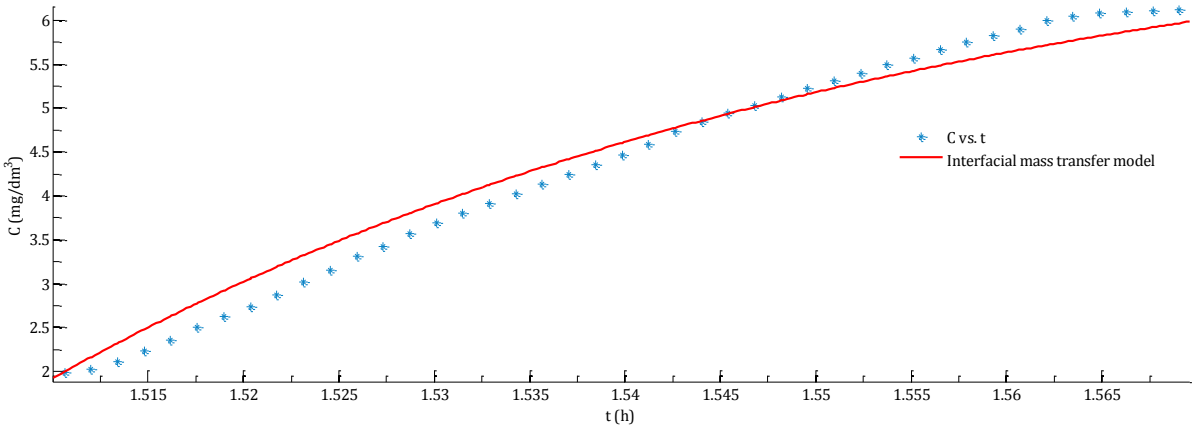

Fig.34: Experiment no.5 best non-linear fit prior to dosing of surfactant effluent: C_{DO} vs. t data set no.5

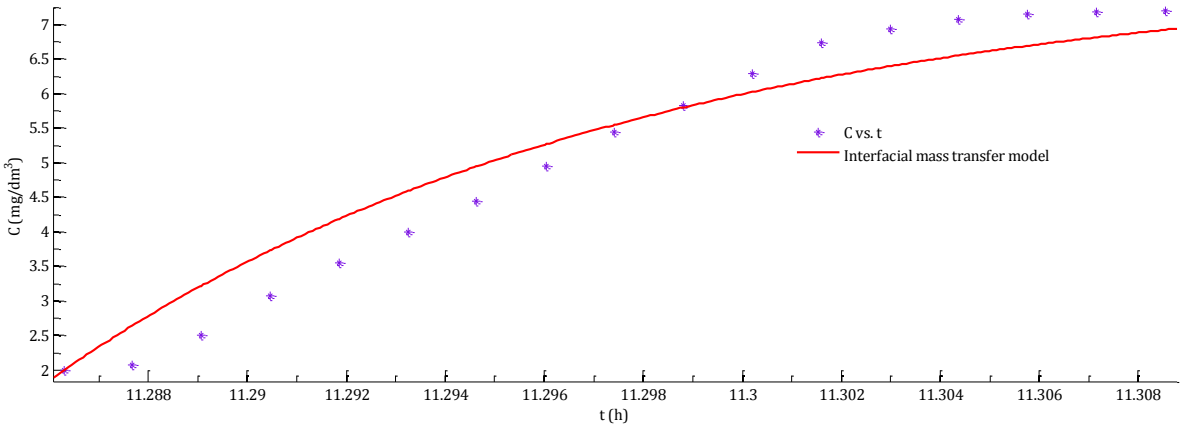

Fig.35: Experiment no.5 best non-linear fit after dosing of surfactant effluent: C_{DO} vs. t data set no.48

5.3 Biodegradability of Surfactant Effluents

For each respirometry experiment, a scatter plot for the OUR vs. t data was provided and on each plot, a baseline respiration rate demarcated the OUR_{exo} vs. t data points from the OUR_{end} vs. t data points. Along the $t-axis$ of each best fit respirogram, an arrow was inserted to indicate the time when a 0.1 dm^3 surfactant effluent load was dosed into the activated sludge system. Biodegradability was computed according to Equation 4.3.3.1.1 and the computation components, m_{S_S} and $m_{COD_{\text{soluble, total}}}$, were respectively computed using Equation 4.3.3.1.3 and Equation 4.3.3.1.4:

5.3.1 Experiment no.1 biodegradability estimates

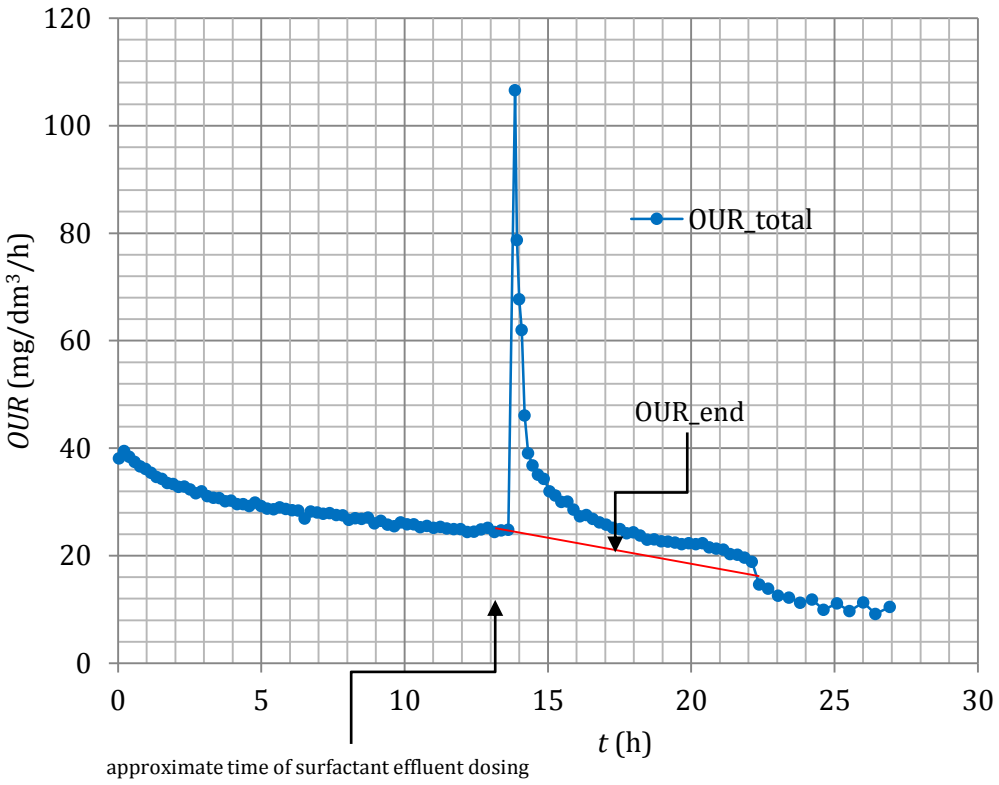

Fig.36: Experiment no.1 scatter plot of OUR vs. t measurements

$m_{S_S} = [125.6678/(1-0.63)]\ \text{mg/dm}^3 \times 1.6\ \text{dm}^3 = 543.428\ \text{mg}$

$m_{COD_{\text{soluble, total}}} = 31630\ \text{mg/dm}^3 \times 0.1\ \text{dm}^3 = 3163\ \text{mg}$

$$biodegradability = \left(\frac{m_{S_S}}{m_{COD_{\text{soluble, total}}}}\right) \times 100\% = (543.428\ \text{mg}/3163\ \text{mg}) \times 100\ \% = 17.18\ \%$$

5.3.2 Experiment no.2 biodegradability estimates

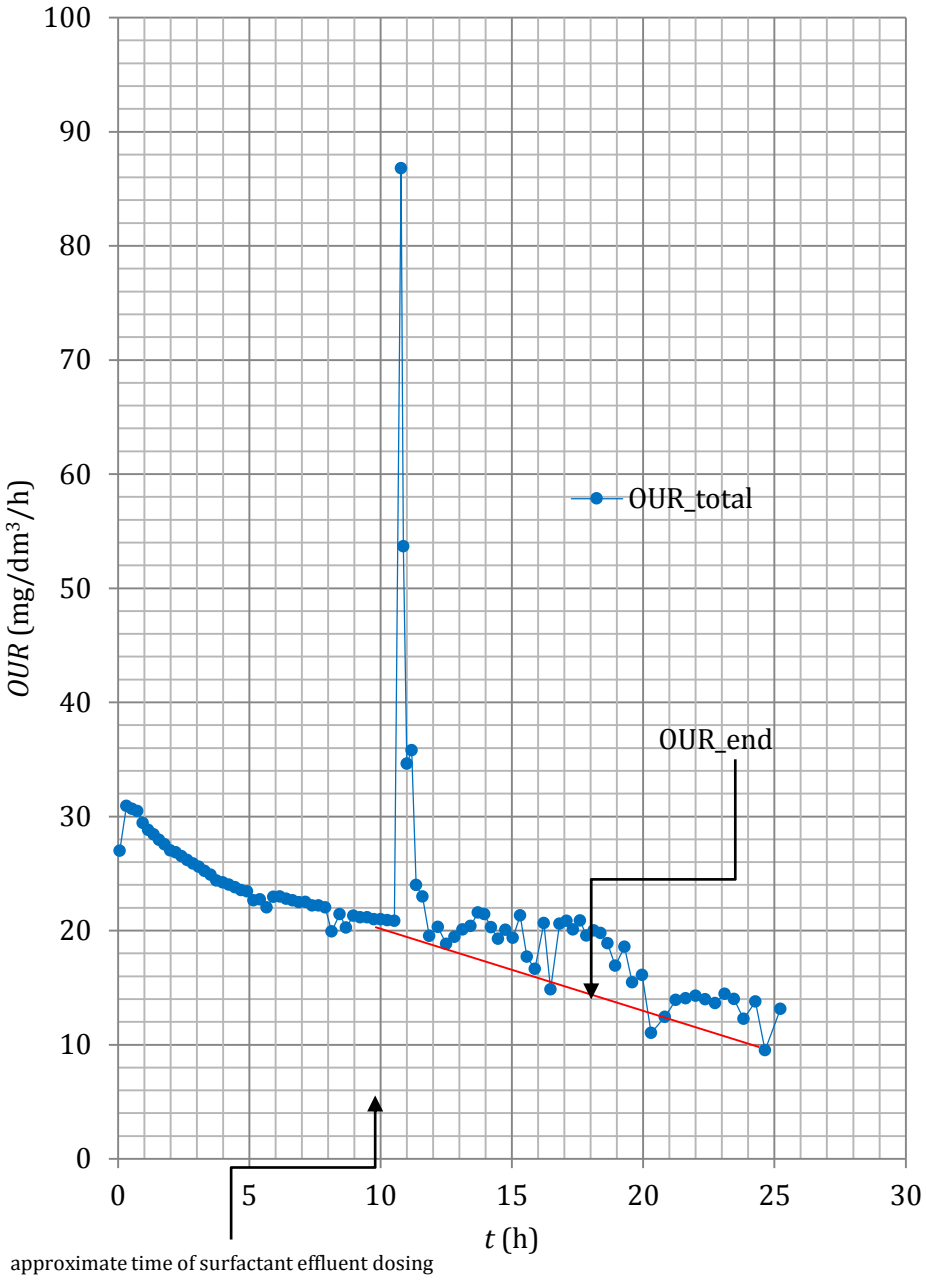

Fig.37: Experiment no.2 plot of OUR vs. t measurements

$m_{S_S} = [\ 152.2620/(1-0.63)]\ \text{mg/dm}^3 \times 1.6\ \text{dm}^3 = 658.43\ \text{mg}$

$m_{COD_{\text{soluble, total}}} = 31630\ \text{mg/dm}^3 \times 0.1\ \text{dm}^3 = 3163\ \text{mg}$

$$biodegradability = \left(\frac{m_{S_S}}{m_{COD_{\text{soluble, total}}}}\right) \times 100\% = (658.43\ \text{mg}/3163\ \text{mg}) \times 100\ \% = 20.82\ \%$$

5.3.3 Experiment no.3 biodegradability estimates

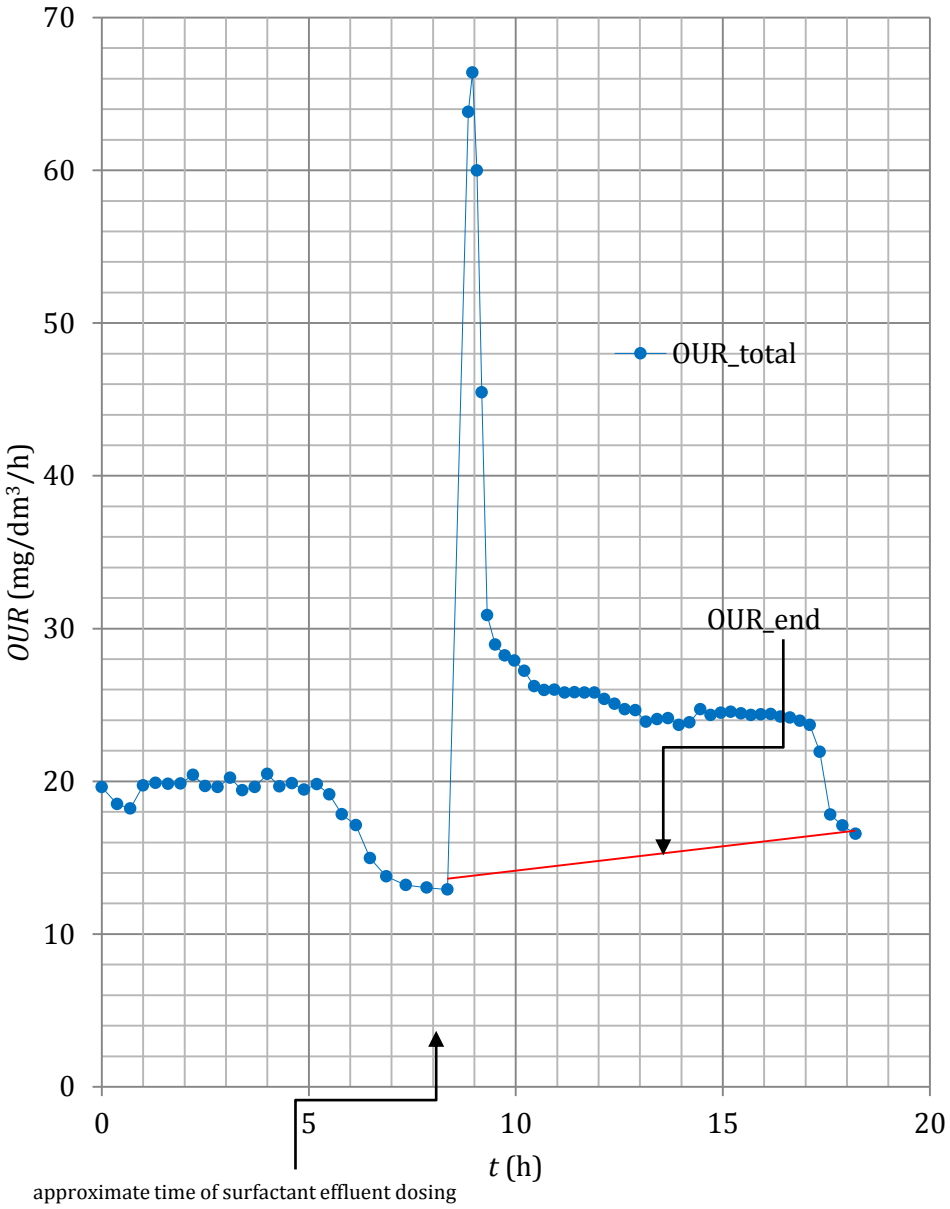

Fig.38: Experiment no.3 plot for OUR vs. t measurements

$m_{S_S} = [83.9102/(1 - 0.63)]\ \text{mg/dm}^3 \times 1.6\ \text{dm}^3 = 362.85\ \text{mg}$

$m_{COD_{\text{soluble, total}}} = 31630\ \text{mg/dm}^3 \times 0.1\ \text{dm}^3 = 3163\ \text{mg}$

$$biodegradability = \left(\frac{m_{S_S}}{m_{COD_{\text{soluble, total}}}}\right) \times 100\% = (362.85\ \text{mg}/3163\ \text{mg}) \times 100\ \% = 11.47\ \%$$

5.3.4 Experiment no.4 biodegradability estimates

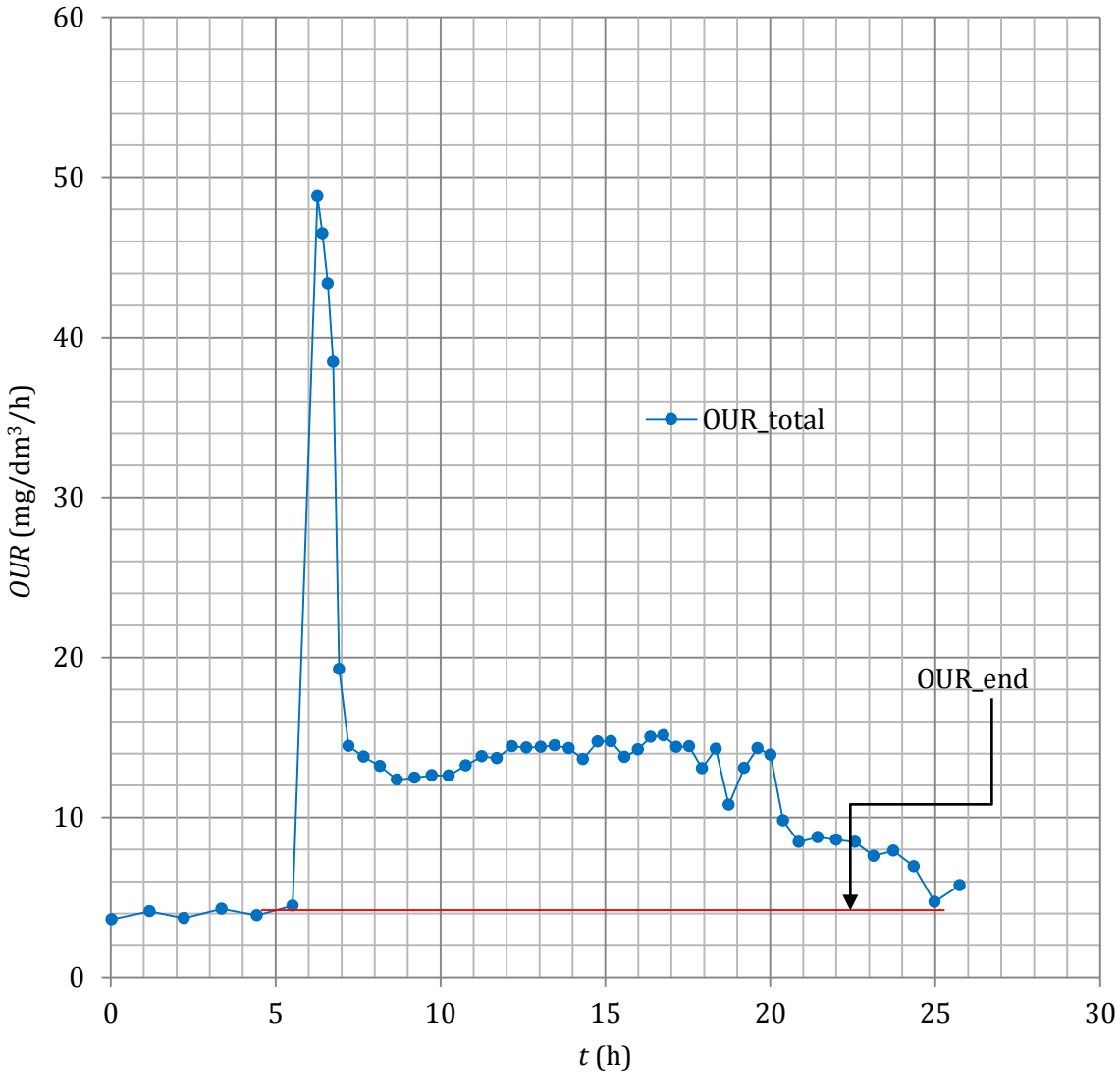

Fig.39: Experiment no.4 plot of OUR vs. t measurements

$m_{S_S} = [182.1141/(1 - 0.63)]\ \text{mg/dm}^3 \times 1.6\ \text{dm}^3 = 787.52\ \text{mg}$

$m_{COD_{\text{soluble, total}}} = 31630\ \text{mg/dm}^3 \times 0.1\ \text{dm}^3 = 3163\ \text{mg}$

$$biodegradability = \left(\frac{m_{S_S}}{m_{COD_{\text{soluble, total}}}}\right) \times 100\% = (787.52\ \text{mg}/3163\ \text{mg}) \times 100\ \% = 24.89\ \%$$

5.3.5 Experiment no.5 biodegradability estimates

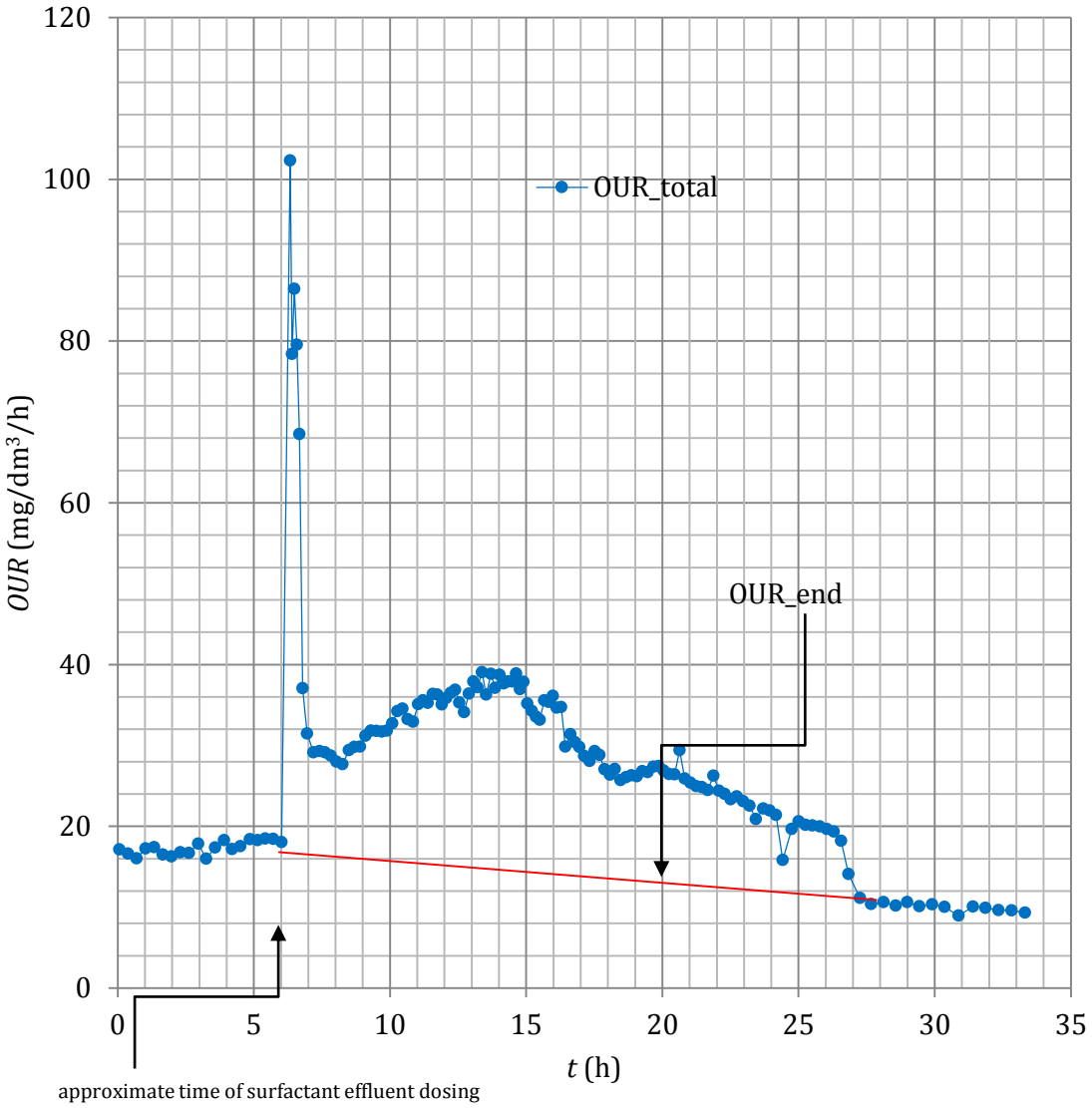

Fig.40: Experiment no.5 plot for OUR vs. t measurements

$m_{S_S} = [380.8685/(1 - 0.63)]\ \text{mg/dm}^3 \times 1.6\ \text{dm}^3 = 1606.02\ \text{mg}$

$m_{COD_{\text{soluble, total}}} = 31630\ \text{mg/dm}^3 \times 0.1\ \text{dm}^3 = 3163\ \text{mg}$

$$biodegradability = \left(\frac{m_{S_S}}{m_{COD_{\text{soluble, total}}}}\right) \times 100\% = (1606.02\ \text{mg}/3163\ \text{mg}) \times 100\ \% = 52.07\ \%$$

6. DISCUSSION

6.1 Soluble Dye Effluents Decolourisation

From the analytical methods and computations employed in this study, the resulting data sets of $m_{\text{dye, adsorbed}}$ vs. t, q vs. t, q vs. C and q_∞ all seemed to support the hypothesised mechanism of biosorption through which decolourisation of soluble dye effluents takes place in receiving municipal activated sludge systems.

For an activated sludge system with a fixed mass of adsorbent (i.e. where there are no microbial growth processes resulting from CH_3COOH dosing), scatter plots of $m_{\text{dye, adsorbed}}$ vs. t show that the mass of the adsorbate particles removed from solution attains an asymptotic value of $m_{\text{dye, solution},\infty} = 0.00407\text{g}$ at $t \cong 1\text{ h}$, when the adsorbate particles (soluble dye effluent) occupy all the adsorption sites on the adsorbent (VSS) surface, with negligible interaction between adsorbed particles on the different adsorption sites being assumed.

In the $m_{\text{dye, adsorbed}}$ vs. t data set, the initial sharp increase in the mass of adsorbate removed from solution in the presence of CH_3COOH dosing at $t \leq 1$ h was likely to have resulted from the non-equilibrium loading of the sludge.

The hypothesised biosorption decolourisation mechanism seems to be further corroborated by q vs. C adsorption equilibrium data which conforms to the adsorption model previously reported by LeVan M.D., Carta G. et al. (1999) to describe a system with a fixed mass of adsorbent and a single adsorbate in solution: $q = KC$, where the computed adsorption parameter, K, for this study was $K = 0.4175\ \text{dm}^3/\text{g}$ adsorbate. For single adsorbate in solution systems, the value of the adsorption parameter is reported to give a measure of the distribution of the adsorbate particles on the adsorbent sites and the value of $K = 0.4175\ \text{dm}^3/\text{g}$ adsorbate that was computed for a laboratory-scale activated sludge system is much lower than those reported for other adsorbents and this shows that the activated sludge system is not a good adsorption system for the removal of soluble dye effluents from solution.

For both systems where there is a fixed mass of adsorbent (no microbial growth processes resulting from CH_3COOH dosing) and where there is a varying mass of the same adsorbent (sludge addition from microbial growth processes resulting from CH_3COOH dosing), similar values for the adsorptive capacity or maximum ratio of the mass of dye adsorbed per unit mass of adsorbent were computed ($q_\infty = 0.0009$ g dye adsorbed/g VSS) and this seems to further support the hypothesis that soluble colour removal in receiving municipal activated sludge system takes place through biosorption as opposed to biodegradation.

From the $m_{\text{dye, adsorbed}}$ vs. t and q vs. t data sets, adsorption equilibrium is reached at $t = 1$ h and if this is compared with the hydraulic residence times of the receiving municipal wastewater treatment plants where:

1. $t_{\text{hydraulic retention}} = 6$ h

2. soluble colour decolourisation through the conventional activated sludge process is completed in much less time than the hydraulic residence time of the plant

this means that soluble colour removal in receiving municipal activated sludge systems will not be rate limited but does not imply that adsorption kinetics were not relevant in this study. They were relevant however, it was not necessary to predict the kinetics accurately.

6.2 Effect of Surfactant Effluents on Oxygen Transfer

For each experiment in Section 5.2, fairly uniform values of $k_{\mathrm{L}}a$ estimates were computed prior to the dosing of the surfactant effluent ($\cong$ 20 1/h). However after dosing the surfactant effluent, there were sudden and pronounced increments in the computed estimates of $k_{\mathrm{L}}a$ which exhibited different maximum values in each experiment.

Furthermore for each experiment, the marked increments in the computed estimates of $k_{\mathrm{L}}a$ coincided with noticeable increments in the non-linear regression confidence level error bounds associated with each $k_{\mathrm{L}}a$ estimate instantaneously after dosing the activated sludge system with a load of surfactant effluent.

The increments in the non-linear regression confidence level error bounds associated with each $k_{\mathrm{L}}a$ estimate after the dosing of the surfactant effluent could be a result of either the sudden fouling on the DO probe's permeable membrane surface in contact with the surfactant effluent or other interferences in the Clark dissolved oxygen sensor's measurement mechanism from the presence of the surfactant effluent. Consequently, this could have adversely impacted the DO probe's response time and resulted in erroneous logging of C_{DO} vs. t data sets.

This supposition seems to be corroborated by exhibitions of individual non-linear fits of the modified Lewis-Whitman interfacial mass transfer model onto C_{DO} vs. t data sets selected prior to and after contacting the activated sludge system with the surfactant effluent where for each experiment prior to the dosing of the surfactant effluent, non-linear fits of the model onto experimental data sets exhibit satisfactory goodness-of-fit graphical outputs as shown in Fig.18 (Experiment no.1), Fig.22 (Experiment no.2), Fig.26 (Experiment no.3), Fig.30 (Experiment no.4) and Fig.34 (Experiment no.5).

However instantaneously after dosing the surfactant effluent, the opposite is observed as exhibited by imperfect fits where the goodness-of-fit graphical outputs with fewer data points as shown on Fig.19 (Experiment no.1), Fig.23 (Experiment no.2), Fig.27 (Experiment no.3), Fig.31 (Experiment no.4) and Fig.35 (Experiment no.5).

This could be direct evidence of retardation of the dissolved oxygen sensor's response time as a result of fouling on the dissolved oxygen sensor's permeable membrane when it comes into contact with the surfactant effluent. It is also highly probable that the surfactant effluent imparted some form of interference to the dissolved oxygen sensor's dissolved oxygen measurement mechanism thus indirectly resulting in the retardation of the electrode's response time.

The sudden and pronounced increments in the computed estimates of $k_{\mathrm{L}}a$ after contacting the activated sludge system with the surfactant effluent could have resulted in the surfactant effluent imparting an increment on either the liquid film mass transfer coefficient (k_{L}) or the interfacial area (a) or both.

There is also the possibility that the marked increase in the computed estimates of $k_{\mathrm{L}}a$ could have resulted from reaction-enhanced mass transfer as evidenced by the ensuing oxygen uptake rates (OUR) measurements after the dosing of the surfactant effluent, where the OUR measurements simultaneously exhibit incredibly similar sudden and pronounced increments instantaneously after the dosing of the surfactant effluent.

Comparative computations of $k_{\mathrm{L}}a$ estimates in the presence of a non-surfactant substrate (CH_3COOH) should be conducted to elucidate the $k_{\mathrm{L}}a$ estimates resulting from reaction-enhanced mass transfer from $k_{\mathrm{L}}a$ estimates resulting from the impact of the surfactant on either the liquid film mass transfer coefficient (k_{L}) or the interfacial area (a) or both.

For each respirometry experiment, the following were observed:

1. towards the end of the experiment as $t \longrightarrow t_{\mathrm{R}}$, $(k_{\mathrm{L}}a)_{t \to t_{\mathrm{R}}} \longrightarrow (k_{\mathrm{L}}a)_{0<t<t_{\text{effluent dosing}}}$

   where

   $t_{\text{effluent dosing}} =$ approximate time of surfactant effluent dosing, (h)

2. at the of each experiment at $t = t_{\mathrm{R}}$, $(k_{\mathrm{L}}a)_{t=t_{\mathrm{R}}} \cong (k_{\mathrm{L}}a)_{0<t<t_{\text{effluent dosing}}}$

It is highly probable that this resulted from the depletion of the readily biodegradable active components of the surfactants responsible for the increase in $k_{\mathrm{L}}a$ and this depletion was through aerobic assimilation by the heterotrophic microbial populations, X_{H}, in the activated sludge system.

Inevitably this could have resulted in a gradual decrement in the values of $k_{\mathrm{L}}a$ estimates computed during exogenous respiration (after dosing of the surfactant effluent) either through:

1. the attenuation of the reaction rates enhancing interfacial oxygen transfer or

2. the decline in the impact of the readily biodegradable active components of the surfactant effluent on k_{L} or a or both

6.3 Biodegradability of Surfactant Effluents

With reference to OUR vs. t plots shown in Section 5.3, the transition of OUR measurements from OUR_{end} to OUR_{exo} at the instant when the surfactant effluent was dosed into the activated sludge system was an indicator for higher dissolved oxygen demand by the respiring microbial populations as a result of assimilation and biodegradation of soluble organic substrates in the effluent.

In all respirometry experiments, numerical estimates of biodegradability ($max \cong 52.07\ \%$) were all far less than the estimates reported in literature by surfactant manufacturers ($\geq 90\ \%$).

Since OUR vs. t measurements were simultaneously logged together with C_{DO} vs. t measurements from the same experiment, it is highly probable that the shortcomings of the analytical protocol described in Section 4.2 which resulted in erratic experimental data points after the dosing of the surfactant effluent also extended to the biodegradability assessment where the surfactant effluent either fouled the Clark dissolved oxygen sensor's permeable membrane surface it was in contact with or imparted some form of interference to the measurement mechanism of the dissolved oxygen sensor.

Retardation of the dissolved oxygen sensor's response time as a result of fouling of the sensor's permeable membrane when it comes into contact with the surfactant effluent could have led to lower estimates of biodegradability being computed in comparison to those cited by surfactant manufacturers. Furthermore, this phenomenon could have also resulted in irreproducible computations of biodegradability in the separate experiments in which the activated sludge system was contacted with the same load of surfactant effluent.

It is also highly probable that the pronounced dissimilarities between the biodegradability estimates computed through the respirometry experiment and the estimates cited in literature by the surfactant manufacturers could have been a result of the following possibilities:

1. the presence of toxic components in the surfactant effluent which resulted in the gradual inhibition of microbial activity and death of active microbial populations in the activated sludge system

   According to the study by Liwarska-Bizukojć and Bizukojć (2005), surfactants exhibit strong adsorbing properties and are highly likely to adsorb onto the activated sludge flocs. This adsorption in combination with toxicity have been reported to inhibit and negate biological activity in the activated sludge system and this ultimately leads to diminished removal of COD and BOD_5.

2. there is a significant amount of slowly biodegradable substrates and inert soluble substrates present in the surfactant effluent and these substrates are not depleted through aerobic utilisation and direct absorption by heterotrophic microbial populations, X_{H}, during the time in which the activated sludge is contacted with the surfactant effluent $\left(t_{\text{effluent dosing}}\ t < t_{\mathrm{R}}\right)$.

   Furthermore there are significant differences between the respirometry experiment and the methodologies employed by the surfactant manufacturers in computing biodegradability.

   The biodegradability reported in literature by the surfactant manufacturers of $> 90\%$ is not necessarily rapid or ready biodegradability but is in fact ultimate biodegradability which was computed after $t = 28\ \mathrm{d} = 672\ \mathrm{h}$ in accordance to the ISO 7827:2010 Biodegradability Testing Protocol for evaluating the rapid or ready and ultimate biodegradability of organic compounds in an aqueous medium through the dissolved organic carbon method of analysis (ISO 7827, 2010).

   Contrasting the respirometry experiment with the ISO 7827:2010 Biodegradability Testing Protocol, the total time of contacting the activated sludge system with surfactant effluent is far lesser than that employed in the ISO 7827:2010 method:
   $\left[\left(t_{\text{effluent dosing}}\ t < t_{\mathrm{R}}\right) \cong 15\ \mathrm{h}\right] \ll 672\ \mathrm{h}$.

The probable implication is that the contact time between the surfactant effluent and the activated sludge system in the respirometry experiment is not sufficient to allow for the biodegradation of slowly biodegradable substrates and inert soluble substrates in the surfactant effluent. This implied the computed biodegradability levels far lesser than those attained through the ISO 7827:2010 methodology ($> 90\%$ after $t = 672$ h).

The presence of slowly biodegradable substrates and inert soluble substrates in the surfactant effluent which both cannot undergo rapid biodegradation as would have been computed by the respirometry experiment is corroborated by the study on aerobic biodegradation of surfactants according to Jurado et al. (2013). In this study, surfactant biodegradation levels of $> 90\%$ through the respirometric test were attained at $t >$ 600 h.

7. CONCLUSION

7.1 Biodegradability of Surfactant Effluents

The analytical protocol that was developed to provide a measure of the extent to which an activated sludge system was be capable of decolourising a soluble dye effluent with a known initial concentration was adequately suitable in exhibiting that soluble dye effluent decolourisation does take place in the activated sludge system.

Furthermore, the postulated decolourisation mechanism of physisorption was confirmed by $m_{\text{dye, adsorbed}}$ vs. t measurements which showed that the mass of soluble dye effluent particles removed from solution rapidly reached an asymptotic equilibrium value at $t \cong 1$ h and the adsorption equilibrium data conformed to an adsorption model for the physical adsorption system for a single adsorbate in solution.

The adsorptive capacity of an activated sludge system with microbial growth processes taking place as a result of the presence of biodegradable substrates was similar to that with a fixed amount of adsorbent and this further supported the hypothesised that the most probable mechanism through which soluble dye effluents are decolourised in receiving municipal wastewater treatment plants is physical adsorption. However, the computed values of the adsorption equilibrium parameter from the adsorption model and adsorptive capacity show that the activated sludge system is a poor adsorbent for the removal of soluble dyes from solution in comparison with other adsorbents reported in literature.

Since adsorption equilibrium is reached in $t \leq 1$ h in the activated sludge system and this is far less than the activated sludge process residence time and also takes place much faster than other activated sludge processes, the removal of soluble colour in receiving municipal activated sludge systems is not a rate limited process and it was therefore concluded that whilst adsorption kinetics were relevant to the study, it was not necessary to predict the kinetics accurately.

7.2 Effect of Surfactant Effluents on Oxygen Transfer

In the study for quantifying the effects of a surfactant effluent on oxygen transfer in an activated sludge system, the analytical methods and computations that were developed for the study did provide adequate and satisfactory suitability in accurately computing estimates of $k_{\mathrm{L}}a$ which were intended to mathematically quantify the effects of the surfactant effluent on oxygen transfer from air to the waster phase of the activated sludge system prior to and after loading the activated sludge system with the surfactant effluent.

Instantaneously after dosing the activated sludge system with the surfactant effluent, computed estimates of $k_{\mathrm{L}}a$ exhibited sudden and strongly marked increments which reached a maximum after which the values of $k_{\mathrm{L}}a$ estimates attenuated with time and eventually approached the initial values computed prior to contacting the activated sludge system with the surfactant effluent. This led to the conclusion that the presence of surfactants increases oxygen transfer from air to the water phase of the activated sludge by imparting an increment to either the liquid film mass transfer coefficient (k_{L}) or the interfacial area (a) or both or both.

It was also concluded that there is the possibility of the marked increase in the computed estimates of $k_{\mathrm{L}}a$ resulting from reaction enhanced mass transfer as evidenced by the ensuing sudden and pronounced increments in the oxygen uptake rates (OUR) measurements after the dosing of the surfactant effluent.

This implies that comparative computations of $k_{\mathrm{L}}a$ estimates in the presence of a non-surfactant substrate such as CH_3COOH should be conducted for purposes of elucidating the $k_{\mathrm{L}}a$ estimates resulting from reaction enhanced mass transfer from $k_{\mathrm{L}}a$ estimates resulting from the impact of the surfactant on either the liquid film mass transfer coefficient (k_{L}) or the interfacial area (a) or both.

Whilst the analytical protocol that was developed for the study can be employed for assessing the effects of surfactant effluents on oxygen transfer in the activated sludge systems of receiving municipal wastewater treatment plants, further refinements into the methodology are required in automating the computation of $k_{\mathrm{L}}a$ estimates and generating scatter plots of $k_{\mathrm{L}}a$ vs. t from automated real-time feeds of C_{DO} vs. t data from dissolved oxygen online instrumentation.

In its present form, the analytical protocol that was developed in this study is exceedingly arduous and cumbersome and has the following shortcomings:

1. there is manual identification of C_{DO} vs. t data sets representing reoxygenation phases of aeration cycles from which $k_L a$ estimates are computed

2. for each reoxygenation phase C_{DO} vs. t data set, the oxygen uptake rate (OUR) component of the modified form of the Lewis-Whitman interfacial mass transfer model has to be manually estimated from the ensuing deoxygenation phase C_{DO} vs. t data set

3. for each computation of $k_L a$, a time offset corresponding to the first t data point in the C_{DO} vs. t data set onto which the model is fitted has to be manually incorporated into model prior to fitting and non-linear regression results from the fit have to be manually collated prior to the generation of $k_L a$ vs. t scatter plots

Through further and separate studies, further automation of the methodology is required for meaningful implementation into the protocol for assessing the performance of receiving municipal activated sludge systems as part of eThekwini Municipality's industrial effluent discharge permitting system.

7.3 Biodegradability of Surfactant Effluents

From the shapes of the scatter plot profiles of OUR vs. t in which there was a transition from OUR_{end} to OUR_{exo} at the instant when a load of surfactant effluent was dosed into the activated sludge system, it was concluded that this seemed to be confirmation of the postulation that a certain fraction of the surfactant effluent was biodegradable.

However the OUR vs. t measurements from which biodegradability was computed were simultaneously logged using the same experimental apparatus and methods constituting the analytical protocol which was developed for computing $k_L a$ estimates from C_{DO} vs. t data sets and this implied that the shortcomings observed in this analytical protocol where there was retardation of the dissolved oxygen sensor's response time as a result of fouling of the sensor's permeable membrane when it comes into contact with the surfactant effluent were also extended to the assessment of biodegradability of the surfactant effluent.

This postulation was corroborated by the computed estimates of biodegradability which were irreproducible across the separate experiments in which the activated sludge system was contacted with the same load of surfactant effluent.

The computed estimates of biodegradability were all far less than those reported in literature by surfactant manufacturers and it was therefore concluded that the analytical protocol that was developed for the study did not provide satisfactory suitability in accurately computing biodegradability of the surfactant effluent.

It was therefore concluded that whilst the methodology showed that a certain fraction surfactant effluents is biodegradable in the activated sludge system, the analytical protocol cannot be sufficiently employed for assessing the biodegradability of surfactant effluents in the activated sludge systems of receiving municipal wastewater treatment plants.

REFERENCES

Abo-Elela, S.I.; El-Gohary, F.A.; Ali H.I.; Wahaab R.Sh. A. Treatability Studies of Textile Wastewater, *Environmental Technology Letters*, **1988**, *9*, (2)

Abramowitz, M.; Stegun, I. A. *Handbook of Mathematical Functions with Formulas, Graphs, and Mathematical Tables*, 9th Edition, **1972**, Courier Dover Publications

Aksu, Z. Biosorption of Reactive Dyes by Dried Activated Sludge, Equilibrium and Kinetic Modelling, *Biochemical Engineering Journal*, **2001**, *7*, 9 – 84

Alam, M.Z. Biosorption of Basic Dyes Using Sewage Treatment Plant Biosolids, *Biotechnology* **2004**, *3*, (2), 200 – 204

Al-Ghouti, M.A.; Khraisheh, M.A.; Allen S.J.; Ahmad M.N. The Removal of Dyes from Textile Wastewater: A Study on the Physical Characteristics and Adsorption Mechanisms of Diatomaceous Earth, *J. Environ. Manage.*, **2003**, *69,* (3), 229 – 38

American Association of Textile Chemists and Colorists. *Color Technology in the Textile Industry*, **1997**, 2nd Edition, AATCC

American Association of Textile Chemists and Colorists. *Textile Chemist and Colorist*, **1999**, *31*, (1 – 8), AATCC

American Public Health Association, American Water Works Association and Water Environment Federation. *Standard Methods for the Examination of Water and Wastewater*, **1995**, American Public Health Association

American Society of Civil Engineers - Oxygen Transfer Standards Subcommittee. *Development of Standard Procedures for Evaluating Oxygen Transfer Devices*, **1983**, EPA-600/2-83-102, U.S. Environmental Protection Agency

Asano, K. *Mass Transfer: From Fundamentals to Modern Industrial Applications*, **2006**, John Wiley and Sons.

ASCE. *Standard-Measurement of Oxygen Transfer in Clean Water*, **1991**, ANSI/ASCE 2 – 91, American Society of Civil Engineers, New York

Ash, M.; Ash, I. *Handbook of Industrial Surfactants: An International Guide to More Than 21,000 Products by Trade Name, Composition, Application and Manufacturer*, 1997, Vol.2 and Vol.7, Gower Publishing

Ash, M.; Ash, I. *Handbook of Green Chemicals*, **2004**, 2nd Edition, Synapse Info Resources

Augustine, A.A.; Orike, B.D.; Edidiong, A.D. Adsorption Kinetics and Modeling Of Cu(II) Ion Sorption From Aqueous Solution By Mercaptoacetic Acid Modified Cassava (Manihot Sculenta Cranz) Wastes, *EJEAFChe*, **2007**, *6*, (4), 2221-2234

Bailey, J.E., Ollis, D.F. *Biochemical Engineering Fundamentals*, **1986**, 2nd Edition, New York, NY: McGraw-Hill

Basibuyuk, M.; Forster, C.F. An Examination of the Treatability of a Simulated Textile Wastewater Containing Maxilon Red BL-N, *Process Biochemistry*, **1997**, *32*, (6), 523 - 527

Beydilli, M. I.; Pavlostathis, S.G.; Tincher, W.C. Biological Decolorization of the Azo Dye Reactive Red 2 under Various Oxidation-Reduction Conditions, *Water Environment Research*, **2000**, *72*, (6), 698 – 705.

Boyd, G.E.; Adamson, A.W.; Myers L.S. The Exchange Adsorption of Ions from Aqueous Solutions by Organic Zeolites. II. Kinetics, *Journal of the American Chemical Society*, **1947**, *69*, (11), 2836 – 2848

Bronshtein, I.N.; Semendyayev, K.A.; Musiol, G.; Muehlig, H. *Handbook of Mathematics*, **2007**, 5th Edition, Springer-Verlag.

Brouwer, H.; Klapwijk, A.; Keesman, K.J. Identification of Activated Sludge and Wastewater Characteristics Using Respirometric Batch-Experiments, *Water Research*, **1998**, *32*, (4), 1240 – 1254

Brusatori, M.A.; van Tassel, P.R. A Kinetic Model of Protein Adsorption/Surface-Induced Transition Kinetics Evaluated by the Scaled Particle Theory, *Journal of Colloid and Interface Science*, **1999**, *219*, (2), 333 – 338

Carr, C.M. *Chemistry of the Textiles Industry*, **1995**, Springer

Carvalho, G.; Nopens, I.; Novais, J. M.; Vanrolleghem, P. A.; Pinheiro, H. M. Modelling of Activated Sludge Acclimisation to a Non-ionic, *Water Science and Technology*, **2001**, *43* (7), 9 – 17, IWA Publishing

Carvalho, G.; Paul E.; Novais, J.M.; Pinheiro, H.M. Studies on Activated Sludge Response to Variations in the Composition of a Synthetic Surfactant-containing Feed Effluent, *Water Science and Technology*, **2000**, *42*, (5, 6), 135 – 143, IWA Publishing

Cheng, W.; Wang, S.G.; Lu, L.; Gong, W.X.; Liu, X.W.; Gao, B.Y.; Zhang, H.Y. Removal of Malachite Green (MG) from Aqueous Solutions by Native and Heat-treated Anaerobic Granular Sludge, *Biochemical Engineering Journal*, **2008**, *39*, (3), 538 – 546

Chiang, L.C.; Chang, J.E.; Tseng, S.C. Electrochemical Oxidation Pretreatment of Refractory Organic Pollutants, *Water Science Technology*, **1997**, 36, (2-3), 123 – 130

Choudhury, A.K.R. *Textile Preparation and Dyeing*, **2006**, Science Publishers

Christie, R.M.; Royal Society of Chemistry. *Colour Chemistry*, **2001**, Royal Society of Chemistry

Chu, H.C.; Chen, K.M. Reuse of Activated Sludge Biomass: Equilibrium Studies for the Adsorption of Basic Dyes on Biomass, *Textile Research Journal*, **2004**, *74* , (8), 677-683

Churchley, J.H. Ozone for Dye Waste Colour Removal: Four Years Operation at Leek STW, *International Ozone Association*, **1998**, *20*, 111 – 120

Ciner, F.; Akal Solmaz, S.K.; Yonar, T.; Ustun, G.E. Treatability Studies on Wastewater from Textile Dyeing Factories in Bursa, Turkey; *International Journal of Environment and Pollution*, **2003**, *19*, (4), 403 – 407

Clark, M.M. *Transport Modeling for Environmental Engineers and Scientists*, **2009**, John Wiley and Sons

Cokgor, E.U.; Zengin, G.E.; Tas, D.O.; Oktay, S.; Randall, C.; Orhon D. Respirometric Assessment of Primary Sludge Fermentation Products, Journal of Environmental Engineering, **2006**, *132*, (1)

Cooney, D.O. *Adsorption Design for Wastewater Treatment*, **1999**, Lewis Publishers, Boca Raton

Cunningham, W.P.; Siago, B.W. *Environmental Science, Global Concern*, **2001**, McGraw Hill, New York.

Damayanti, A.; Ujang, Z.; Salim, M.R.; Olsson, G.; Sulaiman, A.Z.; Respirometric Analysis of Activated Sludge Models from Palm Oil Mill Effluent, *Bioresource Technology*, **2010**, *101*, (1), 144 – 149

Dang, N.D.P.; Karrer, D.A.; Dunn, I.J. Oxygen Transfer Coefficients by Dynamic Model Moment Analysis, *Biotechno. BioEng.* **1977**, *19*

Dizge, N.; Aydiner, C.; Demirbas, E.; Kobya, M.; Kara, S. Adsorption of Reactive Dyes from Aqueous Solutions by Fly Ash: Kinetic and Equilibrium Studies, *J. Hazard. Mater.*, **2008**, *150* (3), 737 – 46

Downing, A.L.; Melbourne, K.V.; Bruce, A.M. The Effect of Contaminants on the Rate of Aeration in Water, *Journal of Applied Chemistry*, **1957**, *7*, (11), 590 – 596

Dwyer® Series VFA and VFB Visi-Float®, Service Manual, 2008, http://www.dwyer-inst.com/PDF_files/vf_iom.pdf

Eckenfelder, W. W. Factors Affecting Aeration Efficiency of Sewage and Industrial Wastes, *Sewage. Ind. Wastes*, **1959**, *31* (60)

Eckenfelder, W.W. *Industrial Water Pollution Control*, **1989**, McGraw-Hill Series in Water Resources and Environmental Engineering

Eckenfelder, W.W.; Grau, P. *Activated Sludge Process Design and Control: Theory and Practice*, **1998**, Technomic Pub.

Eckenfelder, W.W.; Musterman, J.L.; Musterman J. *Activated Sludge Treatment of Industrial Wastewater*, **1995**, Technomic Publishing Company

Elsner, P.; Textiles and the Skin, Current Problems in Dermatology, **2003**, Vol. 31, Karger Publishers

Elvers, B.; Hawkins, S.; Arpe, H.J.; Ullman, F.; Günzler, H.; Russey, W.E.; Gerhartz, W.; Pikart-Müller, M.; Schulz, G.; Buchholz, H.; Weise, E. *Ullmann's Encyclopedia of Industrial Chemistry*, **1993**, 5th Edition, VCH

Fall, C.; Flores, N.A.; Espinoza, M.A.; Vazquez, G.; Loaiza-Návia, J.; van Loosdrecht, M.C.; Hooijmans, C.M. Divergence Between Respirometry and Physicochemical Methods in the Fractionation of the Chemical Oxygen Demand in Municipal Wastewater, *Water Environment Research*, **2011**, *83*, (2), 162 – 72

Fakeeha, A.H.; Jibril, B.Y.; Ibrahim, G.; Abasaeed, A.E. Medium Effects on Oxygen Mass Transfer in a Plunging Jet Loop Reactor with a Downcomer, *Chemical Engineering and Processing: Process Intensification,* **1999**, *38*, (3), 259 – 265

Flick, E.W. *Industrial Surfactants*, **2003**, 2nd Edition, Particle Technology Series, William Andrew

Freundlich, H. *Colloid and Capillary Chemistry*, **1926**, Methuen and Co. Ltd, London

Garcia, D. Simpson's Numerical Integration, *MATLAB® Central File Exchange*, **2009**, http://www.mathworks.com/matlabcentral/fileexchange/25754-simpsons-numerical-integration

García-Montaño, J.; Torrades, F.; García-Hortal, J.A.; Domènech, X.; Peral, J. Degradation of Procion Red H-E7B Reactive Dye by Coupling a Photo-Fenton System with a Sequencing Batch Reactor, *Journal of Hazardous Materials*, **2006**, *134*, (1 – 3), 220 – 229

Ghosh, M.M.; Woodard, F.E.; Sproul, O.J.; Knowlton, P.B.; Guertin, P.D. Treatability Studies and Design Considerations for Textile Wastewater, *Journal of Water Pollution Control Federation*, **1978**, *50*, (8), 1976 – 1985

Gottschalk, C.; Libra, J.A.; Saupe, A. *Ozonation of Water and Waste Water: A Practical Guide to Understanding Ozone and Its Applications*, **2010**, John Wiley and Sons

Goudar, C.; Strevett, K.; Grego, J. Competitive Substrate Biodegradation during Surfactant-Enhanced Remediation, Journal of Environmental Engineering, **1999**, *125*, (12), 1142 – 1148

Gujer, W.; Henze, M.; Mino, T.; van Loosdrecht, M.C.M. Activated Sludge Model No. 3. Wat. Sci. Technol. , **1999**, *39*, (1), 183 – 193

Gulnaz, O.; Kaya, A.; Matyar, F.; Arikan, B. Sorption of Basic Dyes from Aqueous Solution by Activated Sludge, *Journal of Hazardous Materials*, **2004**, *108*, (3), 183 – 188

Gupta, V.K.; Ali, I.; Saini, V.K. Adsorption Studies on the Removal of Vertigo Blue 49 and Orange DNA13 from Aqueous Solutions using Carbon Slurry Developed from a Waste Material, *J. Colloid Interface Sci.*, **2007**, *315*, (1), 87 – 93

Hagman, M.; Jansen, J.C. *Oxygen Uptake Rate Measurements for Application at Wastewater Treatment Plants*, **2007**, Vatten

Hameed, B.H.; El-Khaiary, M.I. Sorption Kinetics and Isotherm Studies of a Cationic Dye Using Agricultural Waste: Broad Bean Peels, *Journal of Hazardous Materials*, **2008**, *154*, (1-3), 639 – 648

Hangos, K.M.; Cameron, I.T. *Process Modelling and Model Analysis, Process Systems Engineering*, **2001**, Vol.4, Academic Press

Hebrard, G.; Zeng, J.; Loubiere, K. Effect of Surfactants on Liquid-Side Mass Transfer Coefficients: A New Insight, *Chemical Engineering Journal*, **2009**, *148*, 132-138

Henze, M.; Grady, C.P.L. Jr.; Gujer, W.; Marais, G.V.R.; Matsuo, T. Activated Sludge Model No. 1. *IAWPRC Scientific and Technical Report No. 1*, **1987**, London

Henze, M.; Gujer, W.; Mino T.; van Loosdrecht M.; International Water Association Task Group on Mathematical Modelling for Design and Operation of Biological Wastewater Treatment, *Activated Sludge Models ASM1, ASM2, ASM2d and ASM3*, **2000**, IWA Publishing

Ho, Y.S. Citation Review of Lagergren Kinetic Rate Equation on Adsorption Reactions, *Scientometrics*, **2004**, *59*, (1), 171 – 177

Ho, Y.S. Review of Second Order Models for Adsorption Systems, Journal of Hazardous Materials, **2006**, *136*, (3), 103 – 111

Ho, Y.S.; McKay, G. Pseudo-second Order Model for Sorption Processes, *Process Biochemistry*, **1999**, *34*, (5), 451 – 465

Ho, Y.S.; McKay, G. A comparison of Chemisorption Kinetic Models Applied to Pollutant Removal on Various Sorbents, *Process Safety and Environmental Protection*, **1998**, *76*, (4),

Iqbal, M. K.; Nadeem, A.; Shafiq, T. Biological Treatment of Textile Wastewater by the Activated Sludge Process, *Jour. Chem. Soc. Pak.*, **2007**, *29*, (5), 397 – 400

ISO 7827, *Water Quality – Evaluation of the "Ready", "Ultimate" Aerobic Biodegradability of Organic Compounds in an Aqueous Medium – Method by Analysis of Dissolved Organic Carbon (DOC)*, **2010**, ISO/TC 147/SC 5 - Biological Methods

Ivey International Inc. *Material Safety Data Sheet: Ivey-sol®*, **2011**, http://www.iveyinternational.com/pdfs/MSDS_Ivey-sol_103_106_1081.pdf

Jakobsen, H.A. *Chemical Reactor Modeling: Multiphase Reactive Flows*, **2008**, Springer

Jeffrey, A., *Advanced Engineering Mathematics*, **2002**, Harcourt/Academic Press

Ju, D.J.; Byun, I.G.; Park, J.J.; Lee, C.H.; Ahn, G.H.; Park, T.J. Biosorption of a Reactive Dye (Rhodamine-B) From an Aqueous Solution Using Dried Biomass of Activated Sludge, *Bioresource Technology*, **2008**, *99*, (17), 7971 – 7975

Judd, S.; Judd, C. *The MBR Book: Principles and Applications of Membrane Bioreactors for Water and Wastewater Treatment*, **2011**, Butterworth Heinemann, Elsevier

Judkins, J. F.; Hornsby, J.S. Color Removal from Textile Dye Waste Using Magnesium Carbonate, *Journal of Water Pollution Control Federation*, **1978**, *50*, (11), 2446 – 2456

Jurado, E.; Fernández-Serrano, M; Ríos, F.; Lechuga, M. Aerobic Biodegradation of Surfactants, Biodegradation - Life of Science, 2013, InTech, http://www.intechopen.com/books/biodegradation-life-of-science/aerobic-biodegradation-of-surfactants

Kapdan, I.; Kargi, F.; McMullan G.; Marchant, R. Comparison of White-Rot Fungi Cultures for Decolorization of Textile Dyestuff, *Bioprocess Engineering*, **2000**, 22, (4), 347 – 351

Karsa, D.R.; Porter, M.R. *Biodegradability of Surfactants*, **1995**, Springer

Katoh, S.; Yoshida, F. *Biochemical Engineering: A Textbook for Engineers, Chemists and Biologists*, **2009**, Wiley-VCH

Kim, C.; Choe, E.K.; Chang, I. Non-steady state Estimation of Biodegradability of Dyeing Wastewater Using a Respirometer, *Korean Journal of Chemical Engineering,* **2008**, *25*, (3), 553 - 557

Kim, T.; Lee, J.; Lee, M. Biodegradability Enhancement of Textile Wastewater by Electron Beam Irradiation, *Radiation Physics and Chemistry*, **2007**, *76*, (6), 1037 – 1041

Knepper, T.P.; Barceló, D.; De Voogt, P. *Analysis and Fate of Surfactants in the Aquatic Environment - Comprehensive Analytical Chemistry*, **2003**, (40), Elsevier

Kok, R.; Zajic, J.E, Dynamic Response of a Clark Dissolved Oxygen Probe, *Biotechnology and Bioengineering*, **1975**, *17*, (4), 527 – 539

Kreyszig, E. *Advanced Engineering Mathematics*, **2011**, 10th Edition, John Wiley & Sons, Inc.

Kulkarni, S.V.; Blackwell, C.D.; Blackard, A.L.; Stackhouse, C.W.; Alexander, M.W. *Textile Dyes and Dyeing Equipment: Classification, Properties and Environmental Aspects*, **1985**, EPA/600/S2-85/010, U.S. Environmental Protection Agency

Kumar, T.A.; Saravanan S. Treatability Studies of Textile Wastewater on an Aerobic Fluidized Bed Biofilm Reactor (FABR): A Case Study, *Water Sci. Technol*. **2009**; *59*, (9), 1817 – 1821

Lacasse, K.; Baumann, W. *Textile Chemicals: Environmental Data and Facts*, **2004**, Springer

Lagergren, S. About the Theory of so-called Adsorption of Soluble Substances, *Kungliga Svenska Vetenskapsakademiens Handlingar*, 1898, 24, (4), 1 – 39

Langmuir, I. The Constitution and Fundamental Properties of Solids and Liquids. Part I. Solids, *Journal of the American Chemical Society*, **1916**, *38*, 2221 – 2295

Lazaridis, N.K.; Asouhidou, D.D. Kinetics of Sorptive Removal of Chromium(VI) from Aqueous Solutions by Calcined Mg-Al-CO_3 Hydrotalcite, *Water Research*, **2003**, *37*, (12), 2875 – 2882

Lehr, J.H.; Keeley, J.W.; Lehr, J.K. *Water Encyclopedia: Domestic, Municipal and Industrial Water Supply and Waste Disposal, Water Encyclopedia*, **2005**, Vol.1, John Wiley & Sons

Leung, S.M.; Little, J.C.; Holst, T.; Love N.G. Air/Water Oxygen Transfer in a Biological Aerated Filter, ASCE, *Journal of Environmental Engineering*, **2006**, *132*, 181 – 189

LeVan, M.D.; Carta, G.; Yon, C.M.; *Perry's Chemical Engineer's Handbook*, **1999,** 7th Edition, McGraw-Hill Chemical Engineering Series

Lewis, W.K.; Whitman, W.C. Principles of Gas Absorption, *Journal of Industrial and Engineering Chemistry*, **1924**, 16, 1215 — 1220

Lichtfouse, E. *Organic Farming, Pest Control and Remediation of Soil Pollutants, Sustainable Agriculture Reviews*, **2009**, Vol.1, Springer

Liwarska-Bizukojć, E.; Bizukojć M. Digital Image Analysis to Estimate the Influence of Sodium Dodecyl Sulphate on Activated Sludge Flocs, *Process Biochemistry*, **2005**, *40*, 2067 – 2072

Loyd, C.K.; Boardman, G.D.; Michelsen, D.L. Anaerobic/Aerobic Treatment of a Textile Dye Wastewater, *Hazard Indust. Wastes*, **1992**, *24*, 593 – 601

Lynch, W.O.; Sawyer, C.N. Physical Behavior of Synthetic Detergents I: Preliminary Studies on Frothing and Oxygen Transfer, *Sew. Ind. Wastes*, **1954**, *26*, 1193

Mancy, K.H.; Okun, D.A. Effects of Surface Active Agents on Bubble Aeration, *J. Wat. Pollut. Control Fed.*, **1960**, *32*, 351 – 364

Mancy, K.H.; Okun, D.A. The Effects of Surface Active Agents on Aeration, *J. Wat. Pollut. Control Fed.*, **1965**, *37*, 212 – 227

Mara, D.; Horan, N.J. *Handbook of Water and Wastewater Microbiology*, **2003**, Academic Press

Marsili-Libelli, S.; Tabani, F. Accuracy Analysis of a Respirometer for Activated Sludge Dynamic Modelling, *Water Research*, **2002**, *36*, (5), 1181−1192

Masutani, G.K. *Dynamic Surface Tension Effects on Oxygen Transfer in Activated Sludge*, PhD Thesis, **1988**, University of California, Los Angeles

MathWorks, Inc. MATLAB® R2012a, **2012**, http://www.mathworks.com/products/matlab

McCutcheon Division. *McCutcheon's Emulsifiers and Detergents*, McCutcheon Division MC Pub, **2001**, Cornell University

Metcalf and Eddy Incorporated. *Wastewater Engineering, Treatment and Reuse*, **2003**, 4th Edition, McGraw Hill Series in Civil and Environmental Engineering

Mhlanga, F. *Modelling of the Mariannridge Wastewater Treatment Plant*, MScEng Chemical Engineering Thesis, 2009, Pollution Research Group, School of Chemical Engineering, University of KwaZulu-Natal, Durban

Michaels, G.B.; Lewis, D.L. Sorption and Toxicity of Azo and Triphenylmethane Dyes to Aquatic Microbial Populations, *Environ. Toxicol. Chem.*, **1985**, *4*, (2), 45 – 50

Michaels, G.B.; Lewis, D.L. Microbial Transformation Rates of Azo and Triphenylmethane Dyes, *Environ. Toxicol. Chem.*, **1986**, *5*, (2), 161 – 166

Mohan, P.K.; Nakhla, G.; Yanful, E.K. Biodegradability of Surfactants under Aerobic, Anoxic, and Anaerobic Conditions, *ASCE Journal of Environmental Engineering*, 2006, *132*, 279 – 283

Mohan, P.K.; Nakhla, G.; Yanful, E.K. Biokenitics of Biodegradability of Surfactants under Aerobic, Anoxic, and Anaerobic Conditions, *Water Research*, **2006**, *40*, (3), 533 – 540

Mueller, J.A.; Boyle, W.C.; Pöpel, H.J. *Aeration: Principles and Practice, Water Quality Management Library*, **2002**, CRC Press

Myers, D. *Surfactant Science and Technology*, **2006**, John Wiley & Sons

Najafpour, G.D. *Biochemical Engineering and Biotechnology*, **2006**, Elsevier

Nielsen, P.H.; Daims, H.; Lemmer, H. FISH Handbook for Biological Wastewater Treatment: Identification and Quantification of Microorganisms in Activated Sludge and Biofilms by FISH, **2009**, IWA Publishing

Nigam, P.; Banat, I.M.; Singh, D.; Marchant, R. Microbial Process for the Decolorization of Textile Effluent Containing Azo, Diazo and Reactive Dyes. *Process Biochem.*, **1996**, *31*, 435 – 442

O'Neill, C.; Hawkes, F.R.; Hawkes, D.L.; Lourenco, N.D.; Pinheiro, H.M.; Delée, W. Colour In Textile Effluents – Sources, Measurement, Discharge Consents and Simulation – A Review, *Journal Chem. Technol. Biotechnol.*, **1999**, *74*, 1009 – 1018

OECD. *OECD Guidelines for the Testing of Chemicals / Section 3: Degradation and Accumulation Test No. 303: Simulation Test - Aerobic Sewage Treatment -- A: Activated Sludge Units; B: Biofilms*, **2001**, OECD Publishing

Oliveira, C.S.; Ordaz, A.; Alba, J.; Alves, M.; Ferreira, E.C.; Thalasso F. Determination of Kinetic and Stoichiometric Parameters of Pseudomonas Putida F1 by Chemostat and In Situ Pulse Respirometry; Chemical Product and Process Modeling, **2009**, *4*, (2), 1 – 16

Orhon, D.; Artan, N.; Büyükmurat, S.; Görgün, E., The Effect of Residual *COD* on the Biological Treatability of Textile Wastewaters, *Water Science & Technology*, **1992**, *26*, (3 – 4), 815 – 825

Orhon, D.; Babuna, F.G.; Karahan, O. *Industrial Wastewater Treatment by Activated Sludge*, **2009**, IWA Publishing

Orupõld, K.; Hellat, K.; Tenno, T. Estimation of Treatability of Different Industrial Wastewaters by Activated Sludge Oxygen Uptake measurements, *Water Science and Technology*, **1999**, *40*, (1), 31 – 36

Pagga, U.; Brown, D. The Degradation of Dyestuffs: Part II — Behaviour of Dyestuffs in Aerobic Biodegradation Tests, Chemosphere, **1986**, *15*, (4), 479 - 491

Parish Supply Corp. *Material Safety Data Sheet: Neutral Stone Cleaner™*, **2012**, http://www.parish-supply.com/msds/0047901.pdf

Philichi, T.; Stenstrom, M.K. The Effect of Dissolved Oxygen Probe Lag upon Oxygen Transfer Parameter Estimation*, Journal of Water Pollution Control Federation*, **1989**, *61* (1), 83 — 86

Press, W.H.; Flannery, B.P.; Teukolsky, S.A.; Vetterling, W.T. *Numerical Recipes in FORTRAN 77: Volume 1 of Fortran Numerical Recipes: The Art of Scientific Computing*, **1992**, 2nd Edition, Cambridge University Press

Press, W.H.; Flannery, B.P.; Teukolsky, S.A.; Vetterling, W.T. *Numerical Recipes in FORTRAN 90: Volume 2 of Fortran Numerical Recipes: The Art of Scientific Computing*, **1996**, 2nd Edition, Cambridge University Press

Punmia, B.C.; Jain, A.K.; Jain, A.K. *Wastewater Engineering*, **1998**, Laxmi Publications

Qiu, H.; Lv, L.; Pan, B.C.; Zhang, Q.J.; Zhang, W.M.; Zhang, Q.X. Critical Review in Adsorption Kinetic Models, *Journal of Zhejiang University Science - A*, **2009**, *10*, (5), 716 – 724

Randall, E.W.; Wilkinson, A.; Ekama, G.A. An Instrument for the Direct Determination of Oxygen Utilisation Rate, *Water SA*, **1991**, *17*, (1), 11 – 18

Reemtsma, T.; Jekel, M. *Organic Pollutants in the Water Cycle: Properties, Occurrence, Analysis and Environmental Relevance of Polar Compounds*, **2007**, John Wiley and Sons

Rosen, M.J.; Kunjappu, J.T. *Surfactants and Interfacial Phenomena*, **2012**, 4th Edition, John Wiley and Sons

Ruchti G., Dunn I. J., Bourne J. R., 1981: Comparison of Dynamic Oxygen Electrode Methods for the Measurement of $k_L a$, *Biotechnology and Bioengineering*, **1981**, *23*, (2), 277–290

Ruzicka, K.; Gabriel, O.; Bletterie, U.; Winkler, S.; Zessner, M. Cause and Effect Relationship between Foam Formation and Treated Wastewater Effluents in a Transboundary River, *Physics and Chemistry of the Earth, Parts A/B/C*, **2009**, *34*, (8 – 9), 565 – 573

Schramm, L.L. *Emulsions, Foams, And Suspensions: Fundamentals And Applications*, **2004**, Wiley-VCH

Schwarz, C.A.; Eilersen, A.M.; Henze, M; Wichern, M.; Wilderer, P.A. Modeling of Storage and Endogenous Respiration with Activated Sludge Model, *International Society for Environmental Information Sciences, Environmental Informatics Archives, Paper EIA03-036*, **2003**, *1*, 357 - 365

Showell, M.S. *Handbook of Detergents - Applications in Textile Processing*, **2005**, CRC Press

Smith, P.G.; Scott, J.S. *Dictionary of Water and Waste Management*, **2005**, 2nd Edition, Elsevier Butterworth-Heinemann

Spanjers, H.; Olsson, G. Modelling of the Dissolved Oxygen Probe Response in the Improvement of the Performance of a Continuous Respiration Meter, *Water Research*, **1992**, *26*, (7), 945 – 954

Spanjers, H.; Vanrolleghem, P. A.; Olsson, G.; Dold, P. L. *Respirometry in Control of the Activated Sludge Process: Principles*, **1998**, IAWQ Scientific and Technical Report No. 7

Spanjers, H.; Vanrolleghem, P.A. Respirometry as a Tool for Rapid Characterization of Wastewater and Activated Sludge, *Wat. Sci. Tech.*, **1995**, *31* (2), 105 – 114

Stewart, J. *Calculus Early Transcendentals*, **2008**, 6th Edition, Thomson Brooks/Cole

Subrata, D. *Textile Effluent Treatment – A Solution to the Environmental Pollution, Fibre2Fashion*, **2006**, Textile Technology Articles, http://www.fibre2fashion.com/industry-article/pdffiles/textile-effluent-treatment.pdf

Sundararajan, A.; Ju, L.K. Biological Oxygen Transfer Enhancement in Wastewater Treatment Systems, *Water Environment Research*, **1995**, *67*, (5), 848 – 854

Suschka, J.; Ferreira, E. Activated Sludge Respirometric Measurements, *Water Research*, **1986**, *20*, (2), 137 – 144

Suzuki, M. Adsorption Engineering, Chemical Engineering Monographs, **1990**, Elsevier B. V.

Sykes, R.M.; Rubin, A.J.; Steven; Rath, A.; Chuan, Chang M. Treatability of a Non-ionic Surfactant by Activated Sludge, *Journal of Water Pollution Control Federation*, **1979**, 51, (1), 71 – 77

Talmage, S.S. *Environmental and Human Safety of Major Surfactants: Alcohol Ethoxylates and Alkylphenol Ethoxylates/ A Report to the Soap and Detergent Association*, **1994**, The Soap and Detergent Association, CRC Press Inc.

The Dow Chemical Company, *Material Safety Data Sheet: TERGITOL™ 15-S-15 Surfactant*, **2009**, http://msdssearch.dow.com/PublishedLiteratureDOWCOM/dh_0157/0901b80380157408.pdf?filepath=surfactants/pdfs/noreg/119-01941.pdf&fromPage=GetDoc

Theodore, L.; Ricci, F. *Mass Transfer Operations for the Practicing Engineer*, **2011**, John Wiley and Sons

Tsoler, U. *Handbook of Detergents: Environmental Impact*, **2004**, Marcel Dekker

Ullmann F. *Ullmann's Fibers: Textile and Dyeing Technologies, High Performance and Optical Fibers*, **2008**, Vol. 2, Wiley-VCH

U.S. Geological Survey. *National Field Manual for the Collection of Water-Quality Data: U.S. Geological Survey Techniques of Water-Resources Investigations*, **2014**, Book 9, Chaps. A1-A9, http://pubs.water.usgs.gov/twri9A

van Haandel, A.; van der Lubbe, J. *Handbook Biological Wastewater Treatment*, **2007**, Quist Publishing, Leidschendam

Vanrolleghem, P.A.; Insel, G.; Petersen B.; Sin, G.; De Pauw, D.; Dovermann, H.; , Weijers, S.; Gernaey, K.; De Dommel, W. A Comprehensive Model Calibration Procedure for Activated Sludge Models, *Proceedings of the Water Environment Federation*, **2003**, WEFTEC Session 31 through Session 40 , 210 – 237

Vanrolleghem, P.A.; Spanjers, H.; Petersen, B.; Ginestet, P.; Takács, I. Estimating (Combinations of) Activated Sludge Model No. 1 Parameters and Components by Respirometry, *Wat. Sci. Tech.*, **1999**, *39*, (1), 195 – 214

Vollertsen, J.; Hvitved-Jacobsen, T. Biodegradability of Wastewater – A Method for COD Fractionation, *Water Science and Technology*, **2002**, *45*, (3), 25 – 34

Von Sperling, M., *Activated Sludge and Aerobic Biofilm Reactors - Biological Wastewater Treatment Series*, **2007**, Vol. 5, IWA Publishing

Wagner, M.; Pöpel, J.H. Surface Active Agents and Their Influence on Oxygen Transfer, *Water Science and Technology*, **1996**, *34*, (3-4), 249 – 256

Wang, L.K.; Hung, Y.T.; Lo, H.H.; Yapijakis, C. *Handbook of Industrial and Hazardous Wastes Treatment*, **2004**, 2nd Edition, CRC Press

Wentzel, M.C.; Mbewe, A.; Lakay, M.T.; Ekama, G.A. Batch Test for Characterisation of the Carbonaceous Materials in Municipal Wastewaters, *Water SA*, **1999**, *25*, (3), 327 – 335

Wolfram Research. *Wolfram Mathematica 8.0*, **2010**, http://www.wolfram.com/mathematica/

Young, J.C. Oxygen Uptake Rate as a Monitoring and Control Parameter for Activated Sludge Processes, *Purdue University Industrial Wastes Technical Conference*, **1999**, WEF Indiana Water Pollution Control Association

Zgajnar, G.A., Zagorc-Koncan, J. Characterization of Textile Wastewater: Its Environmental Impact and Biotreatability, *Chemical and Biochemical Engineering Quarterly, Croatian Society of Chemical Engineers*, **2004**, *18*, (3), 309 – 315

Zollinger, H. *Color Chemistry*, **1991**, 2nd Edition, VCH Publishers, New York

Zollinger, H. Color Chemistry: *Syntheses, Properties and Applications of Organic Dyes and Pigments*, **2003**, 3rd Edition, Helvetica Chimica Acta

APPENDICES

A. Soluble dye effluents decolourisation

A.1 Reagent synthesis

A.1.1 Soluble dye effluent

$required\ mass\ concentration = 0.06\ \mathrm{g/dm^3}$

The soluble dye effluent was synthesised from dissolving 0.3 g of Procion Red H-E7B reactive dye in 5 $\mathrm{dm^3}$ of distilled $\mathrm{H_2O}$ to result in a 0.06 $\mathrm{g/dm^3}$ Procion Red H-E7B reactive dye solution.

A.1.2 Readily biodegradable substrate

$selected\ substrate$: $\mathrm{CH_3COOH}$

$required\ mass\ concentration = 123.44\ \mathrm{g/dm^3}$

The readily biodegradable substrate was synthesised from dissolving 617.2g $\mathrm{CH_3COONa}$ in 5 $\mathrm{dm^3}$ of distilled $\mathrm{H_2O}$ to result in 123.44 $\mathrm{g/dm^3}$ of $\mathrm{CH_3COOH}$ as shown in the hydrolysis reaction:

$$\mathrm{CH_3COONa + H_2O \rightarrow CH_3COOH + NaOH} \qquad \text{(A.1.2.1)}$$

A.2 Measurements and estimations

A.2.1 Volatile Suspended Solids (VSS) estimates

The VSS concentration was computed from measuring the mass of solids that were that were retained by a 0.45 μm fibre glass filter medium after filtering 0.01 dm^3 of activated sludge and then drying the retained solids in an oven at 105 °C until they reached a constant weight.

After determining their final weight, the dried solids were then volatilised in a furnace at 550 °C

The difference in weight between the dried solids and the volatilised solids was divided by the measured volume of the activated sludge to compute estimates of the VSS concentration in terms of g VSS/dm^3 of sludge:

$$VSS = (m_1 - m_2)/V_{\text{sludge}} = (0.0453 - 0.0152)/0.01 \quad \text{(A.2.1.1)}$$

$$\therefore VSS = 3.01 \text{ g VSS}/dm^3 \text{ of sludge}$$

where

$m_1 =$ mass of dried solids prior to volatising, (g)

$m_2 =$ mass of dried solids after volatising, (g)

$V_{\text{sludge}} =$ volume of activated sludge analysed, (dm^3)

A.2.2. Light absorbance dominant wavelength estimates for the soluble dye effluent

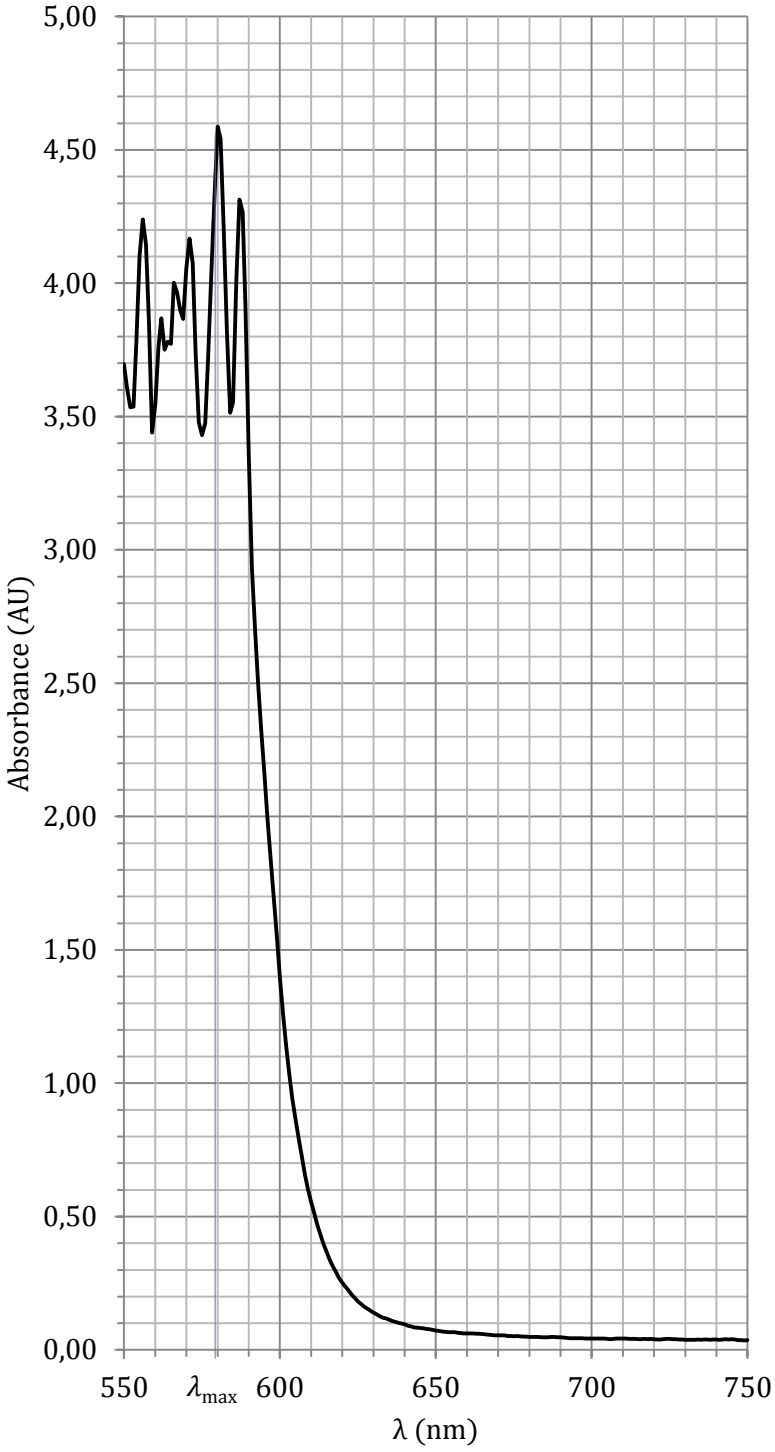

Fig.41: Dye effluent light absorbance spectrum from which the dominant wavelength was computed

As inferred from the light absorbance spectrum shown in Fig.41, $\lambda_{max} = 581$ nm.

A.2.3. Calibration curve for correlating dye concentration in solution to light absorbance

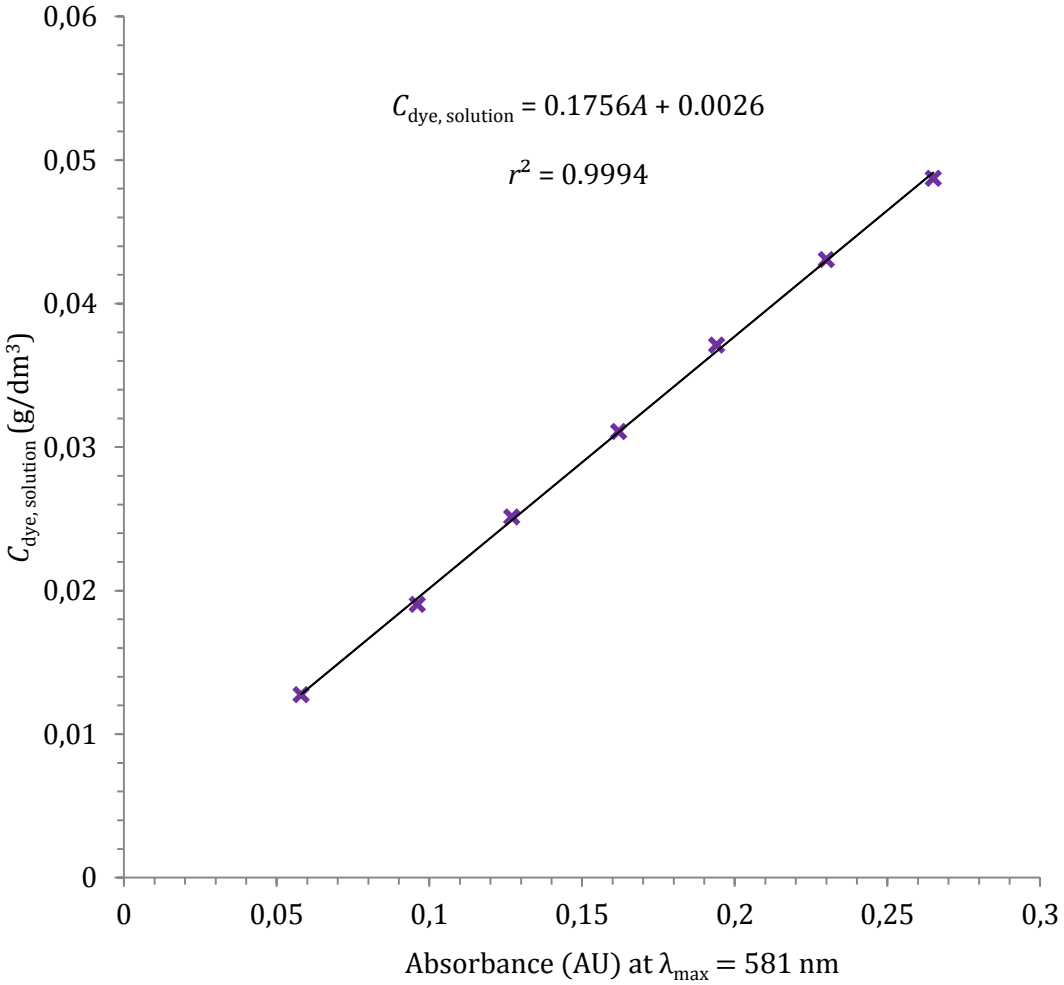

Fig.42: Calibration curve for correlation correlating dye concentration in solution to light absorbance

The correlation between the dye concentration and visible light absorbance was computed through the least squares linear regression method:

$$C_{dye,\ solution} = 0.1756A + 0.0026 \quad \text{(A.2.3.1)}$$

A.2.4. Cumulative volume of CH_3COOH dosed into the activated sludge system

Since CH_3COOH was dosed into the activated sludge system at a volumetric flow rate of 0.012 dm^3/h and a sample was withdrawn from the bioreactor for spectrophotometric analysis at every $t = 0.25$ h interval, the cumulative volume of CH_3COOH dosed into the activated sludge system in successive $t = 0.25$ h intervals from $t = 0$ h to $t = t_R = 2$ h was computed as shown in Table 5:

Table 5: Cumulative volume of CH_3COOH dosed into the activated sludge system at a volumetric flow rate of 0.012 dm^3/h

t (h)	V_{CH_3COOH} (dm^3)
0.00	0.000
0.25	0.003
0.50	0.006
0.75	0.009
1.00	0.012
1.25	0.015
1.50	0.018
1.75	0.021
2.00	0.024

The cumulative total volume of liquid in the activated sludge system resulting from the CH_3COOH dosing in successive $t = 0.25$ h intervals from $t = 0$ h to $t = t_R = 2$ h was computed from the mass balance:

$$V_{total} = V_{supernatant} + V_{dye} + V_{CH_3COOH} \quad \text{(A.2.4.1)}$$

where

$V_{supernatant} = 1.39\ dm^3$

$V_{dye} = 0.50\ dm^3$

Table 6: Cumulative total volume of liquid in the activated sludge system in successive t = 0.25 h intervals from t = 0 h to t = t_R = 2 h

t (h)	V_{total} (dm^3)
0.00	1.8871
0.25	1.8901
0.50	1.8931
0.75	1.8961
1.00	1.8991
1.25	1.9021
1.50	1.9051
1.75	1.9081
2.00	1.9111

A.2.5. Cumulative mass of biomass derived from the readily biodegradable COD dosed into the activated sludge system

Since $dX_{\mathrm{H}}/dt = f(Y_{\mathrm{H}},\ dS_{\mathrm{S}}/dt)$ according to Equation 4.1.3.4.5, where $dS_{\mathrm{S}}/dt = 1.58$ g COD/h and $Y_{\mathrm{H}} = 0.63$ g X_{H}/g X_{STO} , the cumulative mass of biomass that was derived from a readily biodegradable COD mass flow rate of $dS_{\mathrm{S}}/dt = 1.58$ g COD/h in successive $t = 0.25$ h intervals from $t = 0$ h to $t = t_{\mathrm{R}} = 2$ h was computed as shown in Table 7:

Table 7: Cumulative mass of biomass derived from the readily biodegradable COD dosed into the activated sludge system

t (h)	X_{H} (g COD)
0.00	0.000
0.25	0.249
0.50	0.498
0.75	0.747
1.00	0.995
1.25	1.244
1.50	1.493
1.75	1.742
2.00	1.991

Using a conversion factor of 1.42 g COD/g VSS as reported by Metcalf and Eddy Inc. (2003), the cumulative mass of biomass was converted to VSS as shown in Table 8:

Table 8: Cumulative mass of VSS equivalent to the cumulative mass of biomass derived from the readily biodegradable COD dosed into the activated sludge system

t (h)	VSS (g)
0.00	0.000
0.25	0.175
0.50	0.350
0.75	0.526
1.00	0.701
1.25	0.876
1.50	1.051
1.75	1.227
2.00	1.402

The cumulative total mass of VSS in the activated sludge system was computed from the mass balance:

$$\text{g } VSS_{\text{total}} = (V_{\text{sludge}} \times VSS_{\text{initial}}) + \text{g } VSS_{\text{CH}_3\text{COOH dosing}} \quad \text{(A.2.5.1)}$$

where

$\text{g } VSS_{\text{CH}_3\text{COOH dosing}} = \text{mass of } VSS \text{ derived from } \text{CH}_3\text{COOH dosing}$

$VSS_{\text{initial}} = VSS$ concentration in the activated sludge system prior to CH_3COOH dosing $= 3.01 \text{ g } VSS/\text{dm}^3$ of sludge

Table 9: Cumulative total mass of VSS in the activated sludge system in successive $t = 0.25$ h intervals from $t = 0$ h to $t = t_R = 2$ h

t (h)	VSS (g)
0.00	4.515
0.25	4.690
0.50	4.865
0.75	5.041
1.00	5.216
1.25	5.391
1.50	5.566
1.75	5.742
2.00	5.917

B. Effect of surfactant effluents on oxygen transfer

B.1 Reagent synthesis

B.1.1 Surfactant effluent

Given:

1. the concentration of the surfactant effluent at the point of discharge from the factory:

   $C_{\text{effluent, factory}} = 0.23\ \text{g/dm}^3$

2. the volumetric flow rate of the factory effluent at the point of discharge:

   $Q_{\text{effluent, factory}} = 2.579 \times 10^4\ \text{dm}^3/\text{h}$

3. the maximum volumetric flow rate of effluents discharged to the wastewater treatment plant receiving the surfactant effluent:

   $Q_{\text{wastewater treatment plant}} = 2.708 \times 10^5\ \text{dm}^3/\text{h}$

Let:

4. $C_{\text{effluent, wastewater treatment plant}}$ = final concentration of the surfactant effluent when it is received by the wastewater treatment plant, (g/dm^3)

The final concentration of the surfactant effluent when it is received by the wastewater treatment plant was computed as follows:

$$C_{\text{effluent, wastewater treatment plant}} = \left(C_{\text{effluent, factory}} \times Q_{\text{effluent, factory}}\right)/Q_{\text{wastewater treatment plant}} \quad \text{(B.1.1.1)}$$

$$\therefore C_{\text{effluent, wastewater treatment plant}} = (0.23 \times 2.579 \times 10^4)/2.708 \times 10^5 = 0.022\ \text{g/dm}^3$$

The surfactant effluent was synthesised from dissolving 0.11 g of pure surfactant reagent branded Tritec™ obtained from local textile factory called JMV Textiles in 5 dm^3 of distilled H_2O to result in a 0.022 g/dm^3 surfactant effluent.

B.2 Laboratory equipment

B.2.1 YSI 5739 Dissolved Oxygen (DO) probe

DO probe operating specifications

1. temperature range: -5 ℃ to 45 ℃
2. temperature accuracy: $\pm$ 0.2 ℃
3. temperature response time: 30 s for 95 % of change
4. DO range: 0 to 20 mg/dm^3
5. DO accuracy: $\pm$ 0.2 mg/dm^3
6. DO response time: 30 s for 95 % of change at 25 ℃

DO probe calibration

The DO probe was calibrated in an environment with a known oxygen content The following YSI-recommended procedure was used to calibrate the YSI 5739 DO probe:

1. The YSI 5739 DO probe was connected to a DO/OUR meter
2. The DO/OUR meter was turned on and the DO probe was given time to polarise and its readings to stabilize. The stabilisation time took at least 30 min

The probe was then zeroed by flushing it with $N_{2(g)}$ and immersing it in a 0.08 mol/ dm^3 $Na_2SO_{3(aq)}$ solution and allowing the DO readings to stabilise. The zero knob on the DO/OUR meter onto which probe was connected was then adjusted so that a DO reading of 0 mg/dm^3 was registered on the DO/OUR meter.

The gain of the DO probe and DO/OUR meter were set by removing the DO probe from the $Na_2SO_{3(aq)}$ solution and flushing it with fresh H_2O after the probe was transferred into a beaker of fresh H_2O which was saturated with oxygen by continuously sparging air into it.

At a measured temperature and estimated atmospheric pressure, the oxygen solubility was set with the aid of standard tables of DO solubility as function of temperature and pressure and making the necessary adjustments on the gain knob on the DO/OUR meter until the desired saturated dissolved oxygen reading on the DO/OUR meter was obtained.

B.3 Measurements and estimations

B.3.1 Total soluble COD estimates for the surfactant effluent

Estimates of the $COD_{\text{total soluble}}$ were computed through $Cr_2O_7^{2-}$ open reflux method according to the Standard Methods according to the American Public Health Association, American Water Works Association (1995).

Procedure

1. 50 cm^3 of the sample to be analysed was pipetted into a 500 cm^3 reflux flask.

2. to the reflux flask, 1 g of $HgSO_{4(s)}$ and glass beads were added and slowly mixed with 5 cm^3 of pure $H_2SO_{4(l)}$

3. since the addition of $H_2SO_{4(l)}$ was an exothermic process, the mixture was then rapidly cooled to prevent loss of the volatile material.

4. into the 500 cm^3 reflux flask, 25 cm^3 of 0.0417 mol/dm^3 $K_2Cr_2SO_{7(aq)}$ solution was pipetted and mixed.

5. the reflux flask was attached to the Liebig's and 70 cm^3 $H_2SO_{4(l)}$ was added to the reflux mixture thoroughly mixed by swirling prior to application of any heat.

6. the open end of the reflux condenser was covered with a small beaker and refluxed for 2 h

7. after the reflux process, the mixture was diluted with distilled H_2O to twice its initial volume, cooled and titrated with Ferrous Ammonium Sulphate (FAS) titrant in the presence of 2 to 3 drops Ferroin indicator. The end point of the titration was the first sharp change in colour from blue-green to reddish brown.

8. after the titration of the sample, the COD blank was titrated and the blank was equivalent to 50 cm^3 of distilled H_2O. The procedure employed to reflux and titrate the 50 cm^3 of the sample applied to the COD blank and the same titration end point also applied.

Calculation:

$$COD_{\text{total soluble}} = \left[\left(V_{\text{FAS, blank}} - V_{\text{FAS, sample}}\right) \times M_{\text{FAS}} \times 8000\right]/\text{V}_{\text{sample}} \quad \text{(B.3.1.1)}$$

where

$V_{\text{FAS, blank}}$ = volume of FAS used in the titration of the blank, (cm^3)

$V_{\text{FAS, sample}}$ = volume of FAS used in the titration of the sample, (cm^3)

M_{FAS} = molarity of the FAS solution, (mol/dm^3)

$V_{\text{sample}} = 50\ cm^3$

B.3.2 YSI 5739 DO probe response dynamics

The time delay of the DO probe was described using the first order dynamic response model:

$$\frac{dC_{\mathrm{p}}}{dt} = (C - C_{\mathrm{p}})/\tau \tag{B.3.2.1}$$

Using Wolfram Mathematica® according to Wolfram Research (2010) to integrate the model between the boundary conditions according to Philichi and Stenstrom (1989):

$$\int_{C_{\mathrm{p},0}}^{C_{\mathrm{p}}} \left(1/(C - C_{\mathrm{p}})\right) dC_{\mathrm{p}} = \int_{0}^{t} (1/\tau) dt \tag{B.3.2.2}$$

$$\Rightarrow C_{\mathrm{p}} = e^{-t/\tau}\left(C_{\mathrm{p},0} - C + e^{t/\tau}C\right)$$

where

$C_{\mathrm{p},0}$ = first C_{DO} data point from the C_{DO} vs. t measurements logged for a fresh H_2O system

C = dissolved oxygen concentration saturation at the laboratory operating temperature and atmospheric pressure as reported in the National Field Manual for the Collection of Water-Quality Data according to the U.S. Geological Survey (2014)

Estimates of τ were computed from the best fits of C_{DO} vs. t measurements logged for a fresh H_2O system onto the solution of integrating the first order dynamic response model provided by Equation B.3.2.2 and the computations were performed through the Levenberg-Marquardt algorithm implemented on the Curve Fitting Toolbox™ in MATLAB® R2011a according to MathWorks, Inc. (2012).

The experimental procedure of determining the DO probe response dynamics involved equilibrating the probe by immersing it in a 0.08 mol/dm^3 solution of $Na_2SO_{3(aq)}$ and making necessary adjustments on the UCT DO/OUR meter until a stable C_{DO} reading of 0.00 mg/dm^3 was displayed.

The DO probe was then instantaneously transferred to a beaker with 1 dm^3 of fresh H_2O which was saturated with dissolved O_2 by continuously sparging compressed air into the fresh H_2O and maintaining turbulence in the system by agitating the volume of H_2O with a magnetic stirrer.

On instantaneously transferring the DO probe into the beaker with fresh H_2O, measurements of C_{DO} vs. t were logged for a period of 300 seconds in which the logging interval was 0.6 seconds. The designed response time of the YSI 5739 DO probe to reach 90% of its steady-state value at 25 °C specified in the YSI 5739 DO Probe product manual is approximately 10 seconds.

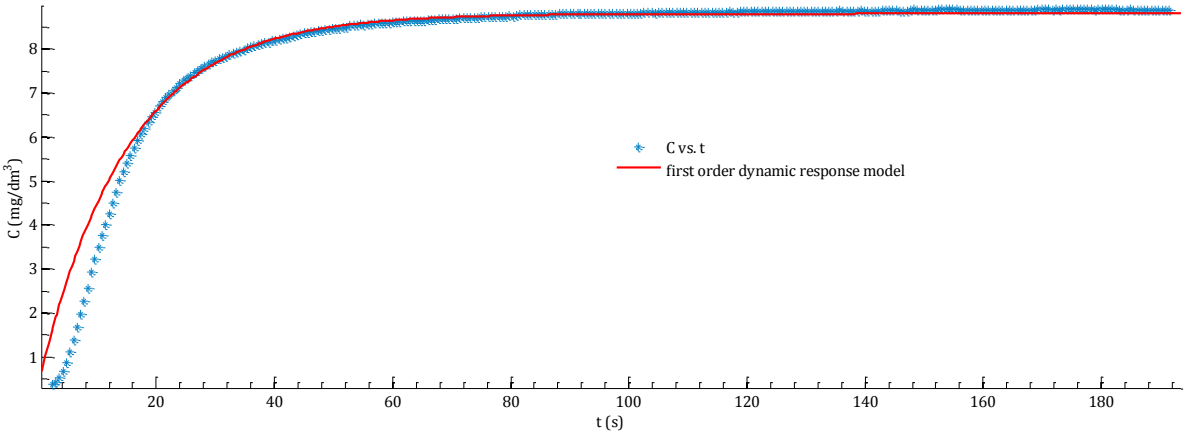

Fig.43: Experiment no.1 non-linear regression best fit of experimental data onto the first order dynamic response model

Table 10: Experiment no.1 estimates of the first order dynamic response model parameters

	best fit value	95% confidence level lower bound		95% confidence level upper bound
τ (s)	14.87	14.77		14.98
	best fit value	min	max	
$R-square$	0.998	0.998	0.998	
SSE	1.724	1.724	1.724	
$RMSE$	0.07398	0.07398	0.07398	

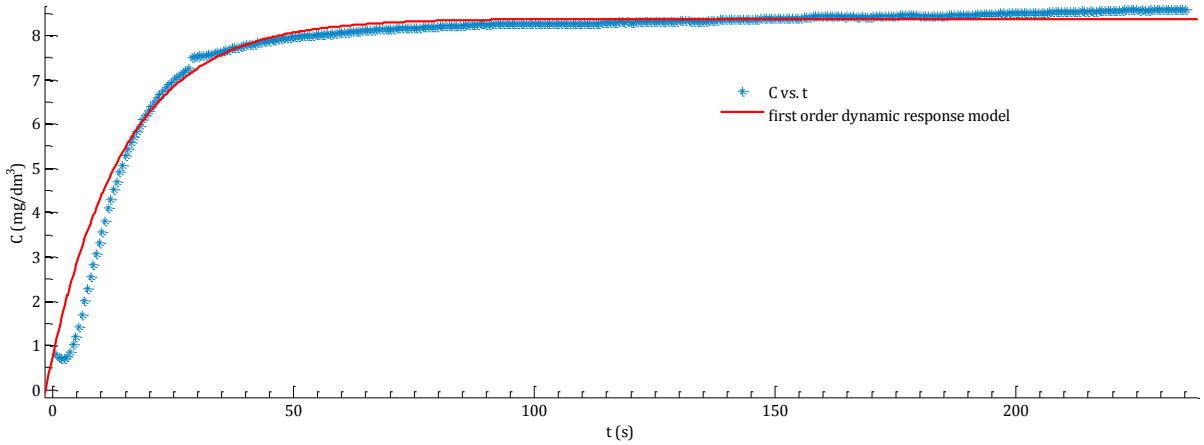

Fig.44: Experiment no.2 non-linear regression best fit of experimental data onto the first order dynamic response model

Table 11: Experiment no.2 estimates of the first order dynamic response model parameters

	best fit value	95% confidence level lower bound		95% confidence level upper bound
τ (s)	15.72	15.51		15.93
	best fit value	min	max	
$R-square$	0.9922	0.9922	0.9922	
SSE	6.818	6.818	6.818	
$RMSE$	0.1321	0.1321	0.1321	

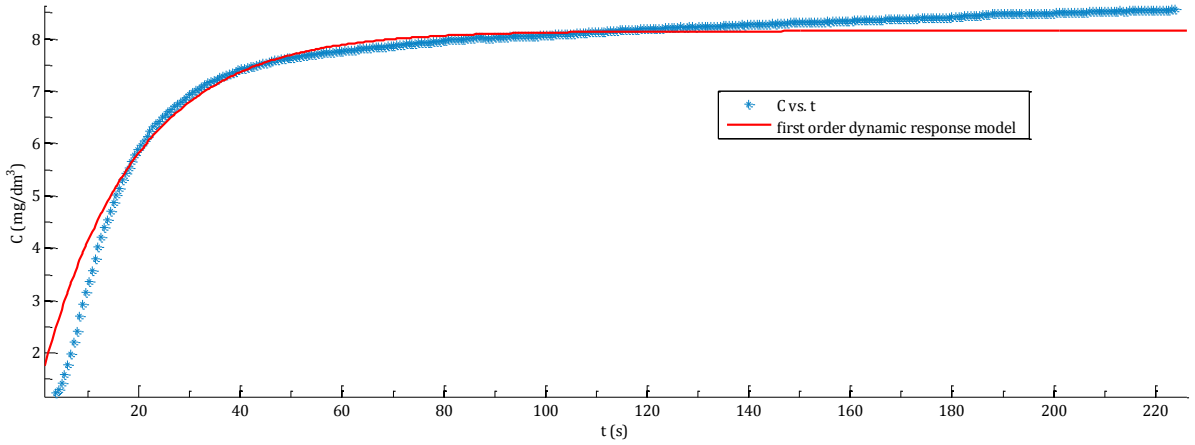

Fig.45: Experiment no.3 non-linear regression best fit of experimental data onto the first order dynamic response model

Table 12: Experiment no.3 estimates of the first order dynamic response model parameters

	best fit value	95% confidence level lower bound		95% confidence level upper bound
τ (s)	18.39	17.96		18.81
	best fit value	min	max	
$R-square$	0.9712	0.9712	0.9712	
SSE	18.25	18.25	18.25	
$RMSE$	0.223	0.223	0.223	

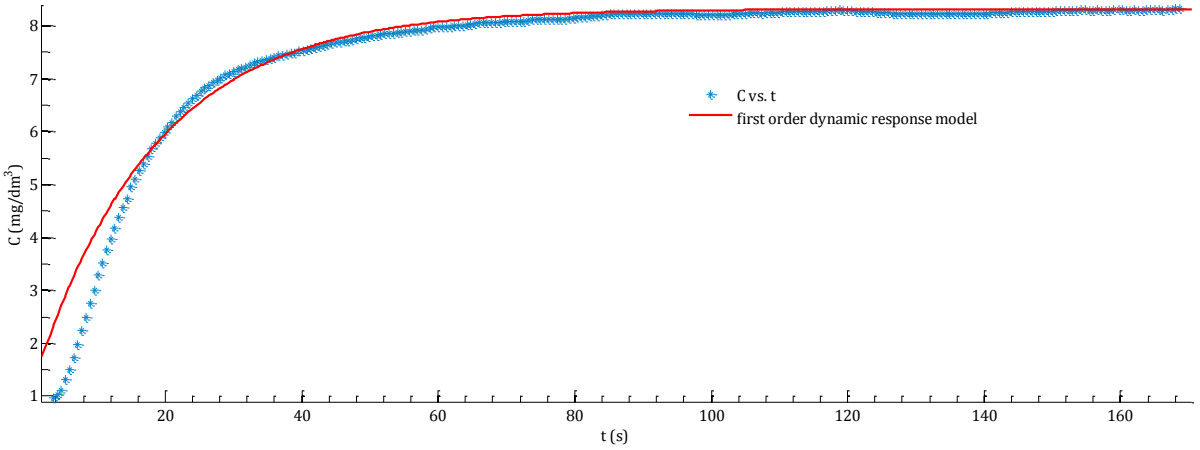

Fig.46: Experiment no.4 non-linear regression best fit of experimental data onto the first order dynamic response model

Table 13: Experiment no.4 estimates of the first order dynamic response model parameters

	best fit value	95% confidence level lower bound		95% confidence level upper bound
τ (s)	17.61	17.45		17.78
	best fit value	min	max	
$R-square$	0.9959	0.9959	0.9959	
SSE	2.445	2.445	2.445	
$RMSE$	0.09428	0.09428	0.09428	

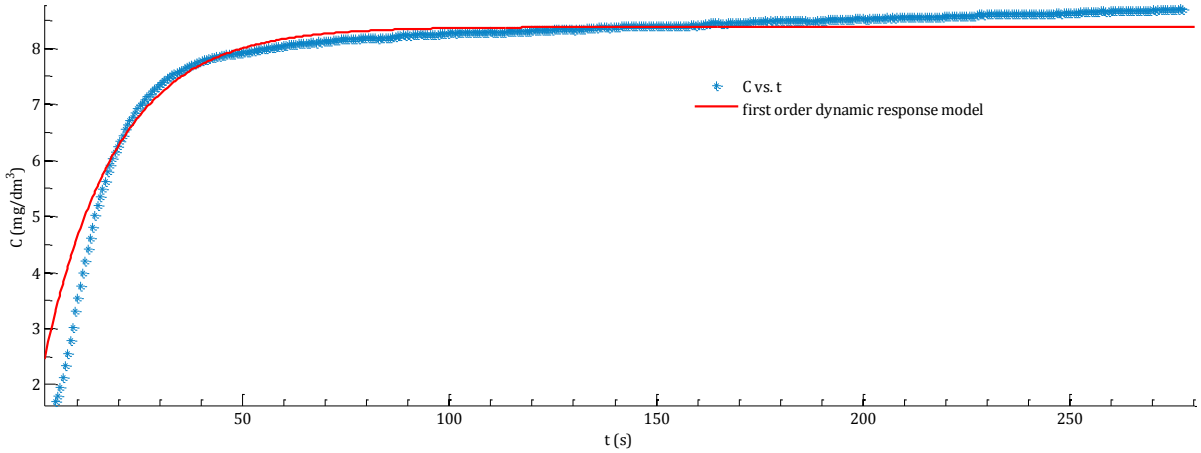

Fig.47: Experiment no.5 non-linear regression best fit of experimental data onto the first order dynamic response model

Table 14: Experiment no.5 estimates of the first order dynamic response model parameters

	best fit value	95% confidence level lower bound		95% confidence level upper bound
τ (s)	17.44	17.11		17.77
	best fit value	min	max	
$R-square$	0.9754	0.9754	0.9754	
SSE	13.39	13.39	13.39	
$RMSE$	0.1717	0.1717	0.1717	

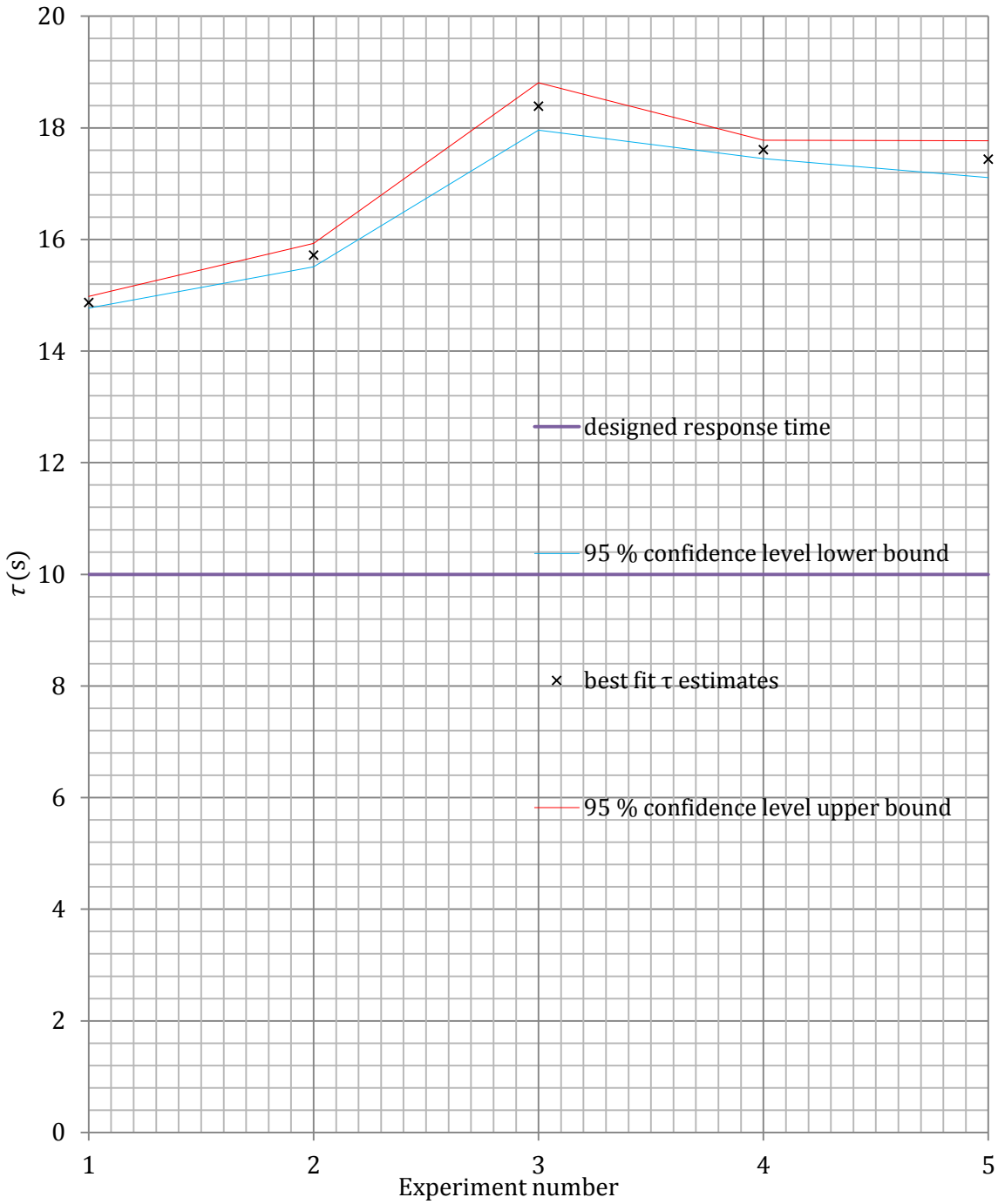

Fig.48: Best fit estimates of τ for the first order dynamic response model

As shown in Fig.48, the computed estimates of τ provided in Table 10, Table 11, Table 12, Table 13 and Table 14 were all greater than the designed response time of 10 seconds and this implied that it was highly probable that there would be the occurrence of inaccuracies when using the YSI 5739 DO Probe to log C_{DO} vs. t measurements.

B.4 Least squares non-linear regression estimates of the oxygen transfer coefficient

The goodness of fit of the modified Lewis-Whitman interfacial mass transfer model onto C_{DO} vs. t data sets from which $k_{\mathrm{L}}a$ estimates were computed was described by the following statistical indicators as described in the documentation of the Curve Fitting Toolbox™ in MATLAB® R2011a according to MathWorks, Inc. (2012):

1. $squared\ correlation\ coefficient$ (R^2): a value $R^2 \cong 1$ showed that a greater portion of variance was accounted for by the model and hence a good fit

2. $sum\ of\ squared\ residuals$ (SSE): a value of $SSE \cong 0$ indicated a good fit

3. $root\ mean\ squared\ error$ ($RMSE$): a value of $SSE \cong 0$ indicated a good fit

B.4.1 Experiment no.1

Table 15: Non-linear regression statistical indicators for experiment no.1 $k_L a$ estimates

t (h)	best fit $k_L a$ estimate (1/h)	95% confidence level lower bound (1/h)	95% confidence level upper bound (1/h)	r^2	*SSE*	*RMSE*
0.1669	23.06	22.37	23.74	0.972	2.199	0.2187
0.38735	24.11	23.35	24.87	0.9704	2.348	0.2284
0.611983333	20.69	20.21	21.17	0.977	2.155	0.1961
0.8394	24.2	23.56	24.84	0.9785	1.681	0.1933
1.058466667	24.16	23.54	24.77	0.9807	1.294	0.1755
1.279616667	24.38	23.61	25.14	0.9722	2.195	0.2234
1.501466667	23.58	22.78	24.37	0.9672	2.671	0.2436
1.7261	24.09	23.33	24.85	0.9717	2.223	0.2248
1.948633333	23.37	22.5	24.23	0.9621	3.042	0.2629
2.178133333	24.19	23.53	24.85	0.9783	1.66	0.1942
2.403483333	23.43	22.73	24.14	0.9737	2.003	0.2134
2.6344	23.68	23.17	24.19	0.9854	1.041	0.1538
2.8625	23.75	23.02	24.49	0.9726	2.127	0.2199
3.089908333	24.03	23.42	24.64	0.9809	1.344	0.1768
3.3201	24.37	23.59	25.14	0.9716	2.268	0.227
3.550325	23.81	23.2	24.42	0.9804	1.529	0.1843
3.78405	24.25	23.56	24.93	0.9775	1.672	0.1972
4.015666667	22.48	21.71	23.24	0.9658	2.822	0.2477
4.24795	23.36	22.5	24.22	0.9641	2.642	0.2508
4.480233333	23.62	22.84	24.4	0.9696	2.426	0.2348
4.714591667	23.63	22.86	24.4	0.971	2.194	0.2259
4.95035	23.69	23.05	24.33	0.979	1.593	0.1903
5.1861	23.16	22.47	23.84	0.9744	2.027	0.2122
5.424633333	22.79	22.03	23.54	0.9689	2.407	0.2339
5.664566667	23.12	22.4	23.84	0.9721	2.231	0.2227
5.902408333	22.58	21.72	23.43	0.9595	3.305	0.271
6.136075	23.41	22.6	24.22	0.9679	2.464	0.2394
6.374616667	23.1	22.43	23.77	0.9756	1.826	0.2037

t (h)	best fit k_La estimate (1/h)	95% confidence level lower bound (1/h)	95% confidence level upper bound (1/h)	r^2	*SSE*	*RMSE*
6.61245	23.35	22.64	24.07	0.9734	2.046	0.2157
6.851833333	40.63	38.64	42.62	0.8836	9.597	0.4568
6.942966667	93.09	82.97	103.2	0.942	2.016	0.3938
7.02365	113.8	92.68	134.8	0.9146	2.409	0.5173
7.105033333	78.05	67.21	88.89	0.9166	2.523	0.4585
7.204483333	68.66	65.5	71.82	0.9839	0.6133	0.1899
7.33455	76.96	72.99	80.93	0.9829	0.6525	0.2019
7.4945	68.23	62.75	73.72	0.9596	2.051	0.3376
7.680191667	58.5	53.19	63.8	0.938	4.455	0.4401
7.879083333	59.28	54.66	63.89	0.9495	3.872	0.3935
8.077983333	61.98	56.63	67.33	0.9489	3.285	0.3955
8.285916667	59.33	54.15	64.51	0.941	4.453	0.4307
8.492466667	61.84	55.82	67.86	0.9378	4.157	0.4449
8.708058333	67.15	62.26	72.04	0.9627	2.291	0.3303
8.920858333	60.98	55.21	66.76	0.9402	3.931	0.4326
9.139933333	63.08	57.52	68.64	0.9475	3.721	0.4112
9.368033333	64.45	60.09	68.81	0.9664	2.177	0.3146
9.596133333	70.74	66.43	75.05	0.9736	1.714	0.2791
9.829816667	65.22	60.65	69.78	0.9619	2.733	0.3375
10.06076667	61.57	55.55	67.6	0.9405	3.733	0.432
10.29721667	58.13	54.48	61.78	0.9608	3.031	0.329
10.53505	57.34	52.97	61.7	0.954	3.325	0.3722
10.77359167	59.25	54.32	64.18	0.9483	3.619	0.3966
11.01143333	63.25	59.44	67.06	0.9726	1.557	0.2723
11.24655833	63.67	59.24	68.11	0.9658	2.075	0.3143
11.48656667	62.46	57.59	67.33	0.9598	2.351	0.3429
11.7314	65.38	61.65	69.1	0.9769	1.247	0.2497
11.974125	63.87	58.96	68.77	0.9622	2.035	0.3272
12.21754167	63.51	59.79	67.23	0.9741	1.461	0.2638
12.45888333	61.46	56.71	66.2	0.9619	1.82	0.3179
12.69811667	60.61	56.38	64.84	0.9656	1.88	0.3066
12.94081667	59.2	54.71	63.69	0.9615	1.98	0.3228
13.18144167	63.75	60.64	66.87	0.9842	0.6397	0.194

t (h)	best fit k_La estimate (1/h)	95% confidence level lower bound (1/h)	95% confidence level upper bound (1/h)	r^2	*SSE*	*RMSE*
13.42136667	56.33	52.48	60.18	0.9681	1.403	0.2792
13.65643333	53.87	49.52	58.21	0.9567	1.927	0.3272
13.89635833	50.77	47.53	54.01	0.9688	1.354	0.267
14.13698333	47.89	45.01	50.76	0.971	1.174	0.2485
14.3783	48.84	46.45	51.23	0.9795	0.8917	0.2112
14.62726667	47.59	45.73	49.44	0.9862	0.5617	0.1676
14.87554167	40.12	37.92	42.32	0.9704	1.178	0.2368
15.12590833	41.13	38.99	43.27	0.9742	1.065	0.2252
15.38948333	31.54	30.21	32.88	0.9758	1.299	0.2154
15.70451667	38.3	36.81	39.8	0.9827	0.8856	0.1882
16.05155	35.55	33.83	37.27	0.9735	1.456	0.2366
16.42846667	34.35	32.68	36.03	0.9713	1.761	0.2508
16.81583333	34.05	32.45	35.65	0.9742	1.475	0.2338
17.23449167	34.23	32.88	35.58	0.9796	1.247	0.2074
17.63855	33.85	32.49	35.21	0.9799	1.173	0.2047
18.10171667	33.56	31.99	35.13	0.9735	1.592	0.2384
18.53708333	34.78	33.62	35.93	0.985	0.9505	0.178
19.01276667	30.68	28.93	32.44	0.9588	2.735	0.3019
19.446025	33.02	31.57	34.46	0.9763	1.49	0.2267
19.94676667	32.18	30.77	33.58	0.9748	1.74	0.2369

B.4.2 Experiment no.2

Table 16: Non-linear regression statistical indicators for experiment no.2 $k_L a$ estimates

t (h)	best fit $k_L a$ estimate (1/h)	95% confidence level lower bound (1/h)	95% confidence level upper bound (1/h)	r^2	*SSE*	*RMSE*
0.169683	21.85	21.44	22.26	0.9844	1.212	0.1527
0.377617	22.7	22.22	23.18	0.9787	1.32	0.1641
0.582767	22.36	21.75	22.97	0.9731	2.091	0.2087
0.790708	22.02	21.28	22.76	0.9624	2.976	0.2516
0.996558	22.11	21.31	22.9	0.959	3.042	0.26
1.2045	22.19	21.55	22.83	0.9719	2.06	0.2116
1.4173	21.65	20.97	22.33	0.9672	2.439	0.2303
1.630117	22.23	21.62	22.85	0.9755	1.672	0.1949
1.8457	22.42	21.76	23.08	0.973	1.903	0.208
2.0606	22.63	21.95	23.3	0.9735	1.831	0.2063
2.279667	22.6	21.98	23.22	0.9764	1.662	0.1943
2.500833	22.53	21.9	23.15	0.9763	1.695	0.1963
2.722675	22.7	22.05	23.35	0.9757	1.681	0.1977
2.945217	22.96	22.37	23.56	0.9802	1.377	0.179
3.16985	22.83	22.22	23.44	0.9791	1.385	0.1816
3.39795	22.52	22.01	23.03	0.9822	0.991	0.1536
3.631617	22.1	21.51	22.69	0.9783	1.525	0.1862
3.8653	21.99	21.3	22.68	0.9713	2.085	0.2177
4.099658	22.4	21.75	23.05	0.9759	1.681	0.1977
4.334017	22.62	21.95	23.29	0.9755	1.657	0.1987
4.569083	22.43	21.69	23.17	0.9707	2.046	0.2207
4.808317	22.49	21.91	23.08	0.9808	1.282	0.1747
5.053808	22.35	21.74	22.95	0.9792	1.48	0.1855
5.30695	21.19	20.54	21.83	0.9727	2.044	0.2131
5.563567	21.71	21.21	22.21	0.9834	1.113	0.1591
5.806275	22.26	21.65	22.87	0.978	1.523	0.1882
6.048983	21.62	20.94	22.3	0.9715	2.08	0.2174
6.293783	22.39	21.72	23.06	0.9754	1.691	0.2007

t (h)	best fit k_La estimate (1/h)	95% confidence level lower bound (1/h)	95% confidence level upper bound (1/h)	r^2	*SSE*	*RMSE*
6.538583	21.7	21.08	22.31	0.976	1.703	0.1967
6.78685	21.7	20.99	22.41	0.9702	2.121	0.2221
7.033733	22.02	21.53	22.51	0.984	1.044	0.154
7.2834	21.23	20.6	21.86	0.9739	1.934	0.2073
7.533758	22.14	21.57	22.7	0.9814	1.287	0.173
7.788292	21.46	20.85	22.07	0.9771	1.926	0.2024
8.0769	20.64	19.74	21.54	0.9268	4.833	0.3173
8.334917	21	20.32	21.68	0.9707	2.255	0.2239
8.609617	20.08	19.24	20.92	0.9506	3.98	0.2941
8.8711	21.32	20.69	21.94	0.9752	1.791	0.2017
9.1298	21.41	20.67	22.15	0.9682	2.203	0.229
9.385733	22.64	22.1	23.19	0.9835	1.084	0.1607
9.643742	21.59	20.98	22.2	0.9776	1.561	0.1905
9.903833	21.29	20.78	21.81	0.9822	1.276	0.1684
10.16811	21.33	20.68	21.98	0.974	1.807	0.205
10.4289	33.49	31.99	34.99	0.9183	5.71	0.3687
10.53391	67.31	59.71	74.91	0.9187	4.888	0.5072
10.67022	59.18	56.06	62.3	0.9753	1.528	0.2577
10.85266	60.26	58.87	61.65	0.9953	0.2926	0.1128
11.02657	54.51	48.94	60.07	0.9301	4.504	0.4631
11.2624	47.09	44	50.17	0.9612	2.455	0.3198
11.51978	45.25	42.89	47.62	0.9721	2.146	0.2768
11.84952	38.24	36.18	40.29	0.967	2.251	0.2835
12.16464	44.62	42.27	46.97	0.9743	1.398	0.2465
12.4749	38.14	36.36	39.91	0.9733	1.544	0.2391
12.78723	37.24	34.96	39.51	0.9524	2.903	0.322
13.08422	42.09	40.73	43.44	0.9881	0.6325	0.1591
13.37074	44.17	42.68	45.65	0.986	0.7002	0.1674
13.6211	46.08	44.74	47.43	0.9909	0.4366	0.1378
13.86937	43.4	41.16	45.65	0.9706	1.495	0.2496
14.1406	39.41	36.92	41.89	0.9586	2.157	0.2998
14.42364	38.95	37.08	40.82	0.9704	1.661	0.2481
14.70112	40.43	38.59	42.27	0.9756	1.373	0.2298

t (h)	best fit k_La estimate (1/h)	95% confidence level lower bound (1/h)	95% confidence level upper bound (1/h)	r^2	*SSE*	*RMSE*
14.98208	38.21	34.45	41.97	0.9122	4.198	0.4368
15.23662	45.8	44.2	47.41	0.986	0.6871	0.1692
15.5454	39.93	38.24	41.62	0.9772	1.162	0.2114
15.87925	35.37	33.04	37.7	0.9492	2.271	0.3076
16.1422	40.83	39.43	42.22	0.9858	0.6266	0.1616
16.47259	33.27	30.53	36	0.9211	4.683	0.4165
16.73826	38.89	37.28	40.51	0.9774	0.8414	0.1913
16.99001	39.02	37.66	40.38	0.9851	0.594	0.1607
17.25149	35.72	34.37	37.08	0.9805	0.8473	0.1841
17.50255	34.24	32.58	35.9	0.9685	1.796	0.2533
17.77586	30.05	28.24	31.86	0.9493	1.935	0.2782
18.03387	33.77	33.08	34.46	0.9918	0.3777	0.1122
18.30162	27.84	27.29	28.4	0.9908	0.5677	0.1239
18.59648	23.06	21.66	24.46	0.919	5.546	0.3771
18.92891	20.57	19.88	21.26	0.9579	3.249	0.2524
19.22238	20.14	19.81	20.47	0.9914	0.6682	0.1168
19.57915	14.13	13.71	14.55	0.9568	4.903	0.2647
19.93452	14.67	14.56	14.79	0.9972	0.2675	0.06415
20.44358	12.85	12.49	13.22	0.9613	5.646	0.2673
20.88178	17.21	17.07	17.36	0.9969	0.2932	0.06933
21.26228	19.55	19.39	19.71	0.9978	0.1709	0.05847
21.64002	18.94	18.69	19.19	0.9936	0.5225	0.09929
22.00593	20.74	20.25	21.23	0.983	1.534	0.1734
22.38917	18.75	18.33	19.16	0.9838	1.253	0.1583
22.75643	21.72	21.35	22.1	0.9917	0.5944	0.1162
23.11122	22.61	22.45	22.77	0.9985	0.1187	0.04973

B.4.3 Experiment no.3

Table 17: Non-linear regression statistical indicators for experiment no.3 $k_L a$ estimates

t (h)	best fit $k_L a$ estimate (1/h)	95% confidence level lower bound (1/h)	95% confidence level upper bound (1/h)	r^2	*SSE*	*RMSE*
0.27359167	17.03	16.69	17.38	0.9826	1.728	0.1683
0.59015	17.5	17.09	17.91	0.9769	2.334	0.1972
0.89198333	17.41	16.98	17.83	0.975	2.533	0.2055
1.19381667	17.86	17.48	18.23	0.9814	1.855	0.1759
1.49358333	18.06	17.68	18.44	0.9817	1.806	0.175
1.79331667	18.02	17.63	18.41	0.9806	1.84	0.1781
2.0875	17.58	17.17	17.99	0.9775	2.205	0.1933
2.38865	17.9	17.51	18.28	0.9809	1.812	0.1768
2.68633333	18.43	18.2	18.66	0.9925	0.6238	0.1037
2.98195	17.63	17.22	18.03	0.9785	2.106	0.1889
3.28308333	17.67	17.27	18.07	0.9789	2.016	0.1864
3.58420833	17.67	17.23	18.11	0.9746	2.519	0.2066
3.87838333	17.92	17.55	18.28	0.9827	1.627	0.1675
4.17743333	17.66	17.26	18.07	0.9779	2.241	0.1933
4.47786667	18.06	17.76	18.35	0.9882	1.145	0.1381
4.78113333	18.77	18.31	19.22	0.975	2.304	0.1993
5.08226667	17.7	17.32	18.09	0.98	2.054	0.1835
5.38896667	18.6	18.52	18.69	0.9991	0.08283	0.03779
5.7186	15.81	15.57	16.05	0.9887	1.171	0.1332
6.06076667	15.95	15.84	16.07	0.9976	0.2516	0.06175
6.4475	13.63	13.57	13.7	0.9987	0.1575	0.04437
6.89396667	10.74	10.68	10.8	0.9966	0.5616	0.06958
7.38569167	10.4	10.34	10.45	0.9971	0.4889	0.06356
7.885025	10.53	10.44	10.62	0.9916	1.396	0.1065
8.38783333	22.47	22.16	22.79	0.9642	5.803	0.2163
8.56946667	54.46	51.47	57.44	0.9645	1.509	0.268
8.67448333	59.33	57.6	61.07	0.9897	0.3722	0.1364
8.7879	47.66	43.86	51.45	0.9359	3.641	0.3979

t (h)	best fit k_La estimate (1/h)	95% confidence level lower bound (1/h)	95% confidence level upper bound (1/h)	r^2	*SSE*	*RMSE*
8.92979167	52.7	49.23	56.16	0.9604	2.333	0.3185
9.1259	50.46	47.98	52.94	0.9738	1.809	0.2589
9.35331667	52.19	49.56	54.82	0.9738	1.751	0.2595
9.58768333	49.4	46.83	51.97	0.968	2.358	0.2851
9.8235	47.56	44.57	50.55	0.9563	3.705	0.3514
10.0648417	49.17	46.1	52.24	0.9583	3.37	0.3409
10.3089333	48.6	45.25	51.96	0.9528	3.844	0.3705
10.5586167	52.29	48.45	56.12	0.9479	4.581	0.3974
10.799275	57.88	54.09	61.66	0.9653	2.25	0.3127
11.0378833	53.6	49.08	58.12	0.944	4.125	0.4146
11.2834417	54.71	49.88	59.54	0.9381	4.912	0.4433
11.5220333	53.86	48.1	59.62	0.9172	6.631	0.5256
11.7598833	53.12	48.45	57.79	0.9396	4.471	0.4316
12.006775	51.56	48.23	54.89	0.9598	3.089	0.3383
12.2571333	52.12	48.68	55.57	0.9591	3.213	0.345
12.5095833	49.58	45.07	54.1	0.9268	6.637	0.4869
12.7641167	42.91	40.02	45.81	0.9499	4.265	0.3771
13.0318583	42.27	39.42	45.12	0.9488	4.577	0.3842
13.2947333	45.68	42.64	48.73	0.9555	3.317	0.3505
13.55485	47.07	43.82	50.32	0.9562	3.002	0.3465
13.8149417	46.01	42.97	49.06	0.9583	2.75	0.3316
14.0715667	46.9	44	49.8	0.9621	2.641	0.3187
14.3240083	47.82	44.43	51.2	0.9516	3.754	0.3729
14.5695	50.21	46.84	53.58	0.96	2.608	0.3296
14.8129167	49.66	46.14	53.19	0.9558	2.918	0.3487
15.05355	49.5	46.13	52.87	0.9588	2.687	0.3346
15.2934833	49.63	46.13	53.13	0.9575	2.619	0.3375
15.5341083	46.3	42.66	49.94	0.9441	3.921	0.396
15.77195	45.67	42.48	48.86	0.9534	3.097	0.352
16.0070083	44.17	40.75	47.59	0.9429	3.793	0.3895
16.2392917	41.87	38.98	44.76	0.9517	2.973	0.3449
16.47435	39.05	36.42	41.67	0.9496	3.342	0.3518
16.7115	34.76	32.14	37.39	0.93	5.31	0.4207

t (h)	best fit k_La estimate (1/h)	95% confidence level lower bound (1/h)	95% confidence level upper bound (1/h)	r^2	*SSE*	*RMSE*
16.9507333	35.45	33.63	37.27	0.9644	2.439	0.2851
17.2038667	31.64	29.85	33.42	0.9558	3.277	0.32
17.5036083	32.06	30.64	33.47	0.972	1.846	0.244
17.8151667	30.3	28.95	31.64	0.9697	2.138	0.2545
18.1329833	28.4	27.04	29.77	0.9634	2.64	0.2787
18.4563667	27.57	26.39	28.74	0.9692	2.211	0.2514
18.7860083	26.88	25.84	27.92	0.9728	2.062	0.2361
19.1177333	25.3	24.15	26.44	0.9626	2.961	0.2791
19.4626667	26.07	25.13	27.01	0.9754	1.89	0.223
19.8145667	25.13	24.08	26.19	0.9675	2.529	0.258
20.1789833	25.02	24.07	25.97	0.9719	2.336	0.2416
20.5461667	25.07	24.06	26.08	0.9697	2.328	0.2475
20.9112833	24.52	23.46	25.58	0.9649	2.837	0.2697
21.2847333	24.4	23.48	25.33	0.9719	2.296	0.2396
21.6700167	25.5	24.68	26.33	0.9799	1.503	0.1989
22.065725	24.55	23.55	25.54	0.9695	2.446	0.2504
22.4614333	24.49	23.51	25.46	0.97	2.507	0.2503
22.8564333	25.09	24.16	26.02	0.9751	1.713	0.2182
23.2549333	23.38	22.35	24.4	0.9623	3.225	0.2805
23.6436833	24.42	23.6	25.24	0.977	1.817	0.2131
24.0192167	23.9	22.97	24.84	0.9694	2.451	0.2475
24.3850333	23.59	22.68	24.5	0.9701	2.358	0.2428

B.4.4 Experiment no.4

Table 18: Non-linear regression statistical indicators for experiment no.4 $k_L a$ estimates

t (h)	best fit $k_L a$ estimate (1/h)	95% confidence level lower bound (1/h)	95% confidence level upper bound (1/h)	r^2	*SSE*	*RMSE*
0.129333	20	19.44	20.55	0.9742	2.362	0.2131
0.400583	21.47	20.93	22.02	0.9811	1.476	0.1791
0.678192	21.41	20.9	21.93	0.9812	1.713	0.1833
0.952217	20.85	20.22	21.48	0.9735	2.17	0.2149
1.233175	20.71	20.01	21.41	0.9677	2.711	0.2402
1.5197	21.04	20.4	21.68	0.9737	2.19	0.2159
1.803458	21.28	20.69	21.88	0.9773	1.878	0.1999
2.090767	21.17	20.53	21.82	0.9733	2.346	0.2211
2.382933	20.9	20.23	21.57	0.9711	2.544	0.2302
2.677158	20.74	20.01	21.48	0.966	2.944	0.2503
2.975517	20.89	20.23	21.56	0.9717	2.512	0.2288
3.278767	21.35	20.72	21.99	0.9758	2.002	0.2086
3.582033	21.15	20.51	21.79	0.9738	2.323	0.22
3.883175	21.31	20.78	21.85	0.9816	1.647	0.1834
4.190558	21.43	20.9	21.97	0.9827	1.33	0.1719
4.49725	21.43	20.85	22	0.9799	1.632	0.1883
4.806033	21.13	20.59	21.67	0.9811	1.62	0.1837
5.116892	21.43	20.92	21.94	0.9838	1.334	0.1685
5.42845	20.98	20.41	21.56	0.9783	1.956	0.1998
5.742792	21.36	20.88	21.84	0.985	1.324	0.1644
6.055742	20.52	19.94	21.09	0.9774	2.014	0.2028
6.37565	20.57	20	21.14	0.9777	1.986	0.2013
6.698333	21.24	20.83	21.64	0.9894	0.8454	0.1341
7.0252	21.22	20.81	21.63	0.989	0.8744	0.1364
7.351367	20.63	20.18	21.07	0.9857	1.268	0.1592
7.678217	20.49	20.02	20.96	0.9839	1.432	0.1692
8.00925	20.33	19.87	20.78	0.9848	1.338	0.1636
8.342375	20.2	19.73	20.67	0.9838	1.373	0.1674

t (h)	best fit k_La estimate (1/h)	95% confidence level lower bound (1/h)	95% confidence level upper bound (1/h)	r^2	*SSE*	*RMSE*
8.678967	20.03	19.6	20.45	0.986	1.248	0.1564
9.01625	20.22	19.85	20.59	0.9893	0.9817	0.1374
9.35425	19.86	19.51	20.22	0.9892	1.021	0.1375
9.695017	19.63	19.25	20.01	0.9877	1.18	0.1478
10.03578	19.18	18.75	19.61	0.9839	1.469	0.1681
10.39393	19.43	19.05	19.82	0.9873	1.173	0.1488
10.74097	19.18	18.8	19.55	0.9878	1.09	0.1448
11.09563	19.2	18.82	19.59	0.9873	1.157	0.1492
11.4524	19.37	19.06	19.67	0.9916	0.7568	0.1195
11.81333	19.01	18.73	19.28	0.9928	0.6548	0.1101
12.17357	19.19	18.95	19.44	0.9944	0.5151	0.09767
12.53312	19.05	18.78	19.32	0.9934	0.5953	0.106
12.89753	20.53	20.14	20.92	0.9866	1.266	0.1517
13.1061	51.38	47.02	55.73	0.9266	3.804	0.4158
13.23827	49.79	47.95	51.64	0.9839	0.845	0.1876
13.39408	43.22	41.94	44.49	0.9905	0.586	0.1501
13.66331	35.59	34.12	37.06	0.9715	2.463	0.258
13.9812	34.72	33.12	36.32	0.9601	3.204	0.2904
14.31304	31.93	30.57	33.29	0.9644	3.234	0.2808
14.65042	33.52	31.99	35.05	0.9617	3.109	0.286
15.00242	34.94	33.51	36.37	0.9703	2.243	0.2496
15.36062	35.04	33.56	36.52	0.9699	2.229	0.2524
15.72643	34.47	32.84	36.1	0.9629	3.137	0.2912
16.08944	38.42	36.56	40.28	0.9681	2.255	0.2697
16.45803	35.65	33.81	37.49	0.9588	3.322	0.3081
16.82383	36.84	34.86	38.82	0.9561	3.584	0.32
17.18268	39.2	37.39	41.01	0.9732	1.779	0.2477
17.54362	36.94	34.92	38.95	0.9605	3.063	0.3094
17.8976	39.21	37.44	40.98	0.9743	1.693	0.2416
18.2474	38.08	36.55	39.6	0.9779	1.438	0.2189
18.5854	36.44	34.63	38.25	0.9683	2.208	0.2713
18.91156	33.81	32.26	35.35	0.9665	2.652	0.2753
19.22242	34.38	32.89	35.87	0.9744	1.678	0.2365

t (h)	best fit k_La estimate (1/h)	95% confidence level lower bound (1/h)	95% confidence level upper bound (1/h)	r^2	*SSE*	*RMSE*
19.53468	33.11	32	34.22	0.98	1.434	0.2024
19.8358	32.24	31.02	33.46	0.9764	1.702	0.2237
20.12858	31.89	30.74	33.05	0.9794	1.45	0.2096
20.42068	30.14	29.1	31.17	0.9796	1.486	0.2061
20.70998	30.37	29.62	31.12	0.9883	0.7797	0.1493
20.98885	27.67	26.79	28.54	0.9797	1.525	0.2003
21.26842	26.37	25.9	26.85	0.992	0.5544	0.1177
21.55147	22.88	22.43	23.32	0.9878	1.025	0.1447
21.84494	20.23	19.87	20.59	0.9884	1.07	0.1395
22.18154	19.44	19.09	19.8	0.9875	1.191	0.1446
22.55013	18.46	18.12	18.81	0.984	1.675	0.1605
22.9194	17.58	17.28	17.87	0.9867	1.397	0.1455
23.30268	16.62	16.3	16.94	0.9816	2.131	0.1733
23.6977	16.43	16.11	16.75	0.9779	2.525	0.1835
24.10037	15.91	15.59	16.23	0.9754	2.887	0.1924
24.51693	15.73	15.38	16.08	0.9676	3.805	0.2167
24.94602	15.03	14.68	15.38	0.9586	5.642	0.2476

B.4.5 Experiment no.5

Table 19: Non-linear regression statistical indicators for experiment no.5 $k_L a$ estimates

t (h)	best fit $k_L a$ estimate (1/h)	95% confidence level lower bound (1/h)	95% confidence level upper bound (1/h)	r^2	*SSE*	*RMSE*
0.258033333	19.76	19.17	20.35	0.9746	2.044	0.2085
0.583533333	20.57	19.81	21.33	0.9667	2.518	0.242
0.915958333	20.86	19.98	21.74	0.9566	3.739	0.2883
1.227516667	21.45	20.56	22.33	0.9601	3.2	0.2728
1.53985	22.14	21.39	22.9	0.9725	2.088	0.223
1.862533333	22.06	21.27	22.85	0.9696	2.567	0.2415
2.1866	21.67	20.75	22.59	0.9594	3.185	0.2754
2.507933333	22.7	22.01	23.39	0.9767	2.084	0.2129
2.841066667	22.61	21.7	23.52	0.9643	2.758	0.2594
3.142883333	22.27	21.33	23.21	0.9628	2.623	0.2594
3.471141667	23.55	22.63	24.47	0.9662	2.959	0.2623
3.798066667	22.76	21.67	23.84	0.9526	3.897	0.3083
4.088783333	22.64	21.56	23.72	0.9553	2.953	0.2825
4.402433333	23.4	22.52	24.28	0.9681	2.874	0.2556
4.739033333	21.49	20.08	22.91	0.9186	6.849	0.4138
5.026933333	24.08	22.98	25.17	0.9601	2.592	0.2683
5.313466667	24.48	23.45	25.52	0.9651	2.267	0.251
5.601383333	24.74	23.86	25.62	0.9733	1.847	0.2205
5.91085	24.18	23.1	25.27	0.9578	3.963	0.3036
6.225916667	43.05	40.35	45.75	0.8683	11.01	0.5248
6.311458333	82.84	68.89	96.79	0.8786	4.822	0.609
6.397	109	88.01	130.1	0.8717	7.472	0.7306
6.483233333	87.28	71.02	103.5	0.8499	9.614	0.7752
6.584075	80.89	63.91	97.87	0.8294	10.36	0.8309
6.693958333	82.19	64.78	99.6	0.8536	9.671	0.8029
6.867133333	89.94	69.13	110.7	0.8338	15.94	0.9409
7.092016667	78.89	66.81	90.97	0.9028	6.422	0.6146
7.314558333	68.72	59.37	78.08	0.9117	5.125	0.549

t (h)	best fit k_La estimate (1/h)	95% confidence level lower bound (1/h)	95% confidence level upper bound (1/h)	r^2	*SSE*	*RMSE*
7.518316667	73.91	62.24	85.58	0.9028	4.423	0.5621
7.72835	72.29	64.14	80.45	0.9346	3.962	0.4692
7.94185	74.91	66.87	82.96	0.9429	3.168	0.4317
8.15675	72.19	58.77	85.61	0.8612	10.75	0.7728
8.395983333	71.64	62.59	80.69	0.9212	4.985	0.5262
8.601833333	74.36	68.59	80.12	0.9629	2.311	0.3399
8.808375	85.28	77.06	93.5	0.9497	4.291	0.4319
9.014225	68.84	62.84	74.84	0.9504	3.29	0.3958
9.211033333	70.01	62.27	77.75	0.9306	4.794	0.4896
9.40855	79.25	69.87	88.62	0.9348	3.854	0.4761
9.6047	80.07	72.51	87.63	0.9524	2.75	0.3909
9.79665	86.15	80.57	91.73	0.9784	1.004	0.2505
9.985816667	80.46	71.25	89.67	0.9413	3.176	0.4455
10.17915	78.95	71.05	86.84	0.9452	3.816	0.4368
10.3697	77.06	69.17	84.95	0.941	4.045	0.4497
10.5526	89.98	78.96	101	0.9368	4.014	0.4859
10.75149167	79.53	70.41	88.65	0.9381	3.632	0.4622
10.94135	85.33	78.78	91.89	0.9679	1.804	0.3166
11.1173	84.77	74.23	95.31	0.932	4.247	0.4998
11.29741667	85.32	74.13	96.51	0.9288	4.175	0.5108
11.47754167	88.88	82.68	95.09	0.9704	1.324	0.279
11.64236667	91.52	87.25	95.79	0.989	0.521	0.1805
11.81065	84.12	76.69	91.54	0.9544	1.89	0.3437
11.9734	90.17	84.16	96.18	0.9745	1.066	0.2581
12.13543333	88.14	82.42	93.86	0.9764	1.149	0.2599
12.296775	99.19	90.62	107.8	0.9717	1.151	0.2976
12.456725	95.92	87.02	104.8	0.9673	1.322	0.3189
12.62571667	83.32	76.67	89.97	0.9644	1.964	0.3303
12.800275	89.43	82.83	96.02	0.9728	1.481	0.2951
12.97205	89.17	83.89	94.46	0.9759	1.069	0.2437
13.12505	84.97	74.67	95.27	0.9396	2.7	0.4392
13.28708333	84.39	76.9	91.87	0.9579	2.192	0.3591
13.44425833	88.73	79.81	97.65	0.951	2.757	0.4027

t (h)	best fit k_La estimate (1/h)	95% confidence level lower bound (1/h)	95% confidence level upper bound (1/h)	r^2	*SSE*	*RMSE*
13.61255833	84.94	78.56	91.32	0.9639	1.568	0.3037
13.76346667	96.17	89.93	102.4	0.9799	0.998	0.2498
13.92550833	78.59	71.96	85.23	0.9597	2.013	0.3441
14.08058333	83.41	75.77	91.05	0.955	2.623	0.3817
14.23636667	81.74	76.84	86.65	0.9786	0.889	0.2357
14.38801667	87.46	83.02	91.9	0.9857	0.629	0.1983
14.537575	115.8	110.1	121.5	0.9921	0.258	0.153
14.67391667	95.3	80.24	110.4	0.9344	1.574	0.4182
14.80470833	87.44	82.66	92.23	0.984	0.642	0.2069
14.95218333	79.87	73.3	86.43	0.9647	1.439	0.3098
15.10453333	71.65	64.29	79.02	0.9541	1.267	0.325
15.25896667	86.06	79.47	92.65	0.9779	0.466	0.2158
15.40506667	72.04	63.42	80.67	0.9415	1.717	0.3783
15.57270833	64.24	60.75	67.74	0.9783	0.831	0.2211
15.72506667	66.71	60.29	73.13	0.9509	1.625	0.3407
15.8781	68.24	61.99	74.5	0.961	0.991	0.2874
16.02905833	68.74	63.5	73.99	0.9636	1.643	0.3109
16.18558333	88.76	80.66	96.86	0.9586	1.064	0.2977
16.33863333	66.83	62.22	71.45	0.9651	1.882	0.3068
16.52228333	66.48	62.35	70.61	0.9772	0.671	0.2189
16.68995	60.71	56.51	64.91	0.967	1.31	0.2776
16.85898333	65.36	62.29	68.43	0.9866	0.378	0.1644
17.03775833	62.91	59.21	66.62	0.9766	0.95	0.2364
17.23115	52.94	49.81	56.07	0.9707	1.207	0.252
17.4141	53.71	48.62	58.79	0.9427	2.015	0.3549
17.60046667	54.41	50.87	57.95	0.9652	1.666	0.2886
17.78128333	54.92	51.45	58.39	0.9718	0.9	0.2371
17.97323333	53.62	49.87	57.38	0.9663	1.092	0.2613
18.16030833	46.41	43.76	49.06	0.9665	1.904	0.2817
18.36059167	41.42	39.74	43.1	0.981	0.844	0.1915
18.56088333	42.64	40.8	44.48	0.9805	0.765	0.1908
18.76325	41.49	39.81	43.16	0.9806	0.926	0.1964
18.96285	40.24	38.26	42.22	0.9725	1.23	0.2312

t (h)	best fit k_La estimate (1/h)	95% confidence level lower bound (1/h)	95% confidence level upper bound (1/h)	r^2	*SSE*	*RMSE*
19.16035833	40.85	37.13	44.58	0.9301	2.57	0.3677
19.35576667	39.72	35.23	44.21	0.8905	5.793	0.5131
19.56858333	38.23	35.28	41.18	0.9394	2.654	0.3473
19.75773333	42.03	40.16	43.91	0.9778	0.925	0.2051
19.94899167	40.45	37.47	43.42	0.9477	2.185	0.3226
20.142325	41.57	39.48	43.65	0.9705	1.591	0.2523
20.3433	39.62	36.26	42.97	0.9321	2.519	0.3549
20.52691667	40.05	37.39	42.7	0.9507	2.526	0.3244
20.7224	38.56	36.62	40.49	0.9688	1.561	0.2499
20.92623333	36.4	34.24	38.57	0.9566	2.363	0.3015
21.1363	38.48	36.73	40.23	0.9748	1.149	0.2189

B.5 MATLAB® implementation of the Simpson's numerical integration function

```
function z = simps(x,y,dim)
%SIMPS  Simpson's numerical integration.
%  Z = SIMPS(Y) computes an approximation of the integral of Y via the
%  Simpson's method (with unit spacing). To compute the integral for
%  spacing different from one, multiply Z by the spacing increment.
%
%  For vectors, SIMPS(Y) is the integral of Y. For matrices, SIMPS(Y) is a
%  row vector with the integral over each column. For N-D arrays, SIMPS(Y)
%  works across the first non-singleton dimension.
%
%  Z = SIMPS(X,Y) computes the integral of Y with respect to X using the
%  Simpson's rule. X and Y must be vectors of the same length, or X must
%  be a column vector and Y an array whose first non-singleton dimension
%  is length(X). SIMPS operates along this dimension.
%
%  Z = SIMPS(X,Y,DIM) or SIMPS(Y,DIM) integrates across dimension DIM of
%  Y. The length of X must be the same as size(Y,DIM).
%
%  Examples:
%  --------
%  % The integration of sin(x) on [0,pi] is 2
%  % Let us compare TRAPZ and SIMPS
%  x = linspace(0,pi,6);
%  y = sin(x);
%  trapz(x,y) % returns 1.9338
%  simps(x,y) % returns 2.0071
%
%  If Y = [0 1 2
%          3 4 5
%          6 7 8]
%  then simps(Y,1) is [6 8 10] and simps(Y,2) is [2; 8; 14]
%
%
%  Class support for inputs X, Y:
%    float: double, single
%
%  -- Damien Garcia -- 08/2007, revised 11/2009
%    directly adapted from TRAPZ
%
%  See also CUMSIMPS, TRAPZ, QUAD.

%%  Make sure x and y are column vectors, or y is a matrix.
perm = []; nshifts = 0;
if nargin == 3 % simps(x,y,dim)
 perm = [dim:max(ndims(y),dim) 1:dim-1];
 yp = permute(y,perm);
 [m,n] = size(yp);
elseif nargin==2 && isscalar(y) % simps(y,dim)
 dim = y; y = x;
 perm = [dim:max(ndims(y),dim) 1:dim-1];
 yp = permute(y,perm);
 [m,n] = size(yp);
 x = 1:m;
else % simps(y) or simps(x,y)
 if nargin < 2, y = x; end
 [yp,nshifts] = shiftdim(y);
```

```
 [m,n] = size(yp);
 if nargin < 2, x = 1:m; end
end
x = x(:);
if length(x) ~= m
 if isempty(perm) % dim argument not given
  error('MATLAB:simps:LengthXmismatchY',...
      'LENGTH(X) must equal the length of the first non-singleton dimension of Y.');
 else
  error('MATLAB:simps:LengthXmismatchY',...
      'LENGTH(X) must equal the length of the DIM''th dimension of Y.');
 end
end

%% The output size for [] is a special case when DIM is not given.
if isempty(perm) && isequal(y,[])
 z = zeros(1,class(y));
 return;
end

%% Use TRAPZ if m<3
if m<3
  if exist('dim','var')
    z = trapz(x,y,dim);
  else
    z = trapz(x,y);
  end
  return
end

%% Simpson's rule
y = yp;
clear yp

dx = repmat(diff(x,1,1),1,n);
dx1 = dx(1:end-1,:);
dx2 = dx(2:end,:);

alpha = (dx1+dx2)./dx1/6;
a0 = alpha.*(2*dx1-dx2);
a1 = alpha.*(dx1+dx2).^2./dx2;
a2 = alpha.*dx1./dx2.*(2*dx2-dx1);

z = sum(a0(1:2:end,:).*y(1:2:m-2,:) +...
  a1(1:2:end,:).*y(2:2:m-1,:) +...
  a2(1:2:end,:).*y(3:2:m,:),1);

if rem(m,2) == 0 % Adjusting if length(x) is even
  state0 = warning('query','MATLAB:nearlySingularMatrix');
  state0 = state0.state;
  warning('off','MATLAB:nearlySingularMatrix')
  C = vander(x(end-2:end))\y(end-2:end,:);
  z = z + C(1,:).*(x(end,:).^3-x(end-1,:).^3)/3 +...
    C(2,:).*(x(end,:).^2-x(end-1,:).^2)/2 +...
    C(3,:).*dx(end,:);
  warning(state0,'MATLAB:nearlySingularMatrix')
end
```

```
%% Resizing
siz = size(y); siz(1) = 1;
z = reshape(z,[ones(1,nshifts),siz]);
if ~isempty(perm), z = ipermute(z,perm); end
```

ANNEXURES

All annexures associated with the study are contained in the CD−ROM entitled: Mashava.Amended.Manuscript.07.2014 under the Annexures directory, i.e. :\Annexures\

The proprietary technical computing platforms that are required for handling the file formats contained in the annexures are as follows:

1. *.xlsx: Microsoft Office Excel, ver. 14.0.4734.100 or later releases

2. *.cfit: Curve Fitting Toolbox™ from MathWorks Inc. MATLAB®, ver. R2011a or later releases

3. *.emf: any Scalable Vector Graphics (SVG) platform

4. *.fig: MathWorks Inc. MATLAB®, ver. R2011a or later releases

5. *.m: MathWorks Inc. MATLAB®, ver. R2011a or later releases

6. *.mat: MathWorks Inc. MATLAB®, ver. R2011a or later releases


Mashava.Amended.Manuscript.07.2014
Annexures
Soluble Dye Effluent Decolourisation
Soluble Dye Effluent Decolourisation.xlsx
Effect of Surfactant Effluent on Oxygen Transfer
DO Experiment no.1
DO Experiment no.2
DO Experiment no.3
DO Experiment no.4
DO Experiment no.5
DO Probe Response Dynamics Experiment no.1
DO Probe Response Dynamics Experiment no.2
DO Probe Response Dynamics Experiment no.3
DO Probe Response Dynamics Experiment no.4
DO Probe Response Dynamics Experiment no.5
DO Probe Time Constant Estimates.xlsx
Biodegradability of Surfactant Effluent
OUR Experiment no.1
Numerical Analysis Computations
OUR Experiment no.2
Numerical Analysis Computations
OUR Experiment no.3
Numerical Analysis Computations
OUR Experiment no.4
Numerical Analysis Computations
OUR Experiment no.5
Numerical Analysis Computations